REPORT 1299

CONTENTS

REPORT 1299

CORRELATION, EVALUATION, AND EXTENSION OF LINEARIZED THEORIES FOR TIRE MOTION AND WHEEL SHIMMY [1]

By Robert F. Smiley

SUMMARY

An evaluation is made of the existing theories of linearized tire motion and wheel shimmy. It is demonstrated that most of the previously published theories represent varying degrees of approximation to a summary theory developed herein which is a minor modification of the basic theory of Von Schlippe and Dietrich. In most cases where strong differences exist between the previously published theories and the summary theory, the previously published theories are shown to possess certain deficiencies.

A series of systematic approximations to the summary theory is developed for the treatment of problems too simple to merit the use of the complete summary theory, and procedures are discussed for applying the summary theory and its systematic approximations to the shimmy of more complex landing-gear structures than have previously been considered.

Comparisons of the existing experimental data with the predictions of the summary theory and the systematic approximations provide a fair substantiation of the more detailed approximate theories. However, some discrepancies exist which may be due to tire hysteresis effects or other unknown influences. Thus, further work may be needed to explain these discrepancies.

INTRODUCTION

In the ground maneuvering of aircraft equipped with swiveling landing gears there sometimes arises the problem of violent oscillations or shimmy of the landing gear which may lead to failure of the gear. In the past this problem has been handled largely by means of various measures based on practical experience. However, this empirical approach has not proved entirely adequate. Moreover, for radically different types of complex flexible landing gears it is highly doubtful whether any empirical approach based purely on past experience could always safely and optimumly take into account all of the possible conditions which a landing gear might be subjected to in actual operation.

A considerable amount of theoretical and experimental work on wheel shimmy has been done, mostly in the past 25 years. (Most of the existing papers on this subject are listed in ref. 1, which also presents a historical discussion of the development of the wheel-shimmy problem.) However, most of these theoretical papers have not been correlated with each other or with the available experimental data, so that essentially there exists at present a large number of at least superficially different theories of wheel shimmy and a fair amount of experimental data which has not been correlated with many of these theories (refs. 2 to 23).

The primary purpose of the present report is to clear up this partial confusion of theories by demonstrating that most of the previously published theories represent various approximations to one basic general linearized theory derived herein and that most of the previously published linearized theories which do not represent approximations to this general theory possess certain undesirable characteristics. This basic general theory, which is henceforth called the summary theory, is derived in such a manner that it makes use of and is compatible with the soundest features of practically all the previously published theories, insofar as this is possible at present; however, in the main this summary theory is a minor modification of the theory proposed by Von Schlippe and Dietrich in references 3, 4, and 5.

A second purpose of this report is to develop a series of systematic approximations to the summary theory suitable for use in the treatment of problems too simple to merit the use of the complete summary theory and to examine both these systematic approximations and the previously published theories to determine how these theories are related to the summary theory and how the predictions of these theories agree with the available experimental data.

A final purpose of this report is to illustrate procedures for applying the summary theory and its approximations to complex types of flexible landing-gear structures.

Although the primary purpose of this report is concerned with the wheel-shimmy problem, most of the material presented is directly applicable to the more general problem of the motion of elastic tires under arbitrary rolling conditions. Thus this material is pertinent to the study of veering-off or ground looping, ground handling, and catapulting stability of aircraft.

The material in this report is arranged as follows. First, a detailed statement of the problem is given, together with a detailed outline of the manner in which it is treated herein. Then, after a brief discussion of the restrictions on the analysis, a linearized derivation is made for the general Von Schlippe-Dietrich type of kinematic equations governing the motion of elastic tires rolling without skidding. This analysis proceeds essentially in accordance with the

[1] Supersedes NACA Technical Note 3632 by Robert F. Smiley, 1956.

theoretical analysis of Von Schlippe and Dietrich except that the present analysis considers the subject of tire tilt in slightly greater detail.

Next, the primary forces and moments acting on a rolling tire are discussed and used to establish the equations of motion for arbitrary rolling conditions. Then a systematic procedure is developed for forming approximations to the summary theory.

The previously published theories are listed, discussed, and compared with the summary theory and these systematic approximations. Finally, the application of the summary and approximate theories to several simplified landing gears is discussed. The first example is chosen primarily to demonstrate the correlation between theory and experiment, the second example to demonstrate the correlation between the summary theory and its systematic approximations, and the remaining example to illustrate the application of the theory to complex problems.

Some of the material presented herein was submitted to the University of Virginia in partial fulfillment of the requirement for a Master of Aeronautical Engineering degree.

SYMBOLS

a trail (perpendicular distance between ground-contact center point and swivel axis)

$a'=a-\xi Lh\frac{\sin\kappa}{r}$

A_1,A_2,A_3 coefficients defined by equations (115b)

B_1,B_2 coefficients defined by equations (115b)

c lateral distance of center of pressure of vertical force from XZ-plane

c_λ change in lateral distance of center of pressure of vertical force from XZ-plane per unit of λ_0

c_γ change in lateral distance of center of pressure of vertical force from XZ-plane per unit of γ

c_1 distance from wheel center to center of gravity of swiveling parts of landing gear

c_2 distance from center of gravity of swiveling parts of landing gear to swivel axis

d_1,d_2 hysteresis constants used in equation (128c)

$\overline{D}$ tire parameter used by Bourcier de Carbon

$D(\ )$ differential operator with respect to distance, $\frac{d(\ )}{dx}$ or $v^{-1}D_t(\ )$

$D_t(\ )$ differential operator with respect to time, $\frac{d(\ )}{dt}$ or $vD(\ )$

$E_0,E_1,\ldots$ coefficients of linear differential equations

E energy dissipated per cycle

f frequency, $\nu/2\pi$

$F_0,F_1,\ldots$ coefficients of linear differential equations

F_{yh} lateral force due to hysteresis effects

F_{yt} lateral inertia force resulting from lateral deformation of tire

F_{yw} net lateral tire force acting on wheel

F_{ys} net lateral structural force acting on wheel

$F_{y\lambda}$ lateral force on tire due to lateral distortion of tire

$F_{y\gamma}$ lateral force on tire due to lateral tilt of tire

F_z vertical load on tire

F_η lateral force on swiveling parts of landing gear due to landing-gear strut

g linear damping constant (Damping moment$=g D_t\psi$)

h half-length of tire-ground contact area

$i=\sqrt{-1}$

$I(\ )$ imaginary part of $(\ )$

I_0 moment of inertia of the swiveling part of a landing gear about an axis parallel to the swivel axis and passing through the center of gravity of the swiveling part

I_{xw} polar moment of inertia of wheel and tire about an axis perpendicular to the wheel axle

I_{yt} polar moment of inertia of tire (excluding solid wheel parts)

I_{yw} total polar moment of inertia of wheel and tire

I_ψ moment of inertia of the swiveling part of a landing gear about the swivel axis

j excess of number of zeros over number of poles

J parameter in stability-determination plots (appendix C)

k lateral spring constant of landing-gear strut

k_n parameter used in appendix A

K_α torsional stiffness of tire

ΔK_α total effective change in tire torsional stiffness due to tire inertia effects

ΔK_{α_t} effective change in torsional stiffness of tire due to lateral acceleration of tire

ΔK_{α_f} change in tire torsional stiffness due to centrifugal forces

K_γ lateral tire force due to tilt per radian of tilt angle

K_λ lateral stiffness of tire

ΔK_λ total effective change in lateral stiffness of tire due to tire inertia effects

ΔK_{λ_t} effective change in lateral stiffness of tire due to lateral acceleration of tire

ΔK_{λ_f} change in lateral stiffness of tire due to centrifugal forces

$l_0,l_1,\ldots$ tire constants; $l_n=\frac{(nL+h)h^{n-1}}{n!}$

L relaxation length

m mass of swiveling parts of landing gear

m_t mass of tire

m_w mass of wheel including tire

m_1 mass of nonswiveling parts of landing gear

M_0 constant friction-damping moment

M_{xs} net structural tilting moment acting on wheel center

$M_{x\theta}$ gyroscopic moment due to swiveling

M_{zh} twisting moment due to hysteresis effects

M_{zt} inertia moment resulting from lateral deformation of tire

M_{zs} net structural swiveling moment acting on wheel center

$M_{z\alpha}$ torsional moment on tire due to twist of tire

$M_{z\gamma}$ gyroscopic moment due to tilting

$M_{z\lambda}$ gyroscopic moment due to lateral distortion of tire

M_θ torsional moment on the swiveling parts of the landing gear due to landing-gear strut and damper unit

M_ψ damping moment about swivel axis

N cornering power (lateral tire force per radian of yaw angle during steady yawed rolling for yaw angle approaching zero)

n_1 parameter used in appendix A

p complex roots of characteristic equations

p_1, p_2 functions defined in appendix D

$p_{1\infty}, p_{2\infty}, p_{11}, p_{12}, p_{21}, p_{22}$ functions defined in and after equations (80)

q_n parameter used in appendix A

r free tire radius

r_g polar radius of gyration of tire

r_3 vertical distance from wheel axle to ground

r_4 radius of cross section of tire torus

$\overline{R}$ tire parameter used by Bourcier de Carbon

R( ) real part of ( )

s circumferential coordinate on tire (fig. 1)

$\overline{S}$ wave length, $2\pi/\nu_1$

$\overline{S}$ tire parameter used by Bourcier de Carbon

t time

Δt time lag due to tire hysteresis

T Moreland's time-lag constant

$\overline{T}$ tire parameter used by Bourcier de Carbon

$T_1, T_2, \ldots$ functions of D_i correlating structural forces, moments, and deflections

T_α time-lag constant for hysteresis moment

T_λ time-lag constant for hysteresis force

$u_\kappa = c_\lambda F_z(\sigma l_1 \cos\kappa - a)\sin\kappa$

$u_{\kappa 1} = c_\lambda F_z(l_1 \cos\kappa - a)\sin\kappa$

v rolling velocity

w width of tire-ground contact area

w_1 density

$w_\kappa = (aK_\gamma - aF_z + c_\gamma F_z \sin\kappa)\sin\kappa$

x horizontal distance parallel to mean direction of rolling motion

X, Y, Z space-fixed coordinate axes; the X-axis is horizontal and parallel to the mean direction of rolling motion, the Z-axis is vertical, and the Y-axis is perpendicular to the XZ-plane. The XY-plane is the ground plane.

y lateral distance of tire equator from XZ-plane

z vertical distance up from XY (ground) plane

y_0, y_1, y_2, y_i, y_g lateral deflection of tire equator from XZ-plane; subscript 0 refers to the center of the ground-contact area, 1 to the foremost point of the ground-contact area, 2 to the rearmost point of the ground-contact area, i to equator points off the ground, and g to equator points on the ground

α twist in tire, radians

$\Delta\alpha$ half-width of twisting-moment—angular-deflection hysteresis loop of tire

γ lateral wheel tilt, radians

γ_λ lateral tire tilt resulting from lateral deformation, radians

ϵ pneumatic caster, K_α/N

$\eta, \eta_0, \eta_1, \eta_3, \eta_a, \eta_i, \eta_g$ lateral deflection of center plane of wheel with respect to the XZ-plane; subscript 0 refers to the point corresponding to the center of the ground-contact area, 1 to the point corresponding to the foremost point of the ground-contact area, 3 to the center point of the wheel, a to the point of attachment of the swiveling parts of the wheel to the swivel axis, i to wheel-plane points off the ground, and g to wheel-plane points on the ground

η_ν inertia-force parameter (eq. (46))

η_z inertia-moment parameter (eq. (49))

η_α hysteresis-moment parameter (eqs. (62))

η_λ hysteresis-force parameter (eqs. (60))

θ angle of rotation of wheel about the vertical Z-axis, radians

κ inclination of swivel axis, radians (fig. 5)

$\lambda, \lambda_0, \lambda_1, \lambda_2, \lambda_i, \lambda_g$ lateral distortion of tire equator with respect to the solid parts of the wheel; subscript 0 refers to the center of the ground contact area, 1 to the foremost point of the ground contact area, 2 to the rearmost point of the ground contact area, i to equator points off the ground, and g to equator points on the ground

$\Delta\lambda_0$ half-width of lateral-force—lateral-deflection hysteresis loop of tire

ν circular frequency of shimmy motion, $2\pi f$ or $\nu_1 v$

ν_1 path frequency of shimmy motion, $v v^{-1}$

ξ tire tilt parameter (eq. (13))

ρ spring constant for a linear restoring moment

$\rho_\kappa = (aK_\gamma - aF_z + ac_\lambda F_z + c_\gamma F_z \sin\kappa)\sin\kappa$

$\sigma = 1 + \xi L h \dfrac{\tan\kappa}{l_1 r}$

σ_1, σ_2 constants representing phase shift

τ constant defined by equations (33) and (50)

τ_1 constant for gyroscopic moment $\left(\approx \dfrac{1}{2}\right)$

$\tau_2 = \dfrac{N l_1 T^2}{I_\psi}$

ψ angle of rotation of wheel about the swivel axis, radians

ω angular velocity of wheel about its axle $\left(\approx \dfrac{v}{r}\right)$

Subscripts:

c critical

max maximum

STATEMENT OF THE PROBLEM AND GENERAL APPROACH

The purpose of this section is to define specifically the problem considered in this report and to clarify further the correlation between the various parts of the report.

The basic problem to be considered is the rolling motion and wheel shimmy of a rigid wheel equipped with an elastic tire, when the wheel is attached to some supporting structure such as a landing-gear strut. The motion of the rigid wheel can, of course, be completely described by six independent variables corresponding to the three degrees of freedom in

translation and rotation of the wheel. In addition to these six degrees of freedom, there exists a seventh degree of freedom which is associated with the distortion of the elastic tire or the track of the tire on the ground which results from the application of a given motion to the rigid wheel. Thus, in general, the motion of a rigid wheel with an elastic tire represents a system of motion involving seven variables, and seven equations correlating these different variables are required to solve for the motion of a landing gear under arbitrary rolling conditions. Six of these equations will usually be the equations expressing the sum of the forces or moments acting along each of the three principal coordinate axes; the seventh relation will be an equation, usually a kinematic equation, which correlates the tire distortion with the other variables.

The present report is not concerned with all seven degrees of freedom. Most of the report is restricted to a consideration of cases of wheel motion in which the wheel is rolling at an approximately constant velocity v without braking, and consequently with constant angular velocity ω, and where no strong vertical oscillations are involved. Thus, for example, effects of acceleration or deceleration, which are known to have at least some influence on the rolling motion (see, for example, the experimental evidence of ref. 17) are not considered. Similarly, fore and aft oscillations of the wheel are excluded.

When these three restrictions are applied, the seven-variable problem of a rolling wheel becomes reduced to the consideration of a system involving the following four degrees of freedom: (1) swiveling of the wheel about a vertical axis through the wheel center point, designated by the symbol θ; (2) lateral tilting of the wheel with respect to a vertical plane parallel to the direction of undisturbed motion, designated by the symbol γ; (3) lateral displacement of the wheel with respect to a space-fixed reference axis parallel to the direction of undisturbed motion, designated by the symbol η with various subscripts; and (4) lateral displacement of the tire footprint on the ground (which is a measure of the tire distortion), designated by the symbol y_0. (These coordinates and their positive directions are illustrated in fig. 1.)

In order to obtain four equations correlating these four variables θ, γ, η, and y_0, the following procedure is used: After some remarks on general restrictions, a kinematic relation between the four variables is derived in the section entitled "Kinematic Relations for the Rolling Tire." Next, the primary forces acting on the wheel from the ground, including wheel inertia forces, are discussed in the section entitled "Forces and Moments on the Wheel." By utilizing these ground forces and moments, the four basic equations of motion for the wheel, including the kinematic equation, are set down in the section entitled "Equations of Motion."

For many applications these equations of motion in their most general form are relatively complicated and, although they are by no means insolvable, it is profitable to simplify the equations for those problems which do not require the detailed equations of the summary theory. Therefore, a number of systematic approximations to the summary theory are formulated in the section entitled "Systematic Approximations to the Summary Theory." A second reason for establishing these systematic approximations lies in the fact that they furnish a framework for comparing the summary theory with the other existing theories of wheel motion, most of which are closely related to these systematic approximations. Such a comparison of the summary theory and its systematic approximations with the existing theories of wheel motion is carried out in the section entitled "Classification and Evaluation of Existing Theories."

In the last major section of this report the summary theory and its systematic approximations are applied to three illustrative types of landing-gear configurations which are chosen either to illustrate agreement between theory and experiment or to illustrate methods for applying the theory to complex problems of wheel shimmy.

GENERAL RESTRICTIONS

Before entering upon the detailed derivation of the equations of motion, some further restrictions on the analysis should be discussed. First of all, the present report is limited almost exclusively to linearized theories. However, there is some question as to whether a linearized theory is sufficient to describe the important features of wheel shimmy. It appears at present that a linearized theory will provide at least a fair qualitative description of stability boundaries for shimmy and will indicate whether a given motion is stable or not. However, agreement between theory and experiment, presented in a subsequent section, is still not good enough quantitatively to warrant the conclusion that nonlinear effects can always be neglected or replaced by equivalent linear effects.

Another limitation of the linearized theory is that it does not permit calculation of the maximum steady-state shimmy amplitude for those steady-state self-excited shimmy motions which sometimes occur on actual landing gears.

Although the preceding considerations suggest that nonlinear effects in landing-gear motions may possibly be of importance for some practical problems, their consideration is beyond the scope of the present report and henceforth only linearized theory is discussed. The only concession to nonlinearity is made in appendix A, which presents a conventional approximate method for converting a nonlinear shimmy damper to an equivalent linear damper. It should, however, be noted that some attention has been given to the development of nonlinear tire-motion theory in references 18 to 21.

Another restriction arises in connection with the assumption adopted throughout this report that the finite width of the tire need not be taken into account in developing a tire-motion theory for single tires of conventional cross section. This assumption appears at present to be at least partly justified on the basis of an experiment by Von Schlippe and Dietrich (ref. 3); on the other hand, since their investigation of this matter was extremely limited in scope, their experimental result may not be completely typical. Consequently, a more thorough evaluation of tire-width effects seems desirable. Some theoretical work on this subject has been done by Von Schlippe and Dietrich (ref. 3) and later by Rotta (ref. 2), but the matter is beyond the scope of the present report.

KINEMATIC RELATIONS FOR THE ROLLING TIRE

In this section the kinematic equations for the motion of a

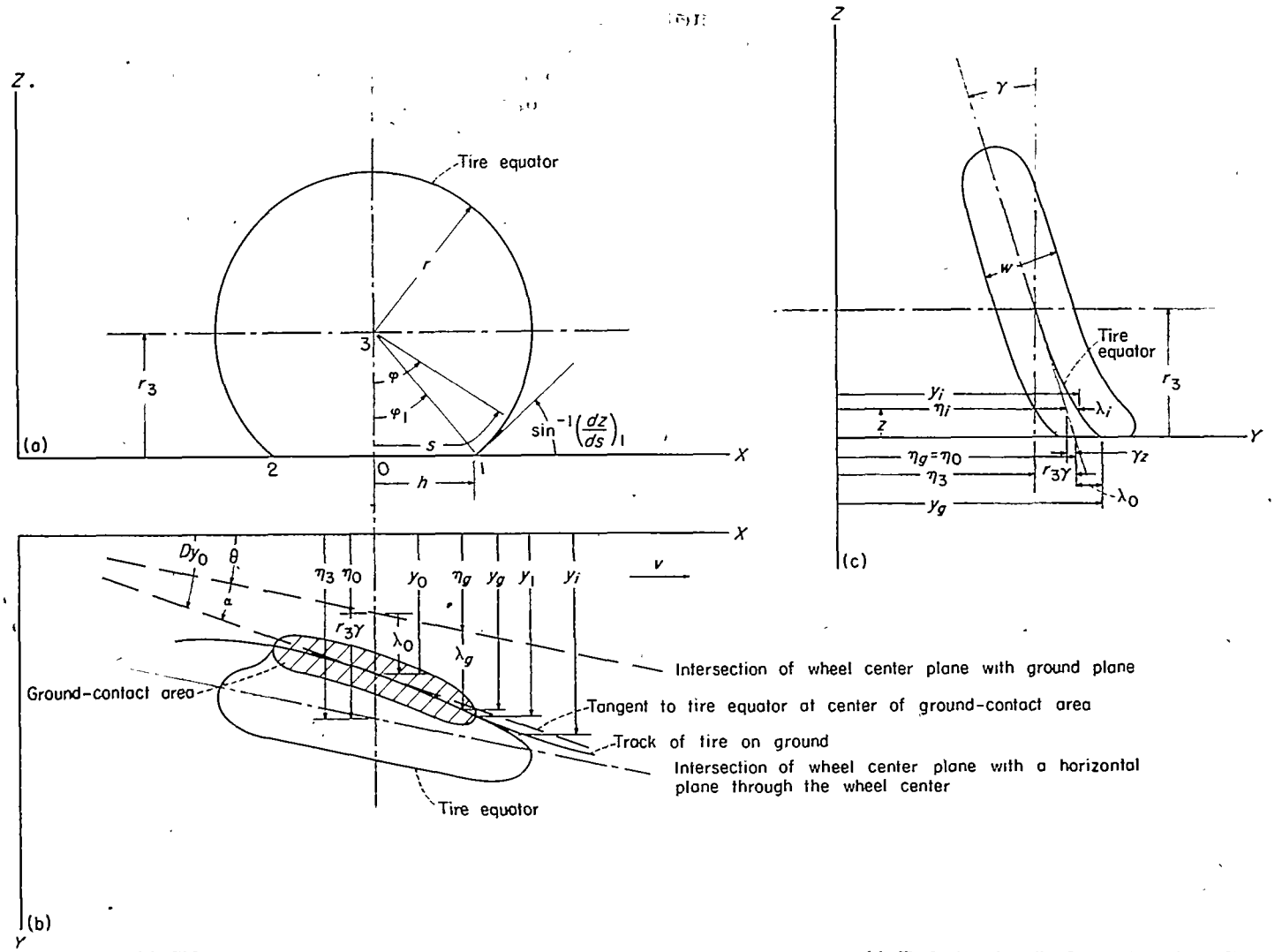

(a) Side view.

(b) Bottom view for tilted swiveled conditions.

(c) End view for tilted unswiveled conditions.

FIGURE 1.—Geometric relations for a rolling elastic tire. (For the sake of clarity parts (b) and (c) of this figure are drawn to different scales. The positive X-axis is the direction of undisturbed motion.)

rolling tilted elastic tire without skidding are derived in accordance with the theoretical analysis of Von Schlippe and Dietrich (ref. 3 or 4). This derivation differs only slightly from that analysis in that it omits some refinements of the theory which are necessary for very wide tires and it includes some influences of tilting of the tire in more detail. While the modifications that are made in regard to tilt may not necessarily be of practical importance in most cases, they may be of interest in a few problems.

Specifically, the object of this section is to obtain a relation correlating the absolute lateral deflection of the center point of the tire ground-contact area y_0 with the corresponding wheel coordinates of lateral deflection η (for example, η_0 or η_3), swivel angle θ, and tilt γ. (See fig. 1.) First, some geometric relations are set down and some background information regarding tire distortion is discussed. Then this information is utilized to obtain a kinematic relation between the lateral deflection of the tire center line or equator at the forward edge of the ground-contact area y_1 and the coordinates η, γ, and θ. Next, a kinematic relation between the lateral deflections of the tire equator at the center and forward edge of the ground-contact area (designated y_0 and y_1, respectively) is established. These two relations are combined to obtain a basic kinematic equation correlating y_0 with η, γ, and θ.

The derivation of these kinematic relations is based upon the following physical concept: As a tire moves forward, the tire material on the circumference just ahead of the ground-contact area is laid down or developed on the ground without skidding and becomes the new forward portion of the ground-contact area, so that the track of the tire is completely determined by the lateral-distortion coordinate of the foremost ground-contact point y_1 and the slope of the distorted center line or equator of the tire at that point.

GEOMETRIC RELATIONS

The primary geometric quantities involved in the problem of a rolling tire are shown in figure 1, which gives an instantaneous view of a distorted tire with respect to an arbitrary space-fixed XYZ coordinate system, the X-axis being horizontal and parallel to the mean direction of wheel motion, the Z-axis being perpendicular to the ground, and the Y-axis being perpendicular to the X- and Z-axes. Parts (a) and (b) of this figure represent side and bottom views,

respectively, of a rolling wheel that is swiveled and tilted. For the sake of clarity, part (c) of this figure, which shows an end view of the rolling tire, has been drawn to a different scale from part (b) and represents the unswiveled condition. In discussing the geometric quantities, the following terminology and symbols are used: The wheel center plane is the plane of symmetry of the wheel perpendicular to the wheel axle. The tire center line or equator comprises the tire points which on the undistorted tire are located at the intersection of the tire outer circumference with the wheel center plane; under the action of moments and lateral forces these tire points are deflected laterally by an amount λ with respect to the wheel center plane. The symbol λ_f designates the lateral deflection of tire equator points which are not in contact with the ground and λ_g designates the lateral deflection of points which are in contact with the ground. The point at the center of the ground-contact area is designated by λ_0.

The lateral distance of the wheel plane from an arbitrary space-fixed XZ-plane is designated by η_f for points off the ground at a vertical height z and by η_g for points on the ground. The lateral distances of tire-equator points from this XZ-plane are similarly designated by y_f and y_g. The difference between y and η is the lateral distortion λ of the tire, or

$$\lambda_f=y_f-\eta_f \tag{1}$$

and

$$\lambda_g=y_g-\eta_g \tag{2}$$

The tire contacts the ground in a finite area having a finite width and a length $2h$. The width of this area is assumed to be negligibly small; that is, the ground-contact area is assumed to be reduced to a ground-contact line. The foremost ground-contact point (in the direction of motion) is designated by the subscript 1, the rearmost point by the subscript 2, and the center point by the subscript 0. Except for braking and accelerating effects, the center point 0 has approximately the same horizontal x-coordinate as the wheel axle.

Distances about the tire equator or circumference are measured in terms of the circumferential coordinate s whose origin is taken at the point 0.

The wheel is assumed to move at constant velocity v approximately in the direction of the X-axis. The wheel is laterally inclined with respect to the vertical Z-axis by the tilt angle γ and is swiveled with respect to the XZ-plane by the swivel angle θ. Both tilt and swivel angles are assumed to be small; that is, $\cos\theta\approx\cos\gamma\approx1$, $\sin\theta\approx\theta$, and $\sin\gamma\approx\gamma$.

The center point of the wheel axle is located at a vertical distance r_3 from the XY (ground) plane, a lateral distance $r_3\gamma$ from the intersection of the wheel plane and the XY-plane, and a lateral distance η_3 from the XZ-plane, where

$$\eta_3=\eta_0-r_3\gamma \tag{3}$$

TIRE DISTORTION

This section contains a short discussion of the features of tire distortion which are pertinent to the derivation of the basic kinematic relations of this report.

Experimental and theoretical considerations (for example, see refs. 3 and 2, respectively) indicate that, if the tire equator in the ground-contact region is subjected to arbitrary lateral distortion, the lateral distortion of the tire equator off the ground λ_f tends to die out as an exponentially decaying function of the circumferential displacement s (for example, see fig. 2(a)). Thus, near tire point 1 off the ground the tire distortion will tend to approach the pattern described by the equation

$$\lambda_f=\lambda_1 e^{-\frac{s-h}{L}} \tag{4}$$

and a similar equation will apply near tire point 2. The exponential constant L is a tire characteristic having the dimension of length and is called the relaxation length. The relaxation length near point 2 is not necessarily exactly the same as that near point 1; however, since the former relaxation length will not be used in this report in any critical calculations, this difference will not be taken into account.

In regard to the accuracy of equation (4) very near point 1, it should be emphasized that this exponential variation is only an expression of the equilibrium condition which the tire-equator distortion would reach in the absence of any restraints. However, it is obvious that conditions exist for which this distortion curve cannot be completely exponential in form. For example, for the case of pure lateral deflection of a stationary tire, the tire equator in the ground-contact zone is (neglecting skidding) a straight line parallel to the wheel center plane and extending from point 1 to point 2 (see solid lines in fig. 2 (b)). Consequently, the existence of an exponential curve just to the right of point 1, and including point 1, would imply the existence of a sharp bend in the tire at point 1 such as is indicated in figure 2 (a). Since a sharp bend is impossible because of finite tire stiffness, it follows that, in general, on a stationary tire the exponential variation given by equation (4) cannot be valid close to point 1. However, experimental evidence indicates that beyond a short transition region ahead of point 1 the tire-equator distortion curve does have an essentially exponential character (see solid lines in fig. 2 (b)). As the wheel rolls ahead the nonexponential transition region of the tire equator is laid down or developed on the ground as it passes into the ground-contact zone, and the more nearly exponential part of the equator curve moves down toward the ground (see dashed lines in fig. 2 (b)) and is eventually developed on the ground, so that after rolling a short distance from rest and during normal rolling conditions (fig. 2 (c)) the tire-equator distortion at the front end of the tire can approach the assumed exponential variation of equation (4).

At the rear end of the tire the equator distortion curve during rolling does not so closely approximate an exponential variation, since at the rear end there is no process of laying down or development such as is responsible for the exponential variation at the front end. However, since the rearward section of the tire equator is not used in any critical calculations in this report, its equator curve is also, for simplicity, assumed to be exponential.

If equation (4) is accepted as the basic equation for

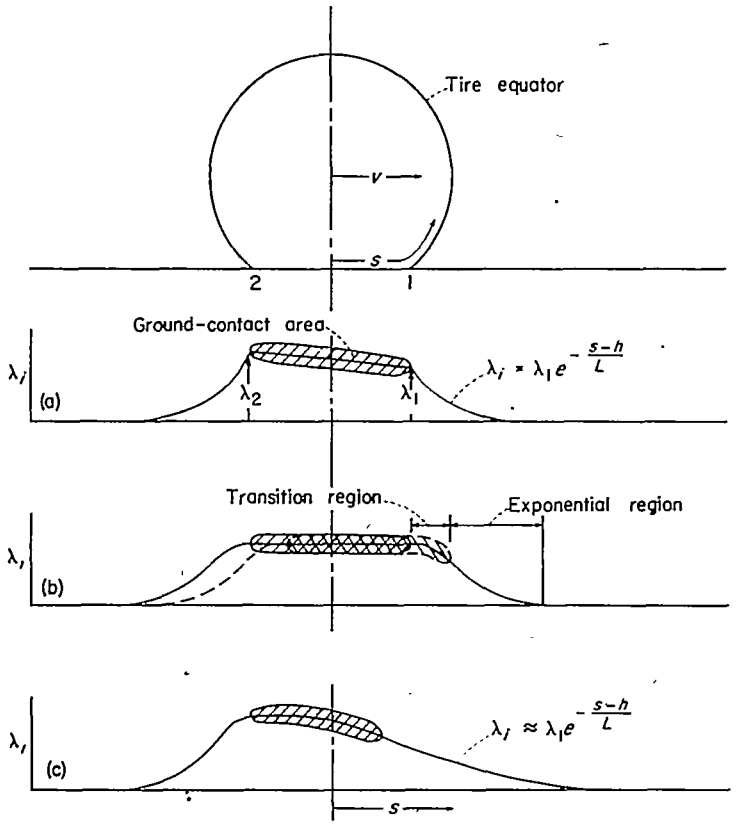

(a) Assumed theoretical shape of tire equator distortion for a stationary twisted tire. $v=0$.

(b) Actual shape of tire equator distortion for an untwisted tire at rest (solid lines) and just after starting to roll (dashed lines).

(c) Actual shape of tire equator distortion for a rolling tire.

FIGURE 2.—Tire equator distortion.

tire-equator lateral distortion near point 1 under rolling conditions, the total lateral displacement of the tire from the XZ-plane in this region can, by use of equation (1), be written in the form

$$y_i=\eta_i+\lambda_1 e^{-\frac{s-h}{L}} \tag{5}$$

Substituting the geometric relation $\eta_i=\eta_g-\gamma z$ (see fig. 1) into equation (5) gives

$$y_i=\eta_g-\gamma z+\lambda_1 e^{-\frac{s-h}{L}} \tag{6}$$

KINEMATIC EQUATION

By making use of the physical concepts discussed previously, together with equation (6), it is now possible to establish as follows the basic differential equation relating the tire deflection at the center of the ground-contact area y_0 with the wheel coordinates η, θ, and γ.

There is assumed to be perfect adhesion between tire and ground, that is, no skidding. As the tire rolls forward (arbitrarily swiveling, tilting, and moving laterally) a distance dx, a new element of the tire of circumferential length ds above and in front of point 1 is laid down or developed on the ground. This tire element, before being laid down on the ground, had the lateral-distortion variation given by equation (6). This equation, after differentiation with respect to s, yields for a given instantaneous position of the tire the following rate of change of distortion:

$$\frac{dy_i}{ds}=\frac{d\eta_g}{ds}-\gamma\frac{dz}{ds}-\frac{1}{L}\lambda_1 e^{-\frac{s-h}{L}} \tag{7}$$

At point 1, where $s=h$ and $y_i=y_1$:

$$\left(\frac{dy_i}{ds}\right)_1=\left(\frac{d\eta_g}{ds}\right)_1-\gamma\left(\frac{dz}{ds}\right)_1-\frac{1}{L}\lambda_1 \tag{8}$$

The term $\left(\frac{dz}{ds}\right)_1$ is simply the sine of the angle between the ground and the tire equator at point 1. (See fig. 1.) Just to the left of point 1 the tire is flattened on the ground, or $\frac{dz}{ds}=0$. If $\left(\frac{dz}{ds}\right)_1$ were not zero, the tire would have to have a sharp bend at point 1. However, because of the finite bending stiffness of an actual tire, a sharp bend is impossible; thus $\left(\frac{dz}{ds}\right)_1=0$ and equation (8) reduces to

$$\left(\frac{dy_i}{ds}\right)_1=\left(\frac{d\eta_g}{ds}\right)_1-\frac{1}{L}\lambda_1 \tag{9}$$

Further, since $\left(\frac{dz}{ds}\right)_1=0$, s is a horizontal coordinate near point 1. The rate of change of wheel lateral displacement η_g with respect to the horizontal coordinate x at any given instant is just the swivel angle θ; hence

$$\left(\frac{dy_i}{ds}\right)_1=\theta-\frac{1}{L}\lambda_1 \tag{10}$$

If the tire is assumed to have no sharp bend at point 1, $\left(\frac{dy_i}{ds}\right)_1=\left(\frac{dy_g}{ds}\right)_1$ at this point. Then, since $\left(\frac{dy_g}{ds}\right)_1$ is the slope of the tire equator on the ground at point 1 and since no skidding is assumed to exist, this slope must coincide with the track of the rolling tire on the ground, which is $\frac{dy_1}{dx}$. Thus,

$$\frac{dy_1}{dx}=\theta-\frac{1}{L}\lambda_1$$

or, if differentiation with respect to x is designated by the operator $D=\frac{d}{dx}$ and the terms are rearranged,

$$L\,Dy_1=L\theta-\lambda_1 \tag{11}$$

(Alternate derivations of this equation are presented in refs. 3 and 4.) A slightly more convenient form of equation (11) is obtained by substitution of the geometric relations $\lambda_1=y_1-\eta_1$ and $\eta_1=\eta_0+h\theta$ (see fig. 1) to give

$$(1+L\,D)y_1=\eta_0+(L+h)\theta \tag{12}$$

Equation (12) is the basic equation for y_1 previously obtained by Von Schlippe and Dietrich (refs. 3 and 4). It should be noted, however, that no tilt terms appear in the equation. Although it is not known whether the effect of tilt on the validity of equation (12) is important, in view of the present lack of a reliable method for taking this tilt effect into account, the following argument is presented to afford at least a crude approach to the problem.

Equation (8) contains the tilt term $\gamma\left(\frac{dz}{ds}\right)_1$ which was set equal to zero on the grounds that the factor $\left(\frac{dz}{ds}\right)_1$ is zero because of the finite bending stiffness of the tire. (See fig. 1.) On the other hand, if it is assumed that the bending stiffness of the tire is zero and if radial tire distortion is neglected, $\left(\frac{dz}{ds}\right)_1$ will be equal to h/r and the tilt term $\gamma h/r$ will enter into equations (9) to (12). As a somewhat questionable approximation, it will now be assumed that a term of this type, but smaller by the reduction factor $\xi<1$, should appear in the differential equations (9) to (12). Equation (12) then becomes

$$(1+L\,D)y_1=\eta_0+\theta(L+h)-\frac{\xi hL}{r}\gamma \tag{13}$$

A similar tilt term was derived by Greidanus (ref. 7) on the basis of a slightly different argument. (Greidanus' term is discussed in a subsequent section of this report.) However, apparently no other detailed tire-motion theory has included such a term.

Equation (13) is the fundamental kinematic relation for tire point 1. The kinematic relations for points 0 and 2 are determined by the condition of perfect adhesion between tire and ground. During the rolling process each tire circumferential element first contacts the ground at point 1, later proceeds to point 0 and then to point 2, after which it leaves the ground. Consequently, with perfect adhesion each tire element at point 2 has the same lateral deflection that it had when it entered the contact zone at point 1 a distance $2h$ ago; that is,

$$y_2(x)=y_1(x-2h) \tag{14}$$

Similarly the kinematic relation for point 0 is

$$y_0(x)=y_1(x-h)$$

or

$$y_1(x)=y_0(x+h) \tag{15}$$

Finally, by combining equations (13), (15), and (3) the equation

$$[1+L\,D]y_0(x+h)=\eta_0(x)+[L+h]\theta(x)-\frac{\xi hL}{r}\gamma(x)$$

$$=\eta_3(x)+[L+h]\theta(x)+\left[r_3-\frac{\xi hL}{r}\right]\gamma(x) \tag{16}$$

is obtained. This is the basic kinematic equation correlating the tire lateral deflection y_0 under rolling conditions with the swivel angle θ, the wheel lateral displacement η_0 or η_3, and the lateral tilt γ for arbitrarily applied variations of θ, η_0 or η_3, and γ. However, this transcendental form of the kinematic equation is not the most convenient form for some purposes in this report. In particular it is expedient to remove the transcendental expression from equation (16) by use of a series expansion.

SERIES EXPANSION OF KINEMATIC EQUATION

The expression $y_0(x+h)$, after expansion in a Taylor series, gives

$$y_0\,(x+h)=y_0\,(x)+h\,Dy_0\,(x)+\frac{h^2}{2}\,D^2y_0\,(x)+\ldots$$

$$=y_0\,(x)+\sum_{n=1}^{\infty}\frac{h^n}{n!}\,D^ny_0(x) \tag{17a}$$

where the operator D^n represents $\frac{d^n}{dx^n}$. An alternative form of equation (17a) which is useful later is

$$y_0\,(x+h)=e^{hD}y_0\,(x) \tag{17b}$$

since the infinite series in hD is the series expansion of the exponential function. A third useful form of this equation is obtained by expressing equation (17b) in terms of a time derivative D_t instead of the space derivative D. Since it is assumed throughout this report that the rolling velocity v is constant, the correlation between these two derivatives is given by the equation

$$D_t(\ )=\frac{d(\ )}{dt}=\frac{dx}{dt}\frac{d(\ )}{dx}=v\frac{d(\ )}{dx}=v\,D(\ )$$

and hence equation (17b) can also be written in the form

$$y_0(x+h)=e^{hv^{-1}D_t}y_0(x) \tag{17c}$$

Differentiation of equations (17) gives the result

$$Dy_0(x+h)=Dy_0(x)+h\,D^2y_0(x)+\frac{1}{2}\,h^2D^3y_0(x)+\ldots$$

$$=\sum_{n=1}^{\infty}\frac{h^{n-1}}{(n-1)!}\,D^ny_0(x) \tag{18a}$$

or

$$Dy_0(x+h)=De^{hD}y_0(x)=v^{-1}D_te^{hv^{-1}D_t}y_0(x) \tag{18b}$$

Substitution of equations (17) and (18) into equation (16) gives after rearrangement, with $y_0(x)$ written simply as y_0 and similar treatment of η_0, η_3, θ, and γ:

$$\eta_0+l_1\theta-\frac{\xi Lh}{r}\gamma=\eta_3+l_1\theta+\left(r_3-\frac{\xi Lh}{r}\right)\gamma$$

$$=(1+l_1\,D+l_2\,D^2+\ldots)y_0$$

$$=\left(1+\sum_{n=1}^{\infty}l_n\,D^n\right)y_0 \tag{19a}$$

where

$$l_1=L+h$$

$$l_2=(2L+h)\frac{h}{2}$$

$$l_n=(nL+h)\frac{h^{n-1}}{n!}$$

or

$$\eta_0+l_1\theta-\frac{\xi Lh}{r}\gamma=\eta_3+l_1\theta+\left(r_3-\frac{\xi Lh}{r}\right)\gamma$$
$$=(1+LD)e^{hD}y_0$$
$$=(1+Lv^{-1}D_t)\,e^{hv^{-1}D_t}y_0 \qquad (19b)$$

Equations (19a) and (19b) are alternative forms of the basic kinematic equation (16) which are useful in subsequent sections of this report.

This concludes the derivation and discussion of the basic kinematic equation correlating the lateral tire deflection y_0 with the wheel coordinates θ, η_0, and γ. Next, attention will be directed to the relationships existing between these coordinates and the forces and moments acting on the wheel.

FORCES AND MOMENTS ON THE WHEEL

In this section the primary forces and moments acting on a rolling wheel are discussed and, where possible, equations are set down for these quantities. These equations are then utilized in later sections, together with the preceding kinematic equation, to establish the equations of motion for a rolling wheel.

The forces and moments considered fall into five general categories: elastic forces and moments due to tire distortion, gyroscopic moments, tire inertia forces and moments, hysteresis forces and moments, and structural forces and moments.

Throughout this discussion, forces along the coordinate axes are considered positive if they tend to move the wheel in the positive directions of the coordinate axes; moments about the coordinate axes X, Y, and Z or other parallel axes are considered positive if they tend to produce wheel rotation from the positive Y-axis toward the positive Z-axis, from the positive Z-axis toward the positive X-axis, and from the positive X-axis toward the positive Y-axis, respectively.

ELASTIC FORCES AND MOMENTS DUE TO TIRE DISTORTION

LATERAL ELASTIC FORCE

The lateral elasticity properties of a tire will be considered first. If a static untilted tire is laterally deflected at its base with respect to its rim by a lateral force $F_{y\lambda}$, it produces an equal spring reaction force roughly proportional to the mean lateral distortion λ_{mean}, or, inversely, a lateral tire distortion λ_{mean} creates a proportional ground force $F_{y\lambda}$. If the lateral distortion of the center of the ground-contact line λ_0 is taken as the mean distortion, then the elastic ground force is

$$F_{y\lambda}=K_\lambda\lambda_0=K_\lambda(y_0-\eta_0)=K_\lambda(y_0-\eta_3-r_3\gamma) \qquad (20)$$

where K_λ is the lateral spring constant or side stiffness of the tire. This relation is used by most investigators. However, in references 2 to 5 a slightly different expression is used. In these references the mean lateral distortion of the tire is defined as the average of the distortions at the leading-edge and trailing-edge points of the ground-contact area (points 1 and 2). The resulting equation for $F_{y\lambda}$ is

$$F_{y\lambda}=\frac{1}{2}K_\lambda(\lambda_1+\lambda_2) \qquad (21)$$

instead of equation (20). The true equation for $F_{y\lambda}$ is probably more complicated than either of these two equations; however, since no plausible means of obtaining a better equation is available, it appears advisable to select one of the above equations for use in this report. Equation (21) may be slightly the better equation for a few special cases of wheel motion, but equation (20) is much simpler to work with, and in most cases of wheel motion it makes little difference which of the two equations is used. Therefore, for the sake of simplicity equation (20) is adopted hereinafter as the basic equation for the lateral force on a wheel due to lateral deformation of the tire.

TORSIONAL ELASTIC MOMENT

The torsional elasticity properties of a tire will be considered next. If a tire is twisted on the ground about a vertical axis through an angle α, there arises a restoring ground moment that is roughly linearly proportional to the twist:

$$M_{z\alpha}=K_\alpha\alpha \qquad (22)$$

The tire twist α is equal to the mean angle between the track of the tire on the ground and the wheel plane; that is, $\alpha=Dy_{mean}-\theta$. Taking the value of Dy_{mean} as Dy_0 gives

$$\alpha=Dy_0-\theta \qquad (23)$$

and thus

$$M_{z\alpha}=K_\alpha(Dy_0-\theta)=K_\alpha(v^{-1}D_ty_0-\theta) \qquad (24)$$

Most investigators of tire motion use this relation. However, in references 2 to 5 the mean angle is taken equal to $(\lambda_1-\lambda_2)/2h$ and thus the moment equation

$$M_{z\alpha}=\frac{K_\alpha}{2h}(\lambda_1-\lambda_2) \qquad (25)$$

is obtained, which leads to relatively more complicated equations of motion than does equation (24). Since there is no strong reason for believing equation (25) to be a significant improvement over the simpler equation (24), the latter is used in the analysis of this report.

Melzer (ref. 10) has used the less accurate relation that the moment due to tire twist is

$$M_{z\alpha}=-K_\alpha\theta \qquad (26)$$

which implies the relation $\theta\gg Dy_0$. (See eq. (24).) Since this relation is not true in all practical cases, Melzer's theory should be viewed with some caution.

TILT ELASTIC FORCE

If a tire is tilted from the vertical Z-axis by an angle γ

without lateral distortion of the equator ($\lambda_0=0$), there arises a restoring ground lateral force that is approximately linearly proportional to the tilt angle (e. g., see ref. 2);

$$F_{y\gamma}=-K_\gamma\gamma \tag{27}$$

where K_γ is the constant of proportionality. Most authors (excepting Rotta in ref. 2) have not considered the effects of this force term although they have considered other effects of the same order of magnitude.

VERTICAL-LOAD CENTER OF PRESSURE

Under some circumstances the vertical load F_z influences the wheel motion. In order to consider this influence it is necessary to know the location of the center of pressure of this force. In the XZ-plane (fig. 1) this center of pressure lies approximately below the wheel axle in line with the point 0. In the YZ-plane the center of pressure is shifted laterally from the intersection of wheel plane and ground η_0 as a result of lateral distortion λ_0 and tilt γ. As a first approximation, this shift may be taken as linearly dependent on λ_0 and γ so that the lateral distance c of the center of pressure from the XZ-plane becomes

$$\begin{aligned} c&=\eta_0+c_\lambda\lambda_0-c_\gamma\gamma \\ &=c_\lambda y_0+(1-c_\lambda)\eta_0-c_\gamma\gamma \\ &=c_\lambda y_0+(1-c_\lambda)\eta_3+[(1-c_\lambda)r_3-c_\gamma]\gamma \end{aligned} \tag{28}$$

where c_λ and c_γ are constants. (The signs of the terms are chosen so that c_λ and c_γ are positive numbers.)

GYROSCOPIC MOMENTS

GYROSCOPIC MOMENT DUE TO LATERAL DISTORTION OF TIRE

The origin of gyroscopic moments on a rolling untilted wheel with lateral distortion of the tire at the ground (fig. 3) is considered next. While the solid rim and axle parts of the wheel are untilted, lateral deformation of the elastic tire causes the tire, on the average, to be tilted with respect to the wheel center plane by an amount $\gamma_\lambda=\frac{\lambda_0\tau_1}{r+r_3}$, where r is the tire radius and τ_1 is a correction factor which indicates the effective fraction of the total tire mass that is tilted at this angle. Kantrowitz (ref. 8), apparently the only investigator who has considered this at least theoretically significant factor, has suggested that $\tau_1\approx 1/2$. This tilting action produces an angular velocity $D_t\gamma_\lambda=\frac{D_t\lambda_0\tau_1}{r+r_3}$, where D_t indicates differentiation with respect to time. This angular velocity, together with the rotational velocity of the tire ω, produces a gyroscopic moment about the Z-axis of magnitude

$$M_{z\lambda}=-I_{yt}\omega\, D_t\gamma_\lambda \tag{29}$$

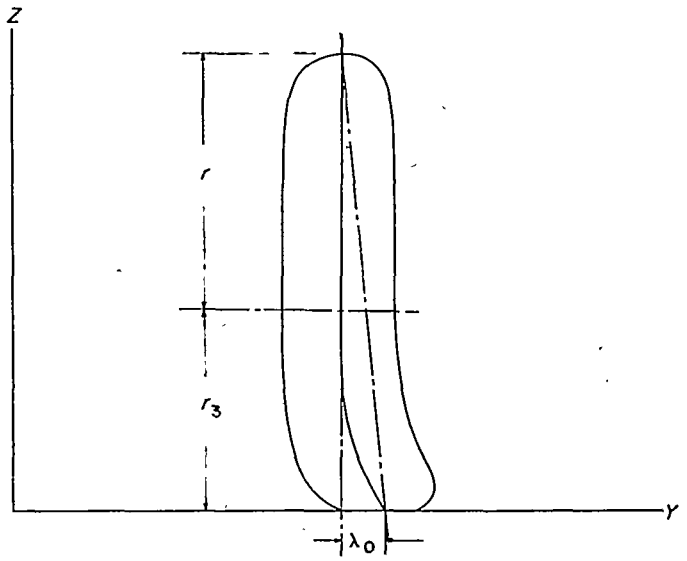

FIGURE 3.—Effective tire tilt due to lateral distortion of tire.

where I_{yt} is the moment of inertia of the tire (excluding the solid rim and axle) about the wheel axle. By using the relation $D_t(\ )=v\,D(\ )$, equation (29) can also be expressed in the form

$$M_{z\lambda}=-I_{yt}v^2\frac{\omega}{v}D\gamma_\lambda \tag{30}$$

where the ratio v/ω is, to a good enough approximation for this secondary term, equal to the tire radius r. Then, substituting for γ_λ and ω/v in equation (30) gives

$$M_{z\lambda}=-\frac{\tau_1 I_{yt}v^2}{r(r+r_3)}D\lambda_0 \tag{31}$$

For later convenience, the result can be expressed in several alternate abbreviated forms:

$$M_{z\lambda}=-\tau v^2 D\lambda_0=-\tau v^2 D(y_0-\eta_0)=-\tau v\,D_t(y_0-\eta_3-r_3\gamma) \tag{32}$$

where

$$\tau=\frac{\tau_1 I_{yt}}{r(r+r_3)} \tag{33}$$

Another method for deriving an expression for τ is discussed in a subsequent section.

GYROSCOPIC MOMENT DUE TO TILTING OF WHEEL

If the entire wheel structure tilts at an angular velocity $D_t\gamma$, another gyroscopic moment arises of magnitude

$$M_{z\gamma}=-I_{yw}\omega\, D_t\gamma\approx-\frac{I_{yw}v}{r}D_t\gamma \tag{34}$$

in addition to the term of equation (29). Here I_{yw} is the total polar moment of inertia of the wheel (including the tire) about its axle.

GYROSCOPIC MOMENT DUE TO SWIVELING OF WHEEL

If the wheel swivels at an angular velocity $D_t\theta$, a tilting gyroscopic moment also arises of magnitude

$$M_{x\theta}=-I_{yw}\omega\, D_t\theta\approx-\frac{I_{yw}v}{r}D_t\theta \tag{35}$$

TIRE INERTIA FORCES AND MOMENTS

This section is concerned with an examination of the influence of tire inertia forces and moments on a wheel rolling at high speeds. Two types of such inertia effects are evaluated now in separate sections: inertia forces and moments associated with lateral distortion and twisting of the tire, and centrifugal forces and moments. Then the overall effects of these two types of inertia forces and moments are considered in another section.

INERTIA FORCES AND MOMENTS DUE TO LATERAL DISTORTION OF TIRE

At high rolling or shimmy velocities, tire inertia forces and moments arise which are proportional to the relative accelerations of the different parts of the tire (including the previously discussed gyroscopic moment due to tire lateral distortion, discussed here from a slightly different point of view). A rough estimate of these forces and moments can be made as follows: One-third of the total mass of the tire m_t is assumed to be located on the periphery of the tire and to be subjected to the same accelerations with respect to the wheel hub as are tire particles on the equator line, while the remaining tire mass is assumed to be substantially undisturbed. The "active" mass of the tire per unit circumferential length is then $m_t/6\pi r$. The lateral acceleration of tire particles on the right-hand side of the tire and off the ground in figure 1(a) will be considered first. The lateral distortion of the tire in this region is given by equation (4). The lateral relative velocity of a tire particle, obtained by differentiating this quantity with respect to time, is

$$D_t\lambda_t=\left(D_t\lambda_1-\frac{\lambda_1}{L}D_t s\right)e^{-\frac{s-h}{L}}$$

The quantity $D_t s$, which represents the peripheral velocity of tire particles with respect to the wheel axle, is approximately equal to the negative of the rolling velocity v, so that the velocity expression becomes

$$D_t\lambda_t=\left(D_t\lambda_t+\frac{v}{L}\lambda_1\right)e^{-\frac{s-h}{L}}$$

Differentiation of this result to give the relative acceleration of the tire particles yields the result

$$D_t^2\lambda_t=\left(D_t^2\lambda_1+\frac{2v}{L}D_t\lambda_1+\frac{v^2}{L^2}\lambda_1\right)e^{-\frac{s-h}{L}}$$

The corresponding inertia force ΔF for this part of the tire is obtained by integrating the product of this acceleration and the active mass per unit length to obtain the force term $-\frac{m_t}{6\pi r}\int_{s=h}^{s\approx\pi r}D_t^2\lambda_t\,ds$. Evaluation of this integral, after replacing the upper limit by infinity for simplification of the result (which introduces no significant error because of the rapidly decaying exponential function in $D_t^2\lambda_t$), yields

$$\Delta F=-\frac{m_tL}{6\pi r}\left(D_t^2\lambda_1+\frac{2v}{L}D_t\lambda_1+\frac{v^2}{L^2}\lambda_1\right) \tag{36}$$

The corresponding inertia moment ΔM is given by the expression

$$-\frac{m_t}{6\pi r}\int_{s=h}^{s\approx\pi r}r\sin\varphi\, D_t^2\lambda_t\,ds$$

where $r\sin\varphi$ is the moment arm (see fig. 1 (a)), s is related to φ by the relation $s-h=r(\varphi-\varphi_1)$, and $\varphi_1=\sin^{-1}\frac{h}{r}$. Therefore, the moment integral may be written in terms of φ in the form

$$\Delta M=-\frac{m_t}{6\pi r}\int_{\varphi_1}^{\pi}r\sin\varphi\left(D_t^2\lambda_1+\frac{2v}{L}D_t\lambda_1+\frac{v^2}{L^2}\lambda_1\right)e^{\frac{r(\varphi-\varphi_1)}{L}}r\,d\varphi$$

Evaluation of this integral, after replacing the upper limit by infinity (which introduces no appreciable error), yields the expression

$$\Delta M=-\frac{m_trL\left(h+L\sqrt{1-\frac{h^2}{r^2}}\right)}{6\pi(L^2+r^2)}\left(D_t^2\lambda_1+\frac{2v}{L}D_t\lambda_1+\frac{v^2}{L^2}\lambda_1\right) \tag{37}$$

In a similar manner, for tire particles off the ground on the left-hand side of the tire in figure 1(a), the following expressions are obtained for the inertia force and moment:

$$\Delta F=-\frac{m_tL}{6\pi r}\left(D_t^2\lambda_2-\frac{2v}{L}D_t\lambda_2+\frac{v^2}{L^2}\lambda_2\right) \tag{38}$$

$$\Delta M=\frac{m_trL\left(h+L\sqrt{1-\frac{h^2}{r^2}}\right)}{6\pi(L^2+r^2)}\left(D_t^2\lambda_2-\frac{2v}{L}D_t\lambda_2+\frac{v^2}{L^2}\lambda_2\right) \tag{39}$$

In these two expressions it is assumed, for reasons previously discussed, that the relaxation length L is the same for both sides of the tire.

In obtaining the inertia forces and moments for tire particles in the ground-contact area, it is recognized that in practically all cases where inertia forces are important the ground-contact line is almost a straight line, so that the lateral distortion for tire particles in this region can be expressed fairly well by the equation

$$\lambda_s=\lambda_0+s\alpha$$

The corresponding velocity and acceleration are

$$D_t\lambda_s=D_t\lambda_0+s\,D_t\alpha-v\alpha$$

$$D_t^2\lambda_s=D_t^2\lambda_0+s\,D_t^2\alpha-2v\,D_t\alpha$$

The total inertia force for this region is then

$$\Delta F=-\frac{m_t}{6\pi r}\int_{s=-h}^{s=h}D_t^2\lambda_s\,ds$$

$$=-\frac{m_t h}{3\pi r}(D_t^2\lambda_0-2v\,D_t\alpha) \tag{40}$$

and the inertia moment is

$$\Delta M=-\frac{m_t}{6\pi r}\int_{s=-h}^{s=h}s\,D_t^2\lambda_s\,ds$$

$$=-\frac{m_t h^3}{9\pi r}D_t^2\alpha \tag{41}$$

The total inertia force F_{yt}, obtained by summing the force terms in equations (36), (38), and (40), can be stated conveniently in terms of λ_0 and α by using the relations $\lambda_1+\lambda_2=2\lambda_0$ and $\lambda_1-\lambda_2=2h\alpha$, which are valid for a substantially straight ground-contact line. The result is

$$F_{yt}=-\frac{m_t}{3\pi r}\left(l_1\,D_t^2\lambda_0+\frac{v^2}{L}\lambda_0\right) \tag{42}$$

where $l_1=L+h$. Similarly, the total inertia moment is

$$M_{zt}=-\frac{m_t}{3\pi}\left\{\left[\frac{rhL\left(h+L\sqrt{1-\frac{h^2}{r^2}}\right)}{L^2+r^2}+\frac{h^3}{3r}\right]D_t^2\alpha+\right.$$

$$\left.\frac{r\left(h+L\sqrt{1-\frac{h^2}{r^2}}\right)}{L^2+r^2}\left(2v\,D_t\lambda_0+\frac{hv^2}{L}\alpha\right)\right\} \tag{43}$$

The significance of these inertia expressions will now be partly evaluated by considering the inertia force for sinusoidal oscillations; that is, where $\lambda_0=\lambda_{0_{max}}\sin\nu t$ and therefore $D_t^2\lambda_0=-\nu^2\lambda_0$, so that equation (42) may be restated as

$$F_{yt}=-\frac{m_t}{3\pi r}\left(\frac{v^2}{L}-l_1\nu^2\right)\lambda_0 \tag{44}$$

(An equation similar to eq. (44) has been derived by Marstrand in ref. 20. Marstrand's equation, however, is based on a cruder representation of the shape of the lateral distortion of the tire.)

In order to interpret the significance of the inertia force it is noted that the tire force quantity which is of importance for the subsequent analysis is the net tire force F_{yn} acting on the wheel, which is equal to the sum of the ground force $F_{y\lambda}$ and the inertia force F_{yt}:

$$F_{yn}=F_{y\lambda}+F_{yt} \tag{45}$$

For a static tire, $F_{y\lambda}$ was set equal to $K_\lambda\lambda_0$ (eq. (20)). In the dynamic case the relation between ground force and lateral distortion of the tire may be modified by the inertia effect. As a first approximation, it will be assumed that the modification of the ground force is proportional to the inertia force, or

$$F_{y\lambda}=K_\lambda\lambda_0-\eta_y F_{yt} \tag{46}$$

where η_y is a number whose absolute value will be less than unity if the modification of the ground force due to the inertia force is less than the inertia force itself.

After combining equations (44), (45), and (46), the following equation for the net tire force F_{yn} is obtained:

$$F_{yn}=F_{y\lambda}+F_{yt}=\left[K_\lambda-(1-\eta_y)\frac{m_t}{3\pi r}\left(\frac{v^2}{L}-l_1\nu^2\right)\right]\lambda_0 \tag{47}$$

From the form of equation (47) it can be seen that, insofar as the ratio of net tire force to lateral deformation is concerned, the effect of the inertia force can be considered equivalent to a change in tire lateral stiffness ΔK_{λ_t} equal to

$$\Delta K_{\lambda_t}=-(1-\eta_y)\frac{m_t}{3\pi r}\left(\frac{v^2}{L}-l_1\nu^2\right) \tag{48}$$

Similarly, from an examination of the terms containing α in the inertia moment equation (43), it can be concluded that part of the effect of this inertia moment is to change the tire torsional stiffness by an amount ΔK_{α_t}, which is defined by

$$\Delta K_{\alpha_t}=-\frac{(1-\eta_z)m_t}{3\pi}\left[\frac{rh\left(h+L\sqrt{1-\frac{h^2}{r^2}}\right)}{L^2+r^2}\left(\frac{v^2}{L}-L\nu^2\right)-\frac{h^3\nu^2}{3r}\right] \tag{49}$$

where η_z is a number representing the torsional stiffness similar to η_y for the lateral stiffness. The remaining inertia-moment term in equation (43), which is proportional to $D_t\lambda_0$, is simply the previously discusssed gyroscopic moment due to lateral tire distortion. By comparing this term with equation (32) it is seen that the coefficient τ may be expressed by the equation

$$\tau=\frac{2m_t r\left(h+L\sqrt{1-\frac{h^2}{r^2}}\right)}{3\pi(L^2+r^2)} \tag{50}$$

Equation (50) gives approximately the same result as equation (33) with Kantrowitz' assumption that $\tau_1\approx\frac{1}{2}$. The discussion of the velocity range in which these stiffness changes are important is postponed until after the effects of centrifugal forces have been considered.

EFFECTS OF CENTRIFUGAL FORCES

Another inertia effect that may become significant at high speeds is produced by the centrifugal forces acting on the individual mass elements of the tire. These centrifugal forces appear to increase the tire stiffness, as will be demonstrated by a crude analysis which gives a qualitative idea of this effect but which should not be regarded as possessing any strong quantitative merit.

For the purpose of this estimate, one-half the mass of the tire is assumed to be concentrated in the side walls and the

other half is assumed to be concentrated on the periphery.

If the tire lateral and torsional stiffnesses K_λ and K_α are assumed to be directly proportional to the tension in the side walls of the tire, there will be two sources of tire stiffness: inflation pressure, which produces a side-wall tension approximately equal to wp per unit circumferential distance (where w is the tire width), and centrifugal force, which produces the side-wall tension $\left(\frac{1}{2}\right)\left(\frac{m_t}{2\pi r}\right)\left(\frac{v^2}{r}\right)$ corresponding to the peripheral tire mass $\frac{1}{2}m_t$. Thus the lateral stiffness of the tire may be expressed in the form

$$K_\lambda \propto 4\pi r^2 wp + m_t v^2$$

or, equivalently, as

$$K_\lambda = K_{\lambda_{static}}\left(1+\frac{m_t v^2}{4\pi r^2 wp}\right)$$

$$= K_{\lambda_{static}} + \frac{m_t v^2 K_{\lambda_{static}}}{4\pi r^2 wp}$$

It is evident from this equation that centrifugal force increases the tire lateral stiffness by an amount ΔK_{λ_j}:

$$\Delta K_{\lambda_j} = \frac{m_t v^2 K_{\lambda_{static}}}{4\pi r^2 wp} \tag{51}$$

and the torsional stiffness by an amount ΔK_{α_j}:

$$\Delta K_{\alpha_j} = \frac{m_t v^2 K_{\alpha_{static}}}{4\pi r^2 wp} \tag{52}$$

SIGNIFICANCE OF TIRE INERTIA EFFECTS WITH RESPECT TO TIRE STIFFNESS

The significance of the two just discussed tire inertia effects on the tire stiffness will now be considered.

For the lateral stiffness of a tire, the effective change ΔK_λ from the static value of K_λ is obtained by adding the two increments given by equations (48) and (51). The resulting effective overall change in tire lateral stiffness as a function of rolling speed and shimmy frequency is

$$\Delta K_\lambda = \frac{(1-\eta_y)m_t l_1 \nu^2}{3\pi r} - \frac{(1-\eta_y)m_t v^2}{3\pi r L} + \frac{m_t v^2 K_{\lambda_{static}}}{4\pi r^2 wp} \tag{53}$$

The first term, which involves the shimmy frequency, appears to be small enough in comparison with K_λ so that it can probably be neglected for most practical conditions. The last two terms have opposite signs if $\eta_y < 1$ and thus may represent two partly counterbalancing effects. The second term arises from the previous considerations of the lateral acceleration of tire particles and tends to reduce the effective lateral stiffness of the tire with increasing rolling velocity if $\eta_y < 1$. The last term arises from the previous considerations of centrifugal forces and tends to increase the lateral stiffness. These last two terms indicate that at high rolling speeds, if $\eta_y < 1$, the tire stiffness may either drastically decrease or drastically increase, depending on which of the two terms is larger. However, both terms happen to be of the same order of magnitude and the derivations of both terms are based on concepts too crude to justify conclusions regarding which term is larger. Thus, the only conclusion that can be drawn is that at sufficiently high rolling speeds drastic changes in tire lateral stiffness may occur. Whether the stiffness increases or decreases can probably be settled only by experiment.

In order to give some quantitative measure of the velocity at which these inertia effects become significant, some calculations were made to determine the velocity at which the magnitude of the second term in equation (53) becomes equal to K_λ. By making use of the static tire data in reference 24 for several modern aircraft tires and assuming that $\eta_y = 0$, it was found that this velocity averaged approximately $400\sqrt{r}$ fps $\approx 270\sqrt{r}$ mph, where r is expressed in feet. Similar estimates for the velocity at which the third term in equation (53) becomes equal to K_λ yielded approximately this same velocity. Moreover, since this velocity is rather high compared with normal present-day landing speeds, the inertia effects on tire lateral stiffness considered here can probably usually be neglected.

For the torsional stiffness of a tire, the overall effective change in torsional stiffness ΔK_α due to tire inertia and centrifugal forces is obtained by adding the two increments given by equations (49) and (52). The result is

$$\Delta K_\alpha = -\frac{(1-\eta_z)m_t}{3\pi}\left[\frac{rh\left(h+L\sqrt{1-\frac{h^2}{r^2}}\right)}{L^2+r^2}\left(\frac{v^2}{L}-L\nu^2\right)-\frac{h^3\nu^2}{3r}\right]+ \frac{m_t v^2 K_{\alpha_{static}}}{4\pi r^2 wp} \tag{54}$$

This equation is parallel to equation (53) for the lateral stiffness, so that statements made previously concerning the lateral stiffness apply here also.

OTHER INERTIA EFFECTS

The preceding discussion suggests that the effects of tire inertia are to change tire stiffness at high speeds and to introduce a gyroscopic moment. However, it should be recognized that other inertia effects will come into play, probably at velocities close to those at which the previously mentioned inertia effects arise. For example, the basic kinematic equation depends on the assumption of an exponentially distorted tire-equator line corresponding to a definite "static" relaxation length. This assumption is valid (if it is valid at all) only when the elastic forces in the tire predominate over the inertia forces. Where inertia forces are strong in comparison with elastic forces, it is at least doubtful whether the relaxation length remains constant.

Although there are undoubtedly other effects of tire inertia in addition to the ones discussed here, it appears probable that the importance of many tire inertia effects can be assessed by means of the following summary statement: The major effects of tire inertia on the rolling motion appear to come into play at a velocity of an order of magnitude of $400\sqrt{r}$ fps $\approx 270\sqrt{r}$ mph where r is expressed in feet. For considerably smaller velocities, most inertia effects can probably be safely neglected; for velocities of this order of

magnitude or higher, many of the basic assumptions of this report, and of most other papers on this subject, may be subject to considerable error.

HYSTERESIS FORCES AND MOMENTS

In addition to the forces and moments previously discussed, certain damping forces and moments arise as a consequence of the sometimes considerable hysteresis losses which arise in the distortion of elastic tires. Apparently the only significant attempt to deal with this hysteresis problem is reported by Von Schlippe and Dietrich in reference 5.[2] This reference provides some valuable insight into the fundamental mechanism of the hysteresis process and presents an equation for the hysteresis moment acting about the swivel axis of a shimmying wheel. However, even though use of this hysteresis-moment equation leads to good agreement between theoretical and experimental stability boundaries for a limited amount of experimental data (as is shown subsequently in the present report), some parts of the analysis seem so unrealistic that it is questionable whether much confidence can be placed in the final results of reference 5. Apparently, the only other significant contribution to the hysteresis problem is provided by the analysis of Moreland in references 11 and 12. In these references tire hysteresis forces as such are not considered, but the idea is introduced that a tire possesses a characteristic time-lag constant. In a subsequent section of the present report it is shown that this time-lag constant may be, at least in part, a consequence of hysteresis effects. However, the interpretation of Moreland's time-lag constant as a hysteresis effect presents some questionable features that are also discussed subsequently.

No completely satisfactory solution of the hysteresis problem has been found yet. However, the following crude analysis of this problem offers another point of view with a few qualitative merits not possessed by the two previous analyses.

Consider the case in which a standing tire is subjected to a periodical lateral deformation λ_0 of the form

$$\lambda_0=\lambda_{0_{max}} \sin \nu t$$

Under these conditions the lateral ground force $F_{y\lambda}$ on the tire is experimentally observed to vary with time in the manner indicated in sketch 1 and the corresponding variation of lateral ground force $F_{y\lambda}$ with lateral tire distortion λ_0, shown in sketch 2, appears in the form of a typical hysteresis loop. As can be seen from sketch 1, the lateral tire deformation λ_0 lags behind the lateral ground force $F_{y\lambda}$ by a time increment Δt, where Δt is approximately equal to the ratio of $\Delta\lambda_0$ to the maximum slope of the curve of λ_0 plotted against time (which is $\lambda_{0_{max}}\nu$ for the assumed variation of λ_0):

$$\Delta t \approx \frac{\Delta\lambda_0}{\lambda_{0_{max}}\nu} \tag{55}$$

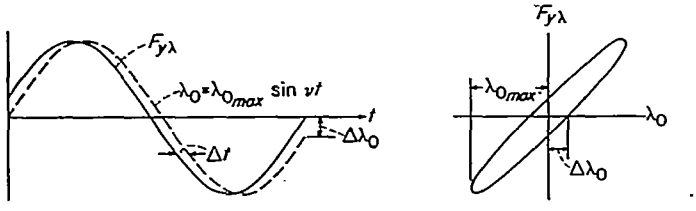

Sketch 1

Sketch 2

[2] Although Von Schlippe and Dietrich considered hysteresis effects in an earlier paper (ref. 4), this earlier analysis leads to some conclusions which are not in agreement with the results of the later, more detailed analysis of reference 5.

As a first approximation for quantitatively including this time-lag concept in the present analysis, a tire is assumed to behave somewhat like a combination of a linear spring and a damper unit such as is indicated in sketch 3, where the

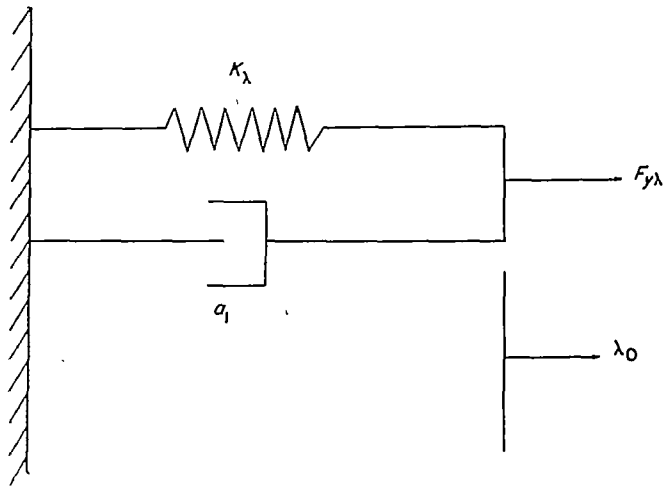

Sketch 3

spring constant corresponds to the previously discussed tire lateral stiffness K_λ and a_1 is the coefficient of an equivalent linear damper. Inertia forces are neglected for the present argument. The differential equation for this system is

$$K_\lambda\lambda_0+a_1 D_t\lambda_0=F_{y\lambda} \tag{56}$$

and its solution for the case of $\lambda_0=\lambda_{0_{max}} \sin \nu t$ gives a hysteresis loop of the form indicated in sketch 2 where the time lag Δt becomes

$$\Delta t=\frac{\tan^{-1}\dfrac{a_1\nu}{K_\lambda}}{\nu} \tag{57}$$

After equating equations (55) and (57), a_1 can be expressed by the relation $a_1=\dfrac{K_\lambda \tan(\Delta\lambda_0/\lambda_{0_{max}})}{\nu}$ so that equation (56) can then be written in the form

$$F_{y\lambda}=K_\lambda\lambda_0+F_{y\hbar}=K_\lambda(\lambda_0+T_\lambda D_t\lambda_0) \tag{58}$$

where $F_{y\hbar}$, the lateral force resulting from hysteresis effects, is

$$F_{y\hbar}=K_\lambda T_\lambda D_t\lambda_0=K_\lambda T_\lambda v D\lambda_0 \tag{59}$$

and where

$$\left.\begin{aligned} T_\lambda&=\frac{\tan(\Delta\lambda_0/\lambda_{0_{max}})}{\nu}=\frac{\eta_\lambda}{\nu}\\ \eta_\lambda&=\tan\frac{\Delta\lambda_0}{\lambda_{0_{max}}}\end{aligned}\right\} \tag{60}$$

With the same type of reasoning the hysteresis twisting moment is given by the equation

$$M_{zh}=K_\alpha T_\alpha D_t\alpha=K_\alpha T_\alpha v D\alpha \tag{61}$$

(compare with eq. (59)), where

$$\left.\begin{aligned} T_\alpha&=\frac{\tan(\Delta\alpha/\alpha_{max})}{v}=\frac{\eta_\alpha}{v}\\ \eta_\alpha&=\tan\frac{\Delta\alpha}{\alpha_{max}}\end{aligned}\right\} \tag{62}$$

It is now seen that the determination of the hysteresis force and moment from equations (59) and (61), respectively, depends on the determination of two quantities T_λ and T_α which have the dimension of time and which will be called time-lag constants. The quantity T_λ, in particular, can be considered closely analogous to Moreland's time-lag constant. In the present case equations have been derived for the time-lag constants as functions of the three variables η_λ, η_α, and ν. (See eqs. (60) and (62).) However, it should be clearly recognized that equations (60) and (62) are based in part on arguments valid only for a standing tire. These arguments may no longer be valid for a rolling tire, and even if the idea of a time-lag constant is still valid, it is likely that the time-lag constants will not be adequately predicted by equations (60) and (62), particularly if the quantities η_y and η_z are evaluated from static hysteresis loops. Moreover, it is basically unsound to assume that the hysteresis force is dependent only on the tire lateral distortion λ_0 and is independent of the tire twist α; actually the hysteresis force (and the hysteresis moment) will in general depend in a complex manner on both λ_0 and α, and even for a first approximation the interaction of these two variables cannot necessarily be neglected. Thus it appears that the preceding hysteresis equations are based on rather speculative and perhaps unsound assumptions, at least from a quantitative point of view, and for this reason these equations will not be incorporated into most of the derivations in subsequent parts of this report. On the other hand, the preceding derivation may be sufficiently plausible to give some idea of the order of magnitude of hysteresis effects, particularly since Moreland has indicated in reference 12 that his experimental data (mostly unpublished) demonstrates the existence of a time-lag effect in tire motion; consequently, in a few parts of this report some mention will be made of the consequences of introducing the hysteresis force and moment terms that have just been derived into a wheel-shimmy analysis.

STRUCTURAL FORCES AND MOMENTS

The preceding discussion covers the major ground forces and moments and the gyroscopic moments acting on the wheel. In addition, forces and moments are exerted on the wheel by the supporting structure. These will be designated as F_{ys} for the net structural force parallel to the Y-axis, M_{xs} for the net structural lateral tilting moment, and M_{zs} for the net structural swiveling moment. These forces and moments include shimmy damper moments, spring restoring moments, inertia forces in a landing-gear structure (exclusive of the wheel inertia force), and spring forces arising from the flexibility of a landing-gear strut or of the fuselage of an airplane. In general, most of these forces and moments can probably be considered approximately linear except shimmy damper moments; however, even these moments can be replaced as a first approximation by equivalent linear damping moments. (See, for example, appendix A.)

Within the scope of a linear theory, these structural forces and moments will depend in a linear manner on the wheel-center coordinates η_3, θ, and γ according to expressions of the type

$$F_{ys}=T_1(D_t)\eta_3+T_2(D_t)\theta+T_3(D_t)\gamma \tag{63}$$

$$M_{xs}=T_4(D_t)\eta_3+T_5(D_t)\theta+T_6(D_t)\gamma \tag{64}$$

$$M_{zs}=T_7(D_t)\eta_3+T_8(D_t)\theta+T_9(D_t)\gamma \tag{65}$$

where the T's are functions of the differential operator D_t, sometimes called transfer functions, whose specific forms will depend on the type of landing gear in question.

This concludes the discussion of the forces and moments acting on a rolling wheel. Now these quantities will be utilized to set up the basic equations of motion for a rolling elastic wheel.

EQUATIONS OF MOTION

DERIVATION OF THE EQUATIONS OF MOTION

In this section the linearized equations of motion for a rolling elastic wheel are set down with the aid of the equations from the preceding sections.

The sum of the lateral forces acting on the wheel parallel to the Y-axis is set equal to the inertia reaction to give (see eqs. (20) and (27))

$$F_{ys}+K_\lambda(y_0-\eta_3-r_3\gamma)-K_\gamma\gamma=m_w D_t^2\eta_3 \tag{66}$$

or, rearranging,

$$F_{ys}+K_\lambda y_0-(K_\lambda+m_w D_t^2)\eta_3-(K_\lambda r_3+K_\gamma)\gamma=0 \tag{67}$$

The first term in equation (66) is the structural force, the second term is the net force on the wheel resulting from tire elastic and inertia forces ($K_\lambda=K_{\lambda_{static}}+\Delta K_\lambda$ where ΔK_λ is given by eq. (53)), the third term is the lateral ground force resulting from tire tilt, and m_w is the mass of the wheel (including the tire). For reasons previously discussed, hysteresis forces and moments are not included either in this equation or in the following equations.

Setting the sum of the lateral tilting moments about the wheel center equal to the inertia reaction gives (see eqs. (20), (27), (28), and (35))

$$M_{xs}+F_z\{c_\lambda y_0+(1-c_\lambda)\eta_3+[(1-c_\lambda)r_3-c_\gamma]\gamma-\eta_3\}+$$
$$[K_\lambda(y_0-\eta_3-r_3\gamma)-K_\gamma\gamma]r_3-\frac{I_{yw}v}{r}D_t\theta=I_{xw}D_t^2\gamma \tag{68}$$

or

$$M_{xs}+(K_\lambda r_3+F_z c_\lambda)y_0-[K_\lambda r_3+F_z c_\lambda]\eta_3-\frac{I_{yw}v}{r}D_t\theta-$$
$$[K_\lambda r_3^2+K_\gamma r_3-F_z r_3(1-c_\lambda)+F_z c_\gamma+I_{xw}D_t^2]\gamma=0 \tag{69}$$

The first term in equation (68) is the structural moment, the second term is the moment resulting from the vertical ground load, the third term is the moment of the ground forces resulting from tire lateral distortion and tilt, the fourth term is the gyroscopic moment resulting from the swiveling motion of the wheel, and I_{xw} is the moment of inertia of the wheel about an axis through its center parallel to the X-axis.

Setting the sum of the swiveling moments about the wheel center equal to zero yields the equation (see eqs. (24), (32), and (34))

$$M_{zs}+K_\alpha(v^{-1}D_t y_0-\theta)-\tau v\,D_t(y_0-\eta_3-r_3\gamma)-\frac{I_{yw}v}{r}D_t\gamma=I_{xw}D_t^2\theta \tag{70}$$

or

$$M_{zs}+(K_\alpha v^{-1}-\tau v)D_t y_0+\tau v\,D_t\eta_3-(K_\alpha+I_{xw}D_t^2)\theta-\left(\frac{I_{yw}}{r}-\tau r_3\right)v\,D_t\gamma=0 \tag{71}$$

The first term in equation (70) is the structural moment, the second term is the net moment resulting from tire elastic and inertia forces exclusive of the gyroscopic moment due to tire lateral distortion ($K_\alpha=K_{\alpha_{static}}+\Delta K_\alpha$ where ΔK_α is given by eq. (54)), the third term is the gyroscopic moment resulting from tire lateral distortion, and the fourth term is the gyroscopic moment resulting from wheel lateral tilt.

Equations (67), (69), (71), and (16) or (19), together with the three auxiliary equations (63) to (65), are the basic equations of motion for an elastic wheel. If the T-functions in equations (63) to (65) are known for a particular landing gear, these equations can be solved simultaneously to determine the rolling behavior of the gear.

Next the question arises as to the most profitable method of solution of these equations for practical landing-gear problems. Essentially, the choice is between exact and approximate solution of the equations. In the past, exact solutions (omitting some of the less important terms previously mentioned) have been made only for the simplest case of a rigid swiveling landing gear attached to a rigid fuselage (refs. 2, 4, and 5). Although the exact solution of these equations for more complex problems does not appear to present any insurmountable difficulties, relatively complex transcendental equations may be involved, so that it is worthwhile to examine the possibility of finding simpler systematic approximations to the general equations.

A second reason for investigating systematic approximations to the summary theory arises in connection with the correlation of the summary theory with the other existing theories. Superficially, in its present form, the summary theory does not closely resemble most of the other existing theories. However, the approximations that are presented subsequently make the correlations between the different theories fairly easy to see.

Subsequent sections of this report will be concerned with the problem of establishing a series of systematic approximations to the general equations and the correlation of these approximations with the other existing theories of wheel motion. However, before proceeding with these two matters it is convenient to digress slightly to consider the exact solution of the general equations for the case of steady yawed rolling, in order to establish several relations which will be useful in later sections.

EQUATIONS FOR STEADY YAWED ROLLING

For an untilted wheel which rolls at constant velocity at a constant small swivel or yaw angle, $y_0(x+h)=y_0(x)=$ Constant, $\theta=$Constant, and $\eta_3=\gamma=0$, so that equations (2) (with y_0 for y_s), (16), (67), and (71) reduce, respectively, to the relations

$$\lambda_0=y_0 \tag{72}$$

$$y_0=(L+h)\theta=l_1\theta \tag{73}$$

$$F_{ys}+K_\lambda y_0=0 \tag{74}$$

$$M_{zs}-K_\alpha\theta=0 \tag{75}$$

By combination of equations (72) and (73) the tire lateral distortion is found to be

$$\lambda_0=l_1\theta \tag{76}$$

By combination of equations (73) and (74) the lateral force on the wheel is found to be

$$F_{ys}=-l_1K_\lambda\theta$$

The quantity l_1K_λ, which represents the lateral force per unit yaw angle, is an important tire characteristic called the cornering power or lateral guiding characteristic of the tire. Later in this report it is found convenient to represent this quantity by a single symbol N, where

$$N=l_1K_\lambda \tag{77}$$

Another property of the steady yawed rolling condition that is of some interest is the distance of the center of pressure of the lateral force behind the center of the tire, which is sometimes called the pneumatic caster $\epsilon=-M_{zs}/F_{ys}$. This quantity, according to equations (73) to (77), is equal to

$$\epsilon=-\frac{M_{zs}}{F_{ys}}=\frac{K_\alpha}{N} \tag{78}$$

SYSTEMATIC APPROXIMATIONS TO THE SUMMARY THEORY

In this section the possibilities for simplifying the preceding equations of motion are discussed, and a series of systematic approximations to the general equations of the summary theory is set down.

All but one of the equations of motion (eqs. (16) or (19), (63) to (65), (67), (69), and (71)) are usually simple linear equations and present no great difficulties. The exception is the kinematic equation, which was originally transcendental in form (eq. (16)) and was later expressed as an infinite series of linear terms (eq. (19a)). The most promising way to simplify the kinematic equation appears to be to assume that the series expansion in equation (19a) is a rapidly convergent

series in which all terms above a certain value of n can be neglected. The rapidity of convergence of the series and its significance cannot be fully determined without a knowledge of the particular landing-gear configuration considered. However, some insight into this question can be obtained by considering the case of purely sinusoidal oscillations of the form $y_0=e^{i\nu_1 x}$, where the quantity ν_1 is the path frequency. Substitution of this expression into the infinite series in y_0 in equation (19a) yields

$$\left(1+\sum_{n=1}^{\infty} l_n D^n\right) y_0=(p_{1\infty}+ip_{2\infty})y_0 \tag{79}$$

where

$$\left.\begin{aligned} p_{1\infty}&=1-l_2\nu_1^2+l_4\nu_1^4-\ \dots \\ p_{2\infty}&=l_1\nu_1-l_3\nu_1^3+l_5\nu_1^5-\ \dots \end{aligned}\right\} \tag{80a}$$

Another form for the p's can be obtained by substituting the relation $y_0=e^{i\nu_1 x}$ into equation (16). The result is

$$\left.\begin{aligned} p_{1\infty}&=\cos\nu_1 h-L\nu_1\sin\nu_1 h \\ p_{2\infty}&=\sin\nu_1 h+L\nu_1\cos\nu_1 h \end{aligned}\right\} \tag{80b}$$

The rate of convergence of the p series of equations (80a) can be tested for any given frequency by substituting numerical values of L, h, and ν_1 into equations (80a) and (80b) and comparing the individual terms. A typical comparison is shown in figure 4 for the conditions $L=0.8r$, and $h=0.5r$. The abscissa of this plot represents the oscillation's wave length $S=2\pi/\nu_1$ and the ordinate represents the p functions. The label p_{12} means that this curve represents the sum of the first two terms in the $p_{1\infty}$ series, and the other labels are analogous. (The approximation symbols will be explained later.) From this figure it is seen that the series converge

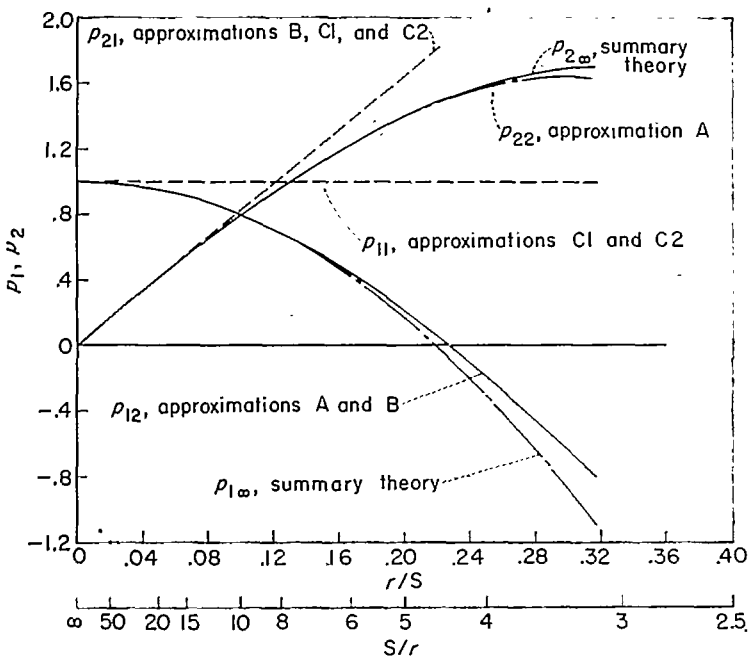

FIGURE 4.—Variation of p_1 and p_2 with shimmy wave length. $L=0.8r$; $h=0.5r$.

very rapidly. From a purely qualitative point of view the figure seems to indicate that, in dealing with shimmy wave lengths greater than approximately 4 tire radii, two terms in each series are sufficient to represent fairly well the exact variations, for wave lengths greater than approximately 6 radii one term in the p_2 series and two in the p_1 series are sufficient, and for wave lengths greater than about 20 radii one term in each series is sufficient. (The wave lengths cited here represent only order of magnitude and are not necessarily quantitatively significant.) To correlate these observations with the conditions of wave length likely to be encountered in practice it can be stated that the experimental data of Von Schlippe and Dietrich (ref. 4 or 5) and Kantrowitz (ref. 8), which are probably fairly typical in this respect, demonstrate wave lengths which are about 4 radii long at zero rolling velocity and which increase with increasing rolling velocity. Thus it appears possible that the use of only a few terms in the series expansion may lead to a reasonable prediction of shimmy characteristics for practical operating conditions.

With the preceding considerations in mind the following approximations to the general wheel-motion equations were established.

APPROXIMATION A

As a first approximation to the general kinematic equation (19a) all terms for $n>3$ will be neglected. This gives the approximate differential equation

$$\begin{aligned} y_0+l_1Dy_0+l_2D^2y_0+l_3D^3y_0&=\eta_0+l_1\theta-\frac{\xi Lh}{r}\gamma \\ &=\eta_3+l_1\theta+\left(r_3-\frac{\xi Lh}{r}\right)\gamma \end{aligned} \tag{81}$$

This equation, together with all the general force and moment equations previously discussed, is referred to hereinafter as approximation A.

APPROXIMATION B

A second, less exact approximation for equation (19a) is obtained by setting $l_n=0$ for $n>2$. Thus

$$\begin{aligned} y_0+l_1Dy_0+l_2D^2y_0&=\eta_0+l_1\theta-\frac{\xi Lh}{r}\gamma \\ &=\eta_3+l_1\theta+\left(r_3-\frac{\xi Lh}{r}\right)\gamma \end{aligned} \tag{82}$$

This equation is referred to as approximation B.

APPROXIMATION C1

Another, cruder approximation for the general differential equation (19a) is obtained by neglecting all terms in the series for $n>1$. This gives the differential equation

$$\begin{aligned} y_0+l_1Dy_0&=\eta_0+l_1\theta-\frac{\xi Lh}{r}\gamma \\ &=\eta_3+l_1\theta+\left(r_3-\frac{\xi Lh}{r}\right)\gamma \end{aligned} \tag{83}$$

which is referred to as approximation C1.

APPROXIMATION C2

As a slight simplification of approximation C1, the relatively unimportant, or at least questionable, term involving ξ may be omitted from equation (83). This gives the differential equation

$$y_0+l_1 Dy_0=\eta_0+l_1\theta=\eta_3+l_1\theta+r_3\gamma \tag{84}$$

which is referred to as approximation C2.

With the aid of equations (2) and (23), equation (84) can be written in the more easily interpreted form

$$\lambda_0=-l_1\alpha \tag{85}$$

or, by using in addition equations (20), (22), and (77), as

$$\lambda_0=-\frac{N}{K_\lambda}\alpha=\frac{F_{y\lambda}}{K_\lambda}=-\frac{NM_{z\alpha}}{K_\lambda K_\alpha} \tag{86}$$

Thus, in this approximation the lateral distortion of the tire is directly proportional to the angular distortion.

The physical meaning of this approximation can be obtained by considering that equation (86) can also be arrived at by letting the ground-contact half-length h approach zero in the general differential equation (19a) (as was mentioned by Rotta in ref. 2), since all terms in the series for $n>1$ and the tilt term are multiplied by h. Then equation (19a) (with $\xi=0$) becomes

$$y_0+L Dy_0=\eta_0+L\theta \tag{87}$$

or, by using in addition equations (2) and (23),

$$\lambda=-L\alpha \tag{88}$$

Also, equation (77) for the yawed rolling becomes

$$N=K_\lambda L \tag{89}$$

and the combination of equations (88) and (89) gives

$$\lambda=-\frac{N}{K_\lambda}\alpha \tag{90}$$

Equation (90) is the same as equation (86) for any given combination of N and K_λ. Thus, when written in the form of equation (86), approximation C2 formally corresponds to the assumption of $h=0$.

Reliable qualitative results should be expected from approximation C2 only when the neglected quantity h is small with respect to the characteristic length of the rolling motion in question (for example, the wave length S of a sinusoidal oscillation). Fortunately, this condition is at least sometimes satisfied for practical rolling conditions.

APPROXIMATION D1

Before considering the next approximation it should be remembered that all of the terms neglected in the preceding approximations were multiplied by the tire ground-contact half-length h; thus these approximations implied the assumption of progressively smaller ground-contact length or progressively larger wave length. In order to simplify the equations further, it is necessary to make some assumptions about the other tire properties. Three such assumptions will now be made to simplify further the equations of approximation C2. For the first approximation, to be called approximation D1, the simplification

$$l_1=0 \tag{91}$$

is adopted. Then it follows from equation (85) that, for finite α,

$$\lambda_0=0 \tag{92}$$

which is the basic equation for this approximation. Thus for this approximation the tire is free to twist but not to deflect laterally. Infinite lateral stiffness is, therefore, also implied:

$$K_\lambda=\infty \tag{93}$$

For the simplest form of wheel shimmy, due to tire elasticity rather than structural elasticity (to be considered subsequently), equation (92) does not provide accurate information. For wheel shimmy due largely to structural elasticity rather than tire elasticity, this approximation may be of some value; actually most existing theories corresponding to this approximation have been developed for the primary purpose of considering the influence of structural elasticity on wheel shimmy.

APPROXIMATION D2

As a second simplification of approximation C2, the assumption

$$l_1=\infty \tag{94}$$

can be adopted. The corresponding theory is designated as approximation D2. From equation (85) it is evident that this approximation implies that, for finite λ_0,

$$\alpha=0 \tag{95}$$

which in turn implies that

$$N=\infty$$

$$K_\alpha=\epsilon N=\infty \tag{96}$$

Thus for approximation D2 the tire is considered to be torsionally rigid but laterally flexible.

APPROXIMATION D3

A third simplification of approximation C2 can be obtained by keeping the quantity l_1 finite but considering the tire to have both infinite lateral stiffness and infinite torsional stiffness, or

$$K_\lambda=K_\alpha=N=\infty \tag{97}$$

This approximation, which is designated as approximation D3, thus represents the case of a rigid tire and consequently also implies that $\alpha=\lambda_0=0$. (Formally, approximation D3 can also be interpreted as the limiting subcase of approximation D1 where $N=\infty$ or as the limiting subcase of approximation D2 where $K_\lambda=\infty$. However, it should not be concluded that approximation D3 is necessarily inferior to these other two approximations.)

A choice of seven simplified approximations based on the

summary theory is now available. The problem remains of determining which, if any, of these approximations is the simplest one which can be used for any particular tire-motion problem. While it is not yet possible to give a completely satisfactory answer to this question, some insight into the answer can be gained by comparing the various approximations with the previously published tire-motion theories, which are at least partly successful and most of which are closely related to these approximations.

CLASSIFICATION AND EVALUATION OF EXISTING THEORIES

In this section the major previously published theories of wheel motion are briefly reviewed, evaluated, and, wherever possible, correlated with the preceding summary theory of this report and its approximations. Each of the major existing theories is first considered individually and then an abbreviated overall summary classification is presented in tabular form.

INDIVIDUAL REVIEW AND EVALUATION OF EXISTING THEORIES

VON SCHLIPPE AND DIETRICH

The tire-motion theory of Von Schlippe and Dietrich (refs. 3 to 5), of course, corresponds directly to the summary theory of this report, since the summary theory was taken from their theory with only minor modifications. These modifications included a more detailed consideration of some of the influences of lateral tilt and of tire inertia forces and moments. It should be noted, however, that the Von Schlippe-Dietrich theory is more advanced than the summary theory of this report in that it partly takes into account the width of the ground-contact area. However, as was previously noted, this factor is probably not of great practical importance.

ROTTA

Rotta's tire-motion theory (ref. 2) corresponds to the summary theory of this report because it also is based on the Von Schlippe-Dietrich theory. Rotta's theory represents a slight extension of the last theory to take into account more adequately most of the effects of tire tilt and the width of the ground-contact area. No inertia forces due to tire lateral distortion or centrifugal forces are discussed.

BOURCIER DE CARBON ADVANCED THEORY

Bourcier de Carbon (ref. 6) has developed two closely related theories of tire motion which are similar to approximations B and C2. The first of these will be referred to as the Bourcier de Carbon advanced theory and the second as the Bourcier de Carbon elementary theory.

Bourcier de Carbon's advanced theory uses five basic tire properties which are correlated with those of the present report through the following relations:

$$\overline{D}=\frac{1}{\overline{N}} \tag{98a}$$

$$\overline{T}=\frac{1}{\overline{K}_\lambda} \tag{98b}$$

$$\overline{S}=\frac{1}{\overline{K}_\alpha} \tag{98c}$$

$$\epsilon\equiv\epsilon=\frac{\overline{K}_\alpha}{\overline{N}} \tag{98d}$$

$$\overline{R}=\frac{l_1}{l_2\overline{K}_\alpha}=\frac{2(L+h)}{\overline{K}_\alpha h(2L+h)} \tag{98e}$$

Equations (98) were obtained by comparing this theory with the corresponding approximation B. The symbols of Bourcier de Carbon are overscored and do not necessarily bear any relation to other symbols in this report designated by the same letters. Although the symbols $\overline{D}$, $\overline{T}$, $\overline{S}$, and $\overline{\epsilon}$ bear a simple relation to the symbols used in the derivations of the present report, the symbol $\overline{R}$ bears a more complicated relation which is worth some detailed consideration.

Bourcier de Carbon defined the tire property $\overline{R}$ as follows: If an untilted wheel is rolled forward while exposed to a constant turning moment about a vertical axis and with no side force, it will move in a circular path of a definite radius; $\overline{R}$ is defined as the reciprocal of the product of the turning moment and the path radius. Unfortunately, however, this constant-moment circle-rolling experiment is not easily performed. Therefore, equation (98e), which expresses $\overline{R}$ in terms of the more easily measured fundamental quantities L, h, and K_α, is of importance for the use of the Bourcier de Carbon advanced theory.

In treating the subject of tilt, Bourcier de Carbon omits many of the details considered in this report. For example, he implicitly assumes that $K_\gamma=c_\lambda=c_\gamma=\xi=0$ and that the inclination angle κ is small (taking $\cos\kappa\approx1$). However, these omitted tilt terms may be as important as the terms considered (as will be shown later); therefore, Bourcier de Carbon's considerations of tilt are incomplete.

It should be noted that in reference 6 certain misconceptions occur in the parts of the paper that deal with comparisons between theory and experiment. In particular, some of the experimental data quoted by Bourcier de Carbon from reference 3 of the present report appears to be either misquoted or misinterpreted. Consequently, Bourcier de Carbon's conclusion that the experimental data of reference 3 provide a remarkable check of his theory is not completely justified; actually these experimental data provide only a fair indirect check of the theory.

GREIDANUS

Another theory similar to approximation B, except for the influence of tilt, is that of Greidanus (ref. 7). Greidanus considers the influence of tilt in much greater detail than does Bourcier de Carbon; however, he also fails to consider the force term proportional to K_γ, and thus his results also do not fully describe the influence of tilt.

In addition, Greidanus' kinematic equation differs from equation (82) for approximation B in that he has introduced a slightly different term associated with tilting of the tire. In the present terminology Greidanus' equation reads

$$y_0+l_1 Dy_0+l_2 D^2y_0=\eta_0+l_1\theta-l_2\frac{\gamma}{r} \tag{99}$$

The difference between the two equations lies in the coefficient of γ. For approximation B (eq. (82)) the coefficient is

$$\frac{\xi L h}{r} \tag{100}$$

and for Greidanus' equation (after substituting for l_2 from eq. (19a)),

$$\frac{\left(L+\frac{h}{2}\right)h}{r} \tag{101}$$

If ξ is set equal to $\left(L+\frac{h}{2}\right)\Big/L$, the two coefficients are identical; thus Greidanus' kinematic equation can be considered to be a particular case of the corresponding equation of approximation B.

No subsequent detailed discussion of Greidanus' theory is included in this report because no complete translation of reference 7 is available.

BOURCIER DE CARBON ELEMENTARY THEORY

Bourcier de Carbon's elementary theory corresponds to approximation C2 of this report except for the minor shortcomings which were discussed in connection with the Bourcier de Carbon advanced theory. The only difference in Bourcier de Carbon's two theories is that the coefficient $\overline{R}$ is taken as infinity in the elementary theory but is finite (see eq. (98e)) for the advanced theory. The infinite value for $\overline{R}$ corresponds to the assumption $l_2=0$, which was previously made in passing from approximation B to approximation C2 (compare eqs. (82) and (84)). The physical significance of $\overline{R}=\infty$ is obvious from equation (98). It means that $h=0$.

MELZER

The Melzer theory of tire motion (ref. 10) is also similar to approximation C2 except for details of the tilting process. Otherwise Melzer's kinematic equation is identical with the kinematic equation of approximation C2 and of Bourcier de Carbon's elementary theory. However, Melzer's theory differs in that it treats the moment due to tire twist as proportional to the swivel angle $-\theta$ rather than to the tire twist angle $Dy_0-\theta$. This assumption would appear justified only if $Dy_0 \ll \theta$, which is not true in general. It is interesting to note that for the simplest case of wheel shimmy (see section entitled "Application to Wheel-Shimmy Problems—Case I") the Melzer approximation leads to one of the same stability boundaries and to the same limiting high-speed shimmy frequency as the more nearly correct approximation that included the term in Dy_0. This restricted agreement, however, hardly justifies the use of Melzer's approximation, since predictions made by means of the two approximations differ with respect to divergence of the shimmy oscillations and with respect to another stability boundary. Moreover, for simple problems the Melzer approximation is not significantly easier to solve than the more nearly correct form including the Dy_0 term.

MORELAND ADVANCED THEORY

Moreland has proposed three versions of a tire-motion theory in references 11 and 12. The most advanced of these versions is governed by the equation

$$\alpha+T\,D_t\alpha=-\frac{\lambda_0}{l_1}=-\frac{F_{y\lambda}}{N} \tag{102}$$

or

$$Tl_1v\,D^2y_0+l_1\,Dy_0+y_0=\eta_0+Tl_1v\,D\theta+l_1\theta \tag{103}$$

where T is a time-lag constant. This theory corresponds to a generalization of approximation C2 (with pneumatic caster neglected, that is, $\epsilon=0$), since for $T=0$ equation (102) is identical with the basic equation for approximation C2. However, for $T\neq 0$ this theory is not directly compatible with the summary theory and its approximations.

Moreland uses the following reasoning to establish this equation: First, it is known that in steady yawed rolling a yaw angle α is developed as a consequence of the application of a lateral force $F_{y\lambda}$ according to the relation

$$\alpha=-\frac{F_{y\lambda}}{N} \tag{104}$$

which is the basic equation for approximation C2. However, for the dynamic rolling case this equilibrium yaw angle obviously cannot be established immediately upon application of a given side force; rather, a finite amount of time will be required for the equilibrium yaw angle to develop. Moreland has attempted to take this finite time lag into account by modifying equation (104) to the new form of equation (102). In the latter equation the constant T is a measure of the time lag of the yaw angle behind the applied force $F_{y\lambda}$.

This time-lag term introduced by Moreland does not correspond exactly to any of the terms in the summary theory, and to this extent Moreland's advanced theory is apparently incompatible with the summary theory. However, a partial reconciliation of the two theories can be obtained through the following considerations of hysteresis effects as applied to approximation C2: According to equation (58) the lateral ground force, if tilt and inertia forces are neglected, is given by the equation

$$\lambda_0+T_\lambda\,D_t\lambda_0=\frac{F_{y\lambda}}{K_\lambda} \tag{105}$$

and the kinematic equation for approximation C2 is (eq. (85))

$$\lambda_0=-l_1\alpha$$

Combining equations (105) and (85) to eliminate λ_0 and substituting $K_\lambda l_1=N$ yields the equation

$$\alpha+T_\lambda\,D_t\alpha=-\frac{F_{y\lambda}}{N} \tag{106}$$

Equation (106) is formally identical with Moreland's basic equation (102) if the hysteresis time constant T_λ is considered equivalent to Moreland's time constant T. The important points to be noted here are: (1) according to both views, the tire twist α lags behind the applied lateral force $F_{y\lambda}$, and (2) Moreland adopts the lateral-force equation $F_{y\lambda}=K_\lambda\lambda_0$ which implies that the lateral force and lateral

deformation are in phase (although lateral force and twist are not in phase), whereas according to approximation C2 (see eq. (105)) the lateral force lags behind the lateral deformation as a consequence of the kinematic relation $\lambda=-l_1\alpha$. In regard to the second point, since there are apparently no pertinent experimental data available, it is not possible to conclude which point of view, if either, is correct.

Why Moreland's time-constant concept has not been incorporated directly into the derivations of the summary theory should be clear from the preceding discussion: It is not certain whether Moreland's time-constant terms are really independent of the terms already contained in the summary theory or whether they are, rather, another way of looking at some terms which are already included in the summary theory. More specifically, Moreland's analysis does not include inertia forces and moments due to tire lateral distortion, hysteresis forces and moments, or the higher l_n terms (l_2, l_3, . . .), and for certain conditions any of these factors could be interpreted as a time-constant effect. In view of these factors and in view of the lack of pertinent experimental data, a completely satisfactory evaluation of the relative values of the summary theory and Moreland's advanced theory cannot be made in the present report.

MORELAND INTERMEDIATE THEORY

As a simpler approximation for his advanced theory, Moreland has implied (ref. 11) that the influence of the time-lag term in the basic equation for his advanced theory (eq. (102)) can be approximated for the usual range of shimmy frequencies by using the simpler kinematic equation

$$40l_1\alpha=-\lambda_0 \tag{107}$$

Inasmuch as approximation C2 has the kinematic equation (85)

$$l_1\alpha=-\lambda_0$$

and approximation D2 has the kinematic equation (95), which could be written in the form

$$\infty\,\alpha\approx-\lambda_0$$

it follows from a comparison of these last three equations that Moreland's intermediate theory falls somewhere between approximations C2 and D2. Since Moreland has not offered any concrete justification for this approximation, further detailed discussion does not appear warranted here.

MORELAND ELEMENTARY THEORY

Moreland's most elementary theory corresponds directly to approximation D3, the case of a completely rigid tire, except that it, like Moreland's other two theories, does not take into account the pneumatic caster ($\epsilon=0$).

TEMPLE ELEMENTARY THEORY

Temple has proposed an elementary theory for the motion of tires which is identical with approximation D1 (ref. 13). Temple has chosen the most general form of this approximation in that he has considered both the tire torsional stiffness K_α (indirectly interpreted as an increase in trail) and the cornering power N.

This theory was developed before experimental evidence pointing to the need for more detailed considerations of tire lateral stiffness was available. Subsequently, Temple has indicated a need for more refined considerations of the tire (ref. 25) and has developed independently a theory (unpublished, but partly described in ref. 21) similar to the theory of Von Schlippe and Dietrich.

MAIER

Maier (ref. 14) has proposed a simplified theory similar to approximation D1, with the difference that he makes the added assumption that the tire torsional stiffness K_α is zero. This theory, too, was developed before there existed much experimental evidence pointing to the need for more refined considerations for shimmy behavior.

TAYLOR

Taylor (ref. 15), in a brief paper, suggested another tire motion theory which corresponds to approximation D2 except that details of the tilt process are omitted.

KANTROWITZ AND WYLIE

The preceding theories for tire motion, which include most of the known theories, may all be considered as closely related to the summary theory of this report. However, two other well-known theories, one by Kantrowitz (ref. 8) and one by Wylie (ref. 9), apparently cannot be derived from the summary theory and thus cannot be accurately classified here with respect to the other theories. They possess some of the merits of approximation B but in other respects are less adequate than approximation C2. To point out the deficiencies of these two theories it is sufficient to consider two simple cases of tire motion as follows:

The first case to be considered is the steady straight-line motion of a nonswiveling, untilted, rolling wheel which is not yawed with respect to its direction of motion ($\alpha=0$), which is inclined by an angle θ (equal to the swivel angle) to the reference X-axis, and which has no lateral forces or moments acting on the wheel. (See sketch 4.) Obviously,

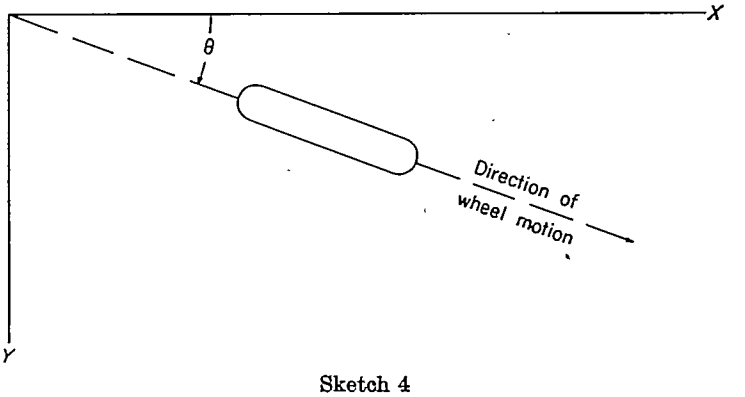

Sketch 4

for this case there will be no lateral distortion of the tire, or

$$\lambda_0=0$$

On the other hand, Kantrowitz' basic equation, which is

$$\lambda_0+L\,D\lambda_0=L\theta-l_2\,D\theta \tag{108}$$

gives for this steady unyawed case (with $D\lambda_0=D\theta=0$)

$$\lambda_0=L\theta$$

This equation is obviously incorrect, since it implies that the lateral distortion of a straight rolling wheel, which actually must be zero, depends on the choice of the coordinate axes to which θ is referred. Only for the special case of a wheel running along the reference axis (that is, for $\theta=0$) is Kantrowitz' theory correct in this respect, and in an actual shimmy problem this condition is possible only for the case of zero trail; hence Kantrowitz' theory cannot necessarily be expected to give reliable results for trails different from zero. Thus Kantrowitz' theory is of at least doubtful value for practical shimmy calculations.

In order to evaluate the Wylie theory, consider the case of steady untilted yawed rolling of a wheel moving parallel to the X-axis. (See sketch 5.) Obviously, the lateral distortion of the tire λ_0 will depend only on the swivel angle θ

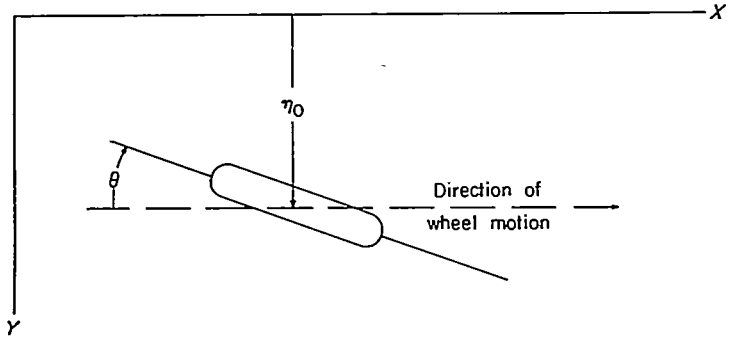

Sketch 5

($\theta=\alpha$) and not at all on the absolute lateral displacement of the wheel η_0. On the other hand the basic equation of Wylie, which in the present terminology is

$$y_0+L\,Dy_0=L\theta-l_2\,D\theta \qquad (109)$$

gives for this steady case (where $Dy_0=D\theta=0$) the relation $y_0=L\theta$ or, by using equation (2),

$$\lambda_0=L\theta-\eta_0$$

This equation states the obviously incorrect conclusion that the tire distortion is dependent on η_0 or, in other words, that it depends on the choice of the coordinate axes. Thus, only for the special case $\eta_0=0$ is Wylie's theory plausible in this respect, and $\eta_0=0$ implies that the reference axis must pass through the path of the wheel. Since this condition is satisfied in an actual shimmy motion only for the special case of zero trail, Wylie's theory, like Kantrowitz', can be fully valid only for zero trail and, consequently, this theory is also of doubtful value for practical shimmy calculations.

It might be noted that the preceding difficulty concerning Wylie's theory could be removed by the logical procedure of adding the term η_0 to the right-hand side of Wylie's equation (109) to give the new basic equation

$$y_0+L\,Dy_0=L\theta-l_2\,D\theta+\eta_0 \qquad (110)$$

Another questionable point in these two theories is that the Kantrowitz theory, as previously noted, predicts that the lateral distortion in yawed rolling parallel to the X-axis (see sketch 5) is

$$\lambda_0=L\theta$$

and so does the Wylie theory if the reference axis is chosen to give $\eta_0=0$. On the other hand, the summary theory has for this yawed case the relation

$$\lambda_0=(L+h)\theta$$

(See eq. (85).) The difference arises from the fact that Kantrowitz and Wylie did not explicitly consider the ground-contact length $2h$ in their derivation.

OTHER THEORIES

In addition to the just discussed theoretical papers dealing particularly with the subject of landing-gear shimmy, a number of relevant papers exist which are either largely of historical interest, which deal particularly with automobile shimmy problems, which deal only briefly with landing-gear shimmy problems, which deal with other tire-motion problems such as yawed rolling and veering-off or ground looping, or which deal with the determination of tire stiffness parameters. Although these papers are of some interest, they do not appear to contain any important contributions which are not contained in the theories just reviewed. The reader is referred to reference 1 for a substantially complete listing and brief discussion of most of the papers in this class.

Of particular historical interest among the investigations not considered here in detail are the work of Broulhiet (ref. 23) and the work of Fromm (discussed in ref. 22). These two investigators independently were apparently the first to recognize the importance of lateral distortion and cornering power of tires in the wheel shimmy problem. Taking these factors into account, both authors developed tire-motion theories whose kinematic relations correspond to that of approximation C2 of the present report.

TABULAR CLASSIFICATION OF EXISTING THEORIES

In order to permit easier visualization and comparison of the merits of the theories discussed, the major assumptions of the various theories of tire motion are collected in table I. This table lists the nature of the assumptions made in regard to the primary tire parameters N, K_λ, K_α, ϵ, and l_n for each of the theories discussed.

APPLICATION TO WHEEL-SHIMMY PROBLEMS

In the preceding sections of this report a set of basic differential equations for the motion of an elastic wheel has been derived and compared with the corresponding equations of most of the previously existing theories. These comparisons have indicated that, from a mostly qualitative point of view, the summary theory of this report and the systematic approximations to it incorporate the major merits of the

TABLE I.—PRIMARY ASSUMPTIONS FOR THE VARIOUS THEORIES OF TIRE MOTION[1]

Theory	N	K_λ	K_α	e	l_1	l_2	l_3	$l_n (n>3)$	Remarks
Summary theory	F	F	F	F	F	F	F	F	
Approximation A	F	F	F	F	F	F	F	0	
Approximation B	F	F	F	F	F	F	0	0	
Approximations C1 and C2	F	F	F	F	F	0	0	0	
Approximation D1	F	∞	F	F	0	0	0	0	Assumes laterally rigid tire
Approximation D2	∞	F	∞	F	∞	0	0	0	Assumes torsionally rigid tire
Approximation D3	∞	∞	∞	F	F	0	0	0	Assumes laterally and torsionally rigid tire
Von Schlippe-Dietrich and Rotta	F	F	F	F	F	F	F	F	
Bourcier de Carbon advanced	F	F	F	F	F	F	0	0	
Greidanus	F	F	F	F	F	F	0	0	
Bourcier de Carbon elementary	F	F	F	F	F	0	0	0	
Melzer	F	F	F	F	F	0	0	0	Assumes tire twist angle=swivel angle
Moreland advanced	F	F	0	0	F	0	0	0	Introduces time-constant term
Moreland intermediate	F	F	0	0	F	0	0	0	Implies extremely large l_1 value
Moreland elementary	∞	∞	∞	0	F	0	0	0	Assumes laterally and torsionally rigid tire
Temple elementary	F	∞	F	F	0	0	0	0	Assumes laterally rigid tire
Maier	F	∞	0	0	0	0	0	0	Assumes laterally rigid tire
Taylor	∞	F	∞	0	∞	0	0	0	Assumes torsionally rigid tire
Kantrowitz	F	F	F	F	F	0	0	0	For trail not equal to zero both of these
Wylie	F	F	F	F	F	0	0	0	theories can lead to erroneous conclusions

[1] The symbol F indicates a finite number.

existing theories of tire motion and avoid some of their disadvantages. However, it still remains to investigate how best to apply the theory to specific landing-gear problems, to investigate the question of the absolute or quantitative accuracy of the summary theory and of the other theories, and, if the summary theory be found satisfactory, to establish the simplest systematic approximation to it which will give reliable information regarding any particular problem in tire motion. The best way to accomplish these various aims appears to be through a discussion of the shimmy of several particular landing-gear configurations. In this section three particular landing-gear configurations are discussed which range in complexity from the simplest case of a rigid swiveling landing gear to the most general case of a gear of arbitrary complexity.

DESCRIPTION OF PARTICULAR CASES CONSIDERED

The first landing-gear configuration considered, which is designated case I, is illustrated in figure 5. It consists of a rigid landing gear whose only degree of freedom other than tire distortion is rotation of the wheel about an inclined swivel axis, which may be opposed by a linear spring or damper. This particular configuration is chosen because most of the existing experimental data have been obtained for such a configuration. Thus, this configuration makes it possible to discuss and evaluate the summary theory, its systematic approximations, and the existing theories with respect to agreement with experiment in regard to the various important characteristics of a shimmy motion, such as stability boundaries, shimmy frequency, and divergence.

The second landing-gear configuration, case II, is an untilted landing gear possessing two degrees of freedom aside from tire distortion. This landing-gear configuration, which is illustrated in figure 6, consists of a wheel free to swivel but not to tilt, which turns about a rigid vertical swivel axis attached by a spring k to the supporting structure. (This spring is an idealized representation of the lateral flexibility of an actual landing-gear strut.) This configuration is discussed for two purposes: (1) to illustrate the effect of structural elasticity on wheel shimmy behavior and (2) to provide

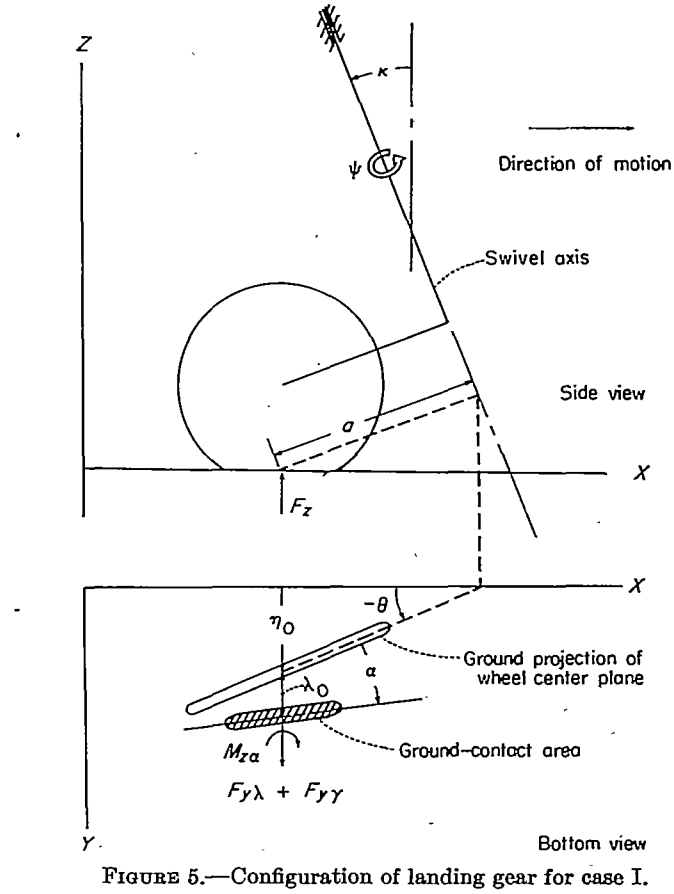

FIGURE 5.—Configuration of landing gear for case I.

an example which is better suited than case I for bringing out the relative merits of several of the systematic approximation theories for a case involving structural flexibility.

The third landing-gear configuration considered is a modification of the gear of case II. In case II the landing gear was considered to be connected to its supporting structure by a single spring; in case III this single spring is replaced by a more complex structure described by some transfer function. This case is chosen mainly to demonstrate the application of the theory to complex problems for which the transfer-function concept may be of value.

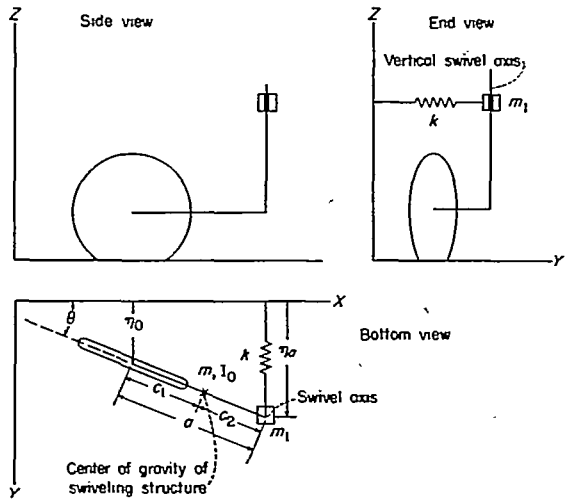

FIGURE 6.—Configuration of landing gear for case II.

CASE I

GENERAL DERIVATION

In this section the basic equation of motion will be derived according to the summary theory for the special case of an inclined, rigid, swiveling landing gear (case I), which is illustrated in figure 5. This equation of motion could be obtained by making use of the previously derived equations of motion for the completely general case; however, it can more easily be derived here in a slightly different form for this particular problem.

The geometric quantities which enter the discussion of this particular landing gear are indicated in figure 5. This gear has a swivel axis lying in the XY-plane and is inclined forward from the vertical Z-axis by a constant angle κ. The perpendicular distance a between the ground-contact center point 0 and the swivel axis is called the trail. The swivel axis is assumed to move with constant velocity v along the X-axis without lateral motion from the XZ-plane.

Rotation of the wheel structure about the inclined swivel axis by an amount ψ results in a component θ of angular rotation about the vertical axis of magnitude

$$\theta=\psi \cos \kappa \tag{111}$$

a component γ of rotation about the X-axis (tilt) of magnitude

$$\gamma=-\psi \sin \kappa \tag{112}$$

and a lateral deflection η_0 of magnitude

$$\eta_0=-a\psi \tag{113}$$

where all angles except κ are considered small.

The sum of all moments about the swivel axis must equal the inertia reaction $I_\psi D_t^2\psi=I_\psi v^2D^2\psi$, where I_ψ is the moment of inertia of the wheel structure (including the wheel) about the swivel axis. The moments about the swivel axis are assumed to consist of the moments resulting from the previously discussed forces and moments that arise from tire distortion and ground loads plus the moments applied to the wheel by the supporting structure, which are assumed to consist of a restoring spring of moment $\rho\psi$ and a linear damper of moment $g\ D_t\psi=gv\ D\psi$, where ρ and g are constants. Thus, summation of the moments about the swivel axis gives the differential equation

$$-[K_\lambda(y_0-\eta_0)-K_\gamma\gamma]a-F_z[c_\lambda y_0+(1-c_\lambda)\eta_0-c_\gamma\gamma] \sin \kappa+ K_\alpha(Dy_0-\theta) \cos \kappa-\tau v^2D(y_0-\eta_0) \cos \kappa-\rho\psi-gv\,D\psi=I_\psi v^2D^2\psi \tag{114}$$

where the first term is the total ground force due to tire lateral distortion and tilt (see eqs. (20) and (27)) times its moment arm a; the second term is the vertical force times its moment-producing fraction $\sin \kappa$ times its moment arm (see eq. (28)); the third term is the moment about the Z-axis due to tire twist (see eq. (24)) corrected by $\cos \psi$ for the component about the swivel axis; the remaining terms on the left-hand side represent the gyroscopic torque due to lateral tire distortion (see eq. (32)), the spring restoring moment, and the linear damper moment. Now by making use of equations (111) to (113), equation (114) can be written in the form

$$A_1\,D^2\psi+A_2\,D\psi+A_3\psi+B_1\,Dy_0+B_2y_0=0 \tag{115a}$$

where

$$\left.\begin{aligned} A_1&=I_\psi v^2\\ A_2&=a\tau v^2 \cos \kappa+gv\\ A_3&=a^2K_\lambda+K_\alpha \cos^2 \kappa+\rho+\rho_\kappa\\ B_1&=-K_\alpha \cos \kappa+\tau v^2 \cos \kappa\\ B_2&=aK_\lambda+c_\lambda F_z \sin \kappa \end{aligned}\right\} \tag{115b}$$

and

$$\rho_\kappa=aK_\gamma \sin \kappa-aF_z \sin \kappa+ac_\lambda F_z \sin \kappa+c_\gamma F_z \sin^2 \kappa \tag{115c}$$

The general relation between ψ and y_0 for this case is found by substituting for η_0, γ, and θ, according to equations (111) to (113) in the general kinematic equation (19a). Thus

$$y_0+\sum_{n=1}^{\infty} l_n D^n y_0=-a\psi+l_1\psi \cos \kappa+\frac{\xi Lh}{r}\psi \sin \kappa$$

or, abbreviating,

$$\sigma=1+\frac{\xi Lh}{rl_1} \tan \kappa \tag{116}$$

and rearranging,

$$(\sigma l_1 \cos \kappa-a)\psi=y_0+\sum_{n=1}^{\infty} l_n D^n y_0=\sum_{n=0}^{\infty} l_n\,D^n y_0 \tag{117}$$

since $l_0=1$. Differentiating this result gives

$$(\sigma l_1 \cos \kappa-a)D\psi=\sum_{n=0}^{\infty} l_n\,D^{n+1}y_0$$

which can also be written as

$$(\sigma l_1 \cos \kappa-a)D\psi=\sum_{n=1}^{\infty} l_{n-1}\,D^n y_0 \tag{118}$$

and, similarly,

$$(\sigma l_1 \cos \kappa-a)D^2\psi=\sum_{n=2}^{\infty} l_{n-2}\,D^n y_0 \tag{119}$$

Substituting these relations into equation (115) and multiplying through by $\sigma l_1 \cos\kappa - a$ gives

$$A_1 \sum_{n=2}^{\infty} l_{n-2} D^n y_0 + A_2 \sum_{n=1}^{\infty} l_{n-1} D^n y_0 + A_3 \sum_{n=0}^{\infty} l_n D^n y_0 +$$

$$B_1(\sigma l_1 \cos\kappa - a) D y_0 + B_2(\sigma l_1 \cos\kappa - a) y_0 = 0$$

Finally, after adding all terms of like order, substituting $N = l_1 K_\lambda$ (eq. (77)), substituting for some of the A's, and using equation (116), there results the equation

$$\sum_{n=0}^{\infty} F_n D^n y_0 = 0 \tag{120a}$$

where

$$\left.\begin{aligned} F_0 &= \sigma a N \cos\kappa + K_\alpha \cos^2\kappa + \rho + \rho_\kappa + u_\kappa \\ F_1 &= a^2 N + a' K_\alpha \cos\kappa + \rho l_1 + \rho_\kappa l_1 + g v + \sigma l_1 \tau v^2 \cos^2\kappa \\ F_2 &= A_1 + A_2 l_1 + A_3 l_2 \\ F_n &= A_1 l_{n-2} + A_2 l_{n-1} + A_3 l_n \qquad (n>2) \end{aligned}\right\} \tag{120b}$$

and

$$\left.\begin{aligned} u_\kappa &= c_\lambda F_z (\sigma l_1 \cos\kappa - a) \sin\kappa \\ a' &= a + (1-\sigma) l_1 \cos\kappa = a - \frac{\xi L h}{r} \sin\kappa \end{aligned}\right\} \tag{120c}$$

SYSTEMATIC APPROXIMATIONS

Equations (120) provide the general differential equation of free motion for case I. The corresponding equations for the systematic approximations A to D3 are obtained as follows.

Approximation A.—The basic equation for approximation A is obtained by setting l_n equal to 0 for $n>3$ in equations (120). The resulting equation can be stated in the following form:

$$E_0 D^5 y_0 + E_1 D^4 y_0 + E_2 D^3 y_0 + E_3 D^2 y_0 + E_4 D y_0 + E_5 y_0 = 0 \tag{121a}$$

where

$$\left.\begin{aligned} E_0 &= I_\psi v^2 l_3 \\ E_1 &= I_\psi v^2 l_2 + (a\tau v^2 \cos\kappa + g v) l_3 \\ E_2 &= I_\psi v^2 l_1 + (a\tau v^2 \cos\kappa + g v) l_2 + (a^2 K_\lambda + K_\alpha \cos^2\kappa + \rho + \rho_\kappa) l_3 \\ E_3 &= I_\psi v^2 + (a\tau v^2 \cos\kappa + g v) l_1 + (a^2 K_\lambda + K_\alpha \cos^2\kappa + \rho + \rho_\kappa) l_2 \\ E_4 &= a^2 N + a' K_\alpha \cos\kappa + \rho l_1 + \rho_\kappa l_1 + g v + \sigma l_1 \tau v^2 \cos^2\kappa \\ E_5 &= \sigma a N \cos\kappa + K_\alpha \cos^2\kappa + \rho + \rho_\kappa + u_\kappa \end{aligned}\right\} \tag{121b}$$

and

$$\left.\begin{aligned} \rho_\kappa &= (a K_\gamma - a F_z + a c_\lambda F_z + c_\gamma F_z \sin\kappa) \sin\kappa \\ u_\kappa &= c_\lambda F_z (\sigma l_1 \cos\kappa - a) \sin\kappa \end{aligned}\right\} \tag{121c}$$

Approximation B.—In order to obtain approximation B, set l_3 equal to 0 in equations (121b). This gives the differential equation

$$E_0 D^4 y_0 + E_1 D^3 y_0 + E_2 D^2 y_0 + E_3 D y_0 + E_4 y_0 = 0 \tag{122a}$$

where

$$\left.\begin{aligned} E_0 &= I_\psi v^2 l_2 \\ E_1 &= I_\psi v^2 l_1 + (a\tau v^2 \cos\kappa + g v) l_2 \\ E_2 &= I_\psi v^2 + (a\tau v^2 \cos\kappa + g v) l_1 + (a^2 K_\lambda + K_\alpha \cos^2\kappa + \rho + \rho_\kappa) l_2 \\ E_3 &= a^2 N + a' K_\alpha \cos\kappa + \rho l_1 + \rho_\kappa l_1 + g v + \sigma l_1 \tau v^2 \cos^2\kappa \\ E_4 &= \sigma a N \cos\kappa + K_\alpha \cos^2\kappa + \rho + \rho_\kappa + u_\kappa \end{aligned}\right\} \tag{122b}$$

(The corresponding equation with inclusion of hysteresis effects is listed in appendix B.)

Approximation C1.—The equation for approximation C1 is obtained by setting l_2 equal to 0 in the equation for approximation B. The resulting differential equation is

$$E_0 D^3 y_0 + E_1 D^2 y_0 + E_2 D y_0 + E_3 y_0 = 0 \tag{123a}$$

where

$$\left.\begin{aligned} E_0 &= I_\psi v^2 l_1 \\ E_1 &= I_\psi v^2 + (a\tau v^2 \cos\kappa + g v) l_1 \\ E_2 &= a^2 N + a' K_\alpha \cos\kappa + \rho l_1 + \rho_\kappa l_1 + g v + \sigma l_1 \tau v^2 \cos^2\kappa \\ E_3 &= \sigma a N \cos\kappa + K_\alpha \cos^2\kappa + \rho + \rho_\kappa + u_\kappa \end{aligned}\right\} \tag{123b}$$

Approximation C2.—The equation for approximation C2 is obtained by setting ξ equal to 0 in the equation for approximation C1. The resulting differential equation is

$$E_0 D^3 y_0 + E_1 D^2 y_0 + E_2 D y_0 + E_3 y_0 = 0 \tag{124a}$$

where

$$\left.\begin{aligned} E_0 &= I_\psi v^2 l_1 \\ E_1 &= I_\psi v^2 + (a\tau v^2 \cos\kappa + g v) l_1 \\ E_2 &= a^2 N + a K_\alpha \cos\kappa + \rho l_1 + \rho_\kappa l_1 + g v + l_1 \tau v^2 \cos^2\kappa \\ E_3 &= a N \cos\kappa + K_\alpha \cos^2\kappa + \rho + \rho_\kappa + u_{\kappa 1} \end{aligned}\right\} \tag{124b}$$

and

$$u_{\kappa 1} = c_\lambda F_z (l_1 \cos\kappa - a) \sin\kappa \tag{124c}$$

(The corresponding equation, with hysteresis effects included, is listed in appendix B.)

Approximation D1.—The differential equation for approximation D1 is obtained by setting l_1 equal to 0 in the equation for approximation C2. The result is the differential equation

$$E_0 D^2 y_0 + E_1 D y_0 + E_2 y_0 = 0 \tag{125a}$$

where

$$\left.\begin{aligned} E_0 &= I_\psi v^2 \\ E_1 &= a^2 N + a K_\alpha \cos\kappa + g v \\ E_2 &= a N \cos\kappa + K_\alpha \cos^2\kappa + \rho + w_\kappa \end{aligned}\right\} \tag{125b}$$

and

$$w_\kappa=(aK_\gamma-aF_z+c_\gamma F_z \sin\kappa)\sin\kappa \qquad (125c)$$

Approximation D2.—The differential equation for approximation D2 is obtained by dividing all terms in equations (124) by l_1 and then setting l_1 equal to ∞ and using the relations $N/l_1=K_\lambda$ and $K_\alpha/l_1=\epsilon K_\lambda$. The resulting equation is

$$E_0 D^3y_0+E_1 D^2y_0+E_2 Dy_0+E_3y_0=0 \qquad (126a)$$

where

$$\left.\begin{aligned} E_0&=I_\psi v^2\\ E_1&=a\tau v^2\cos\kappa+gv\\ E_2&=a^2K_\lambda+a\epsilon K_\lambda\cos\kappa+\rho+\rho_\epsilon+\tau v^2\cos^2\kappa\\ E_3&=aK_\lambda\cos\kappa+\epsilon K_\lambda\cos^2\kappa+c_\lambda F_z\sin\kappa\cos\kappa \end{aligned}\right\} \qquad (126b)$$

Approximation D3.—The differential equation for approximation D3 is obtained by dividing the E's for approximation D1 by N and then setting N equal to ∞. The resulting differential equation is

$$a Dy_0+y_0\cos\kappa=0 \qquad (127)$$

PREVIOUSLY PUBLISHED THEORIES

In the preceding section the differential equations are set down for case I according to the summary theory and the systematic approximations thereto, complete with all pertinent details, including a number of second-order terms so as to enable the direct application of these equations to actual problems. In the present section the differential equations for the previously published theories are listed for the purpose of making clear the differences in the basic structure of the differential equations resulting from the application of these theories to case I. In order to avoid obscuring the more important differences between the equations of the various theories, all terms are omitted whose inclusion in any shimmy theory should be completely straight-forward (such as the spring restoring-moment coefficient ρ and the damping coefficient g) and also all inclination effects. Although the latter effects are not necessarily negligible, they do appear to be of second-order importance and their omission here should not alter the basic structure of these equations. With these omissions—that is, for $g=\rho=\kappa=0$—the differential equations for case I according to the previously published theories are as follows in the terminology of the present report:

Von Schlippe-Dietrich and Rotta theories.—The basic equation of motion for this case according to the Von Schlippe-Dietrich theory, after neglect of the effects of tire width, corresponding to equation (120a) for the summary theory, is

$$\sum_{n=0}^{\infty} F_n' D^n y_0=0 \qquad (128a)$$

where

$$\left.\begin{aligned} F_0'&=aN+K_\alpha\\ F_1'&=a^2N+aK_\alpha+g_1v\\ F_n'&=I_\psi v^2 l_{n-2}+g_1 v l_{n-1}+(a^2K_\lambda+K_\alpha)l_n+\left[\frac{1}{n!}ah^nK_\lambda(l_1-a)\right] \qquad (n=2,4,\ldots)\\ F_n'&=I_\psi v^2 l_{n-2}+g_1 v l_{n-1}+(a^2K_\lambda+K_\alpha)l_n-\left[\frac{1}{n!}h^{n-1}K_\alpha(l_1-a)\right] \qquad (n=3,5,\ldots) \end{aligned}\right\} \qquad (128b)$$

The symbol g_1 is a hysteresis damping coefficient defined by the equation

$$g_1=\frac{d_1}{\sqrt{\nu^2+d_2^2\omega^2}} \qquad (128c)$$

where d_1 and d_2 are hysteresis constants. Aside from the omission of some inclination effects and other terms, as discussed previously, the only differences between equations (128) and equations (120) for the summary theory lies in the inclusion of the hysteresis term involving g_1 and in the addition of the terms in brackets in equations (128b). Rotta's corresponding equations, after neglect of tire width effects, would be the same as equations (128) except that Rotta omitted the hysteresis term. As was previously noted, the Von Schlippe-Dietrich theory and Rotta's theory differ only slightly in their respective considerations of the influences of tilt and tire width, neither of which effects are considered here.

Bourcier de Carbon advanced theory.—The Bourcier de Carbon advanced theory leads to the fourth-order differential equation

$$E_0 D^4y_0+E_1 D^3y_0+E_2 D^2y_0+E_3 Dy_0+E_4y_0=0 \qquad (129a)$$

where

$$\left.\begin{aligned} E_0&=I_\psi v^2 l_2\\ E_1&=I_\psi v^2 l_1\\ E_2&=I_\psi v^2+(a^2K_\lambda+K_\alpha)l_2\\ E_3&=a^2N+aK_\alpha\\ E_4&=aN+K_\alpha \end{aligned}\right\} \qquad (129b)$$

Bourcier de Carbon elementary theory.—The coefficients for the Bourcier de Carbon elementary theory are obtained by setting l_2 equal to 0 in equations (129) for the advanced theory. The resulting third-order differential equation is

$$E_0 D^3y_0+E_1 D^2y_0+E_2 Dy_0+E_3y_0=0 \qquad (130a)$$

where

$$\left.\begin{aligned} E_0&=I_\psi v^2 l_1\\ E_1&=I_\psi v^2\\ E_2&=a^2N+aK_\alpha\\ E_3&=aN+K_\alpha \end{aligned}\right\} \qquad (130b)$$

Melzer.—Melzer's theory gives the third-order differential equation

$$E_0\,D^3y_0+E_1\,D^2y_0+E_2\,Dy_0+E_3y_0=0 \qquad (131a)$$

where

$$\left.\begin{aligned} E_0&=I_\psi v^2 l_1\\ E_1&=I_\psi v^2\\ E_2&=a^2N+l_1K_\alpha\\ E_3&=aN+K_\alpha \end{aligned}\right\} \qquad (131b)$$

Moreland advanced theory.—Moreland's advanced theory leads to the fourth-order differential equation

$$E_0\,D^4y_0+E_1\,D^3y_0+E_2\,D^2y_0+E_3\,Dy_0+E_4y_0=0 \qquad (132a)$$

where

$$\left.\begin{aligned} E_0&=I_\psi Tl_1v^3\\ E_1&=I_\psi l_1v^2\\ E_2&=I_\psi v^2+a^2TNv\\ E_3&=a^2N+aTNv\\ E_4&=aN \end{aligned}\right\} \qquad (132b)$$

Moreland elementary theory.—Moreland's elementary theory gives the differential equation

$$a\,Dy_0+y_0=0 \qquad (133)$$

Taylor.—Taylor's theory leads to the third-order differential equation

$$E_0\,D^3y_0+E_1\,D^2y_0+E_2\,Dy_0+E_3y_0=0 \qquad (134a)$$

where

$$\left.\begin{aligned} E_0&=Iv^2\\ E_1&=0\\ E_2&=K_\lambda a^2\\ E_3&=K_\lambda a \end{aligned}\right\} \qquad (134b)$$

Temple elementary theory.—The second-order differential equation for the Temple elementary theory is

$$E_0\,D^2y_0+E_1\,Dy_0+E_2y_0=0 \qquad (135a)$$

where

$$\left.\begin{aligned} E_0&=I_\psi v^2\\ E_1&=a^2N+aK_\alpha\\ E_2&=aN+K_\alpha \end{aligned}\right\} \qquad (135b)$$

Maier.—The second-order differential equation of Maier's theory is

$$E_0\,D^2y_0+E_1\,Dy_0+E_2y_0=0 \qquad (136a)$$

where

$$\left.\begin{aligned} E_0&=I_\psi v^2\\ E_1&=a^2N\\ E_2&=aN \end{aligned}\right\} \qquad (136b)$$

Kantrowitz.—Kantrowitz' theory leads to the third-order differential equation

$$E_0\,D^3y_0+E_1\,D^2y_0+E_2\,Dy_0+E_3y_0=0 \qquad (137a)$$

where

$$\left.\begin{aligned} E_0&=Iv^2L\\ E_1&=Iv^2+al_2N+l_2K_\alpha\\ E_2&=0\\ E_3&=aN+K_\alpha \end{aligned}\right\} \qquad (137b)$$

Wylie.—Wylie's theory leads to the third-order differential equation

$$E_0\,D^3y_0+E_1\,D^2y_0+E_2\,Dy_0+E_3y_0=0 \qquad (138a)$$

where

$$\left.\begin{aligned} E_0&=Iv^2L\\ E_1&=Iv^2+al_2N+l_2K_\alpha\\ E_2&=a^2N+aK_\alpha\\ E_3&=(aN+K_\alpha)\left(1+\frac{a}{L}\right) \end{aligned}\right\} \qquad (138b)$$

STABILITY OF MOTION

The basic equations of motion having been established according to the various theories for a rigid swiveling landing gear, attention will be directed next to the meaning of these different equations with respect to prediction of the shimmy behavior of the landing gear. However, before going into this subject in detail it may be useful to discuss briefly what sort of information is desired about the motion of a landing gear. Basically, the most important question is whether or not the motion is stable—that is, does the wheel tend to move in a straight line (with decaying shimmy oscillations or decaying aperiodic motion) or does the tire tend to move laterally out from its rectilinear course (with divergent shimmy oscillations or divergent aperiodic motion). To answer this question of stability for linear systems, the

analytic methods of Routh (ref. 26) or Hurwitz (ref. 27) or graphical methods similar to those introduced by Nyquist (refs. 28 to 31) are available. A brief discussion of these methods is given in appendix C. Any of these methods will provide for most cases a procedure for determining whether any particular combination of landing-gear parameters and rolling velocity is stable or unstable.

In general, for complicated problems, rather than investigate the stability of a landing gear by these methods for all possible conditions it may be more convenient and sometimes more valuable to draw various types of stability diagrams describing the system in question. For example, for case I a typical experimental type of stability diagram is shown in figure 7, which presents boundaries between the regions of stability and instability as functions of trail and rolling velocity for a specific landing-gear model. Another useful type of stability diagram for some problems might be a plot of boundaries between stable and unstable regions as functions of damping moment and rolling velocity.

In determining these stability boundaries, use is made of the well-known fact that the motion of a linear system can change from a stable to an unstable condition only where the motion is purely oscillatory—that is, where any variable, for example ψ, is of the form

$$\psi=\psi_m e^{i\nu_1 x} \tag{139}$$

or where the motion is purely uniform, of the form

$$\psi=\psi_m \tag{140}$$

Thus all possible stability boundaries can be obtained by directly substituting expressions of the form of equations (139) and (140) into the basic differential equations. In connection with the question of what form of the differential equation to use, it is of some importance to note that the final form, where the equation is expressed in terms of one variable, is often not the most convenient form to use. For example, for case I the purely oscillatory boundaries are most advantageously obtained by using equations (115) and (117) with the substitutions

$$\left.\begin{aligned}\psi&=\psi_m e^{i\nu_1 x}\\ y_0&=y_{0_{max}} e^{i(\nu_1 x+\sigma_1)}\end{aligned}\right\} \tag{141}$$

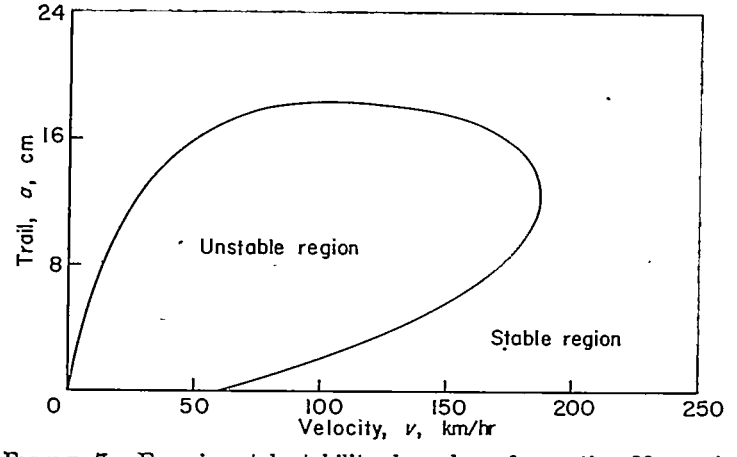

FIGURE 7.—Experimental stability boundary for a tire 29 cm in diameter (from ref. 17).

The advantage of this particular choice arises from the fact that it leads to two algebraic equations, one of which does not include the damping parameter g. This isolation of the parameter g usually eases slightly the mathematical labor of solving for the purely oscillatory boundaries.

The equations governing the stability boundaries for case I for the general theory and for the systematic approximations are listed in appendix D.

COMPARISON AND EVALUATION OF THE SUMMARY THEORY AND ITS SYSTEMATIC APPROXIMATIONS

The dual object of the present section is (1) to assess further the value of the summary theory by comparisons between the predictions of this theory and the available experimental data for case I conditions and (2) to determine, by comparison of the relative predictions of the summary theory and its systematic approximations, what is the simplest satisfactory systematic approximation to the summary theory. Discussion of the previously published theories, as applied to case I conditions, is contained in a subsequent section.

For convenience the following discussion is divided into separate considerations of stability-boundary conditions and unstable shimmy conditions.

Stability-boundary conditions.—The present section discusses theoretical and experimental stability-boundary conditions insofar as they are influenced by the tire parameters l_n (where $n=1, 2, \ldots$), ξ, K_γ, c_λ, N, and τ and by hysteresis effects. In the major part of this discussion the stability boundaries to be considered will be of the type obtained by plotting curves of trail against rolling velocity for those trail conditions that separate regions of stability and instability. The general shapes of these stability boundaries for case I, according to the summary theory and the systematic approximation theories A to D3, are sketched in figure 8 for the special condition of no damping or gyroscopic moments ($g=\tau=0$). It is seen that the summary theory and approximations A to C2 each predict that at high speeds the motion is stable for large trails and unstable for small trails; the horizontal boundary line is the same for each case, and is generally located at a trail roughly equal to the tire radius. (This boundary is theoretically completely independent of the spring restoring moment $\rho D_t\psi$ and is relatively independent of swivel-axis inclination κ.) Approximations D1, D2, and D3 fail to predict this boundary. Also, these three approximations, together with approximations C1 and C2, fail to predict any effect of rolling velocity on the low-speed stability boundaries, whereas, according to approximation B, for sufficiently small speeds the motion becomes stable for all small trails and, according to the higher theories, for most of the small-trail region. Also, at low speeds and large (usually impractical) trails the higher theories (B and above) indicate that the motion becomes unstable at sufficiently small speeds. The effects of the omitted damper and gyroscopic-moment terms would be to reduce the size of the regions of instability.

(a) Effect of higher l_n terms: As a first test of the summary theory and its systematic approximations there are available the experimental data of Von Schlippe and Dietrich (refs. 3, 4, and 5) which were obtained with a small model landing gear equipped with a pneumatic tire of 26 cm

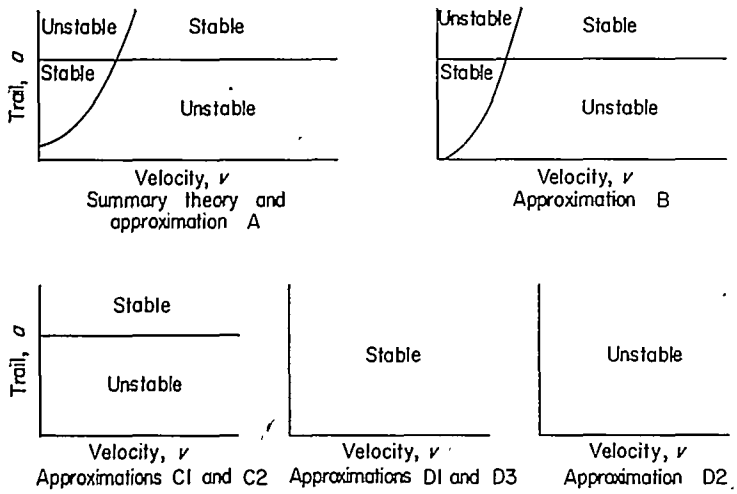

FIGURE 8.—Qualitative comparison of the stability-boundary predictions for case I according to the summary and systematic approximation theories neglecting damper and gyroscopic moments ($g=\tau=0$).

(10 in.) diameter. This model landing gear was tested at relatively low speed conditions where the higher l_n terms (l_2, l_3, . . .) are of some importance; consequently, these data provide an opportunity for testing the relative and absolute validity of the summary theory and the higher approximations A to C2 (which differ essentially only by their inclusion or omission of the higher l_n terms.)

The basic landing gear and tire constants for the Von Schlippe-Dietrich model, which was tested only in the untilted condition ($\kappa=0$), as taken from references 3 and 5, are as follows:

$$\kappa=\rho=g=0$$

$$I_\psi \approx 0.53+0.0025a^2 \text{ cm-kg-sec}^2$$

$$L=10 \text{ cm}$$

$$N=640 \text{ kg/radian}$$

$$K_\alpha=3{,}040 \text{ cm-kg/radian}$$

$$K_\lambda=45 \text{ kg/cm}$$

The quantities l_1, h, and the higher l_n's were calculated from the previously discussed relations $l_1=N/K_\lambda$, $h=l_1-L$, and $l_n=(nL+h)h^{n-1}/n!$. (See eqs. (77) and (19a).)

The experimental data obtained by Von Schlippe and Dietrich for this model are shown in figures 9 and 10, together with the corresponding predictions of the summary theory and the systematic approximations A to C2. (Also shown are the predictions of the theory of Von Schlippe and Dietrich which are discussed in a later section.) Figure 9 presents stability-boundary plots of trail against velocity, and figure 10 presents the frequency at these stability boundaries as a function of velocity. No theoretical curves are shown on these figures for approximations D1, D2, and D3 since these approximations are too crude to give any detailed information for this problem; they predict either completely stable or completely unstable motion for all positive trails (see fig. 8). The equations used to calculate the theoretical curves in these two figures are given in appendix

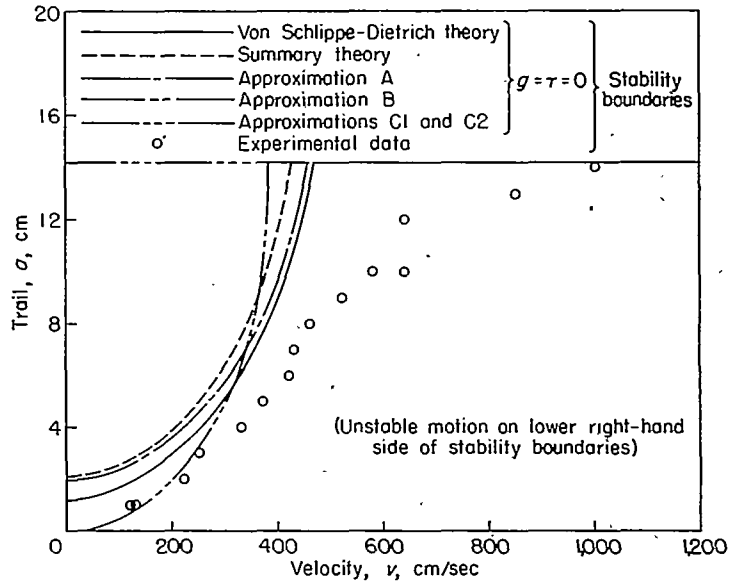

FIGURE 9.—Comparison of theoretical and experimental predictions of the stability boundaries for the Von Schlippe-Dietrich test model of references 3 to 5. (Hysteresis effects are neglected in these theoretical curves.)

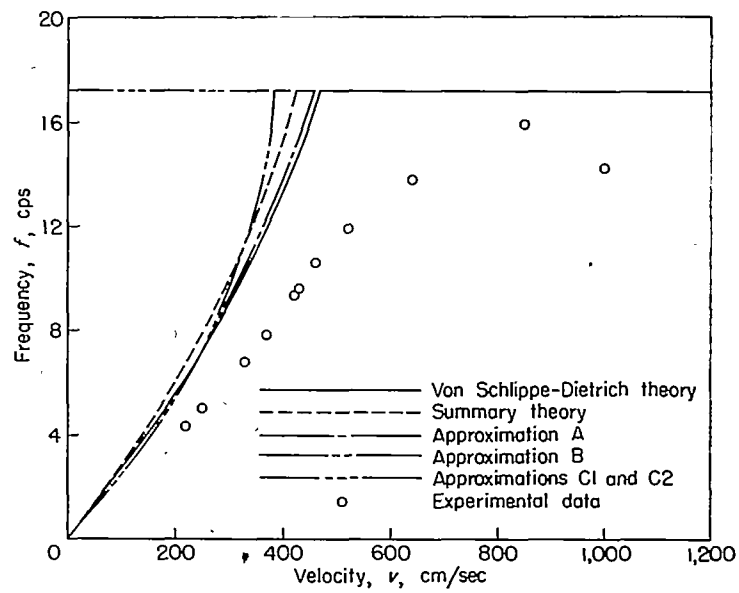

FIGURE 10.—Comparison of theoretical and experimental shimmy frequencies on the stability boundary for the Von Schlippe-Dietrich test model of references 3 to 5. (Hysteresis effects are neglected in these theoretical curves.)

D. In these calculations the gyroscopic torque term involving τ has been neglected since τ is unknown for these data. A rough value of τ could perhaps be estimated, but such a dubious estimate did not appear necessary because the term involving τ, according to any reasonable estimate of τ, would be of no importance in the velocity range of these experimental data.

In comparing the theoretical curves in figures 9 and 10 it is observed that approximation A gives a boundary very close to that of the summary theory. Approximation B does not give as close agreement but it is still fairly good and, more important, for most of the trail range the difference between approximation B and the summary theory is small as compared with the difference between the summary theory and the experimental data. As was previously noted, approximations C1 and C2 (which are identical for the

present condition of $\kappa=0$) predict a trail-velocity stability boundary which is independent of velocity so that this approximation is an inadequate representation of the summary theory at low velocities. However, at high speeds approximations C1 and C2 give the same stability boundary and frequency as the higher approximations.

As a further aid in comparing the different systematic approximations with the summary theory, figure 11 presents a plot of the linear damping coefficient g required to stabilize the motion of the Von Schlippe-Dietrich model at a medium trail of 7 cm as calculated according to the summary theory and the various systematic approximations (the equations used are presented in appendix D). This figure confirms the conclusions drawn from figures 9 and 10 that approximation A is a very good representation of the summary theory and that approximation B is also a good representation of the summary theory. However, more importantly, figure 11 demonstrates that approximations C1 and C2 also give a fairly good representation of the summary theory with respect to prediction of the maximum amount of damping (i. e., the maximum value of g) required for stabilizing the motion. Approximations D1, D2, and D3 are seen to give inadequate representations of the summary theory.

The preceding conclusions are, of course, only proven to be valid for the specific conditions of the Von Schlippe-Dietrich model tests. However, they are believed to be valid for most practical rolling conditions.

In considering the correlation between theory and experiment for the Von Schlippe-Dietrich test conditions, it is noted that the experimental stability boundary in figure 9 is of the same general shape as that given by the summary theory and approximations A and B but that it lies to the right of the theoretical curves and thus indicates that the experimental system is more stable than the theoretical system. Similarly, the experimental frequency-velocity curve in figure 10 falls below the theoretical curves. These discrepancies are perhaps a result of the neglect of hysteresis damping in the calculation of the theoretical curves of figures 9 and 10 and are discussed more fully in the next section.

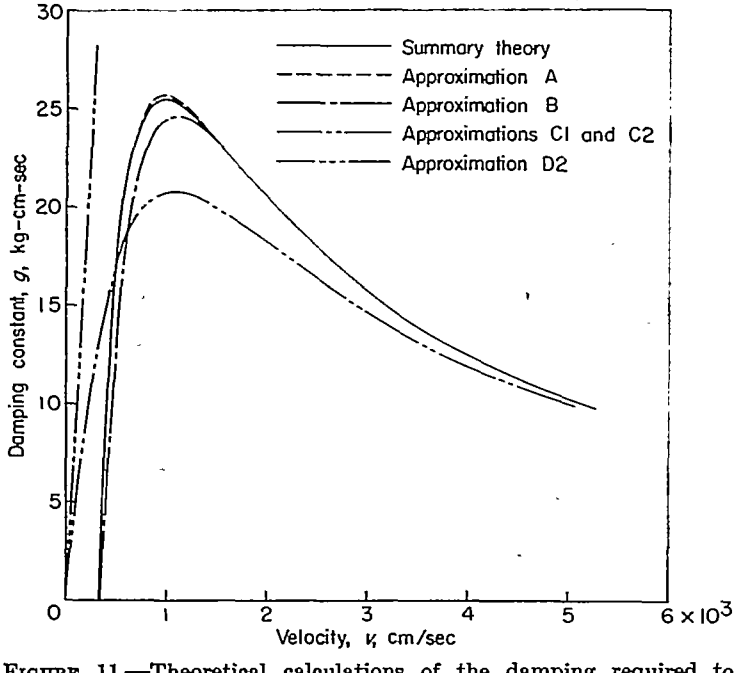

FIGURE 11.—Theoretical calculations of the damping required to stabilize the motion of the Von Schlippe-Dietrich model landing gear at a trail of 7 cm. (No damping required according to approximations D1 and D3.)

(b) Effect of hysteresis: In order to investigate whether the discrepancies between theory and experiment shown in figures 9 and 10 might be explained by a consideration of hysteresis effects, some results of calculations involving hysteresis effects are shown in figures 12 and 13 for the same test conditions as in figures 9 and 10. Figures 12 and 13 present theoretical calculations of trail-velocity and frequency-velocity stability boundaries, respectively, both with and without consideration of hysteresis effects, together with Von Schlippe and Dietrich's experimental data. The curves for the Von Schlippe-Dietrich theory were calculated by using Von Schlippe and Dietrich's theory with their hysteresis equations (see eqs. 128), whereas the curves for

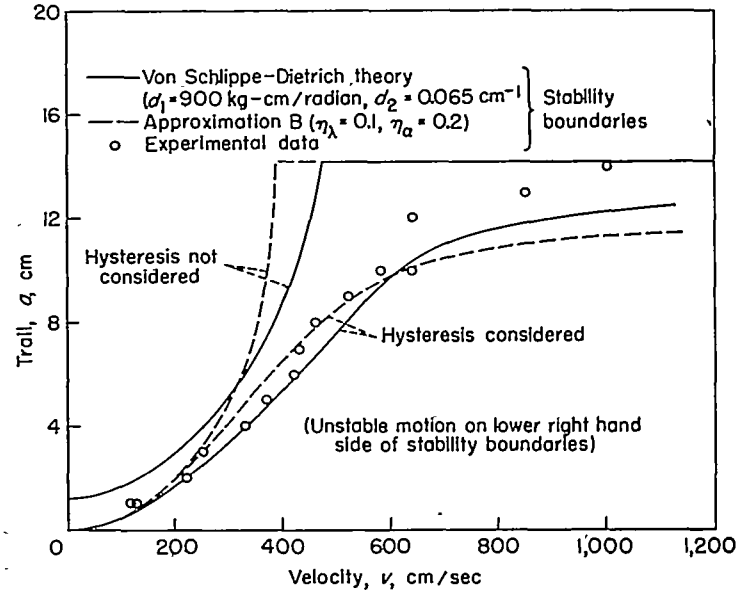

FIGURE 12.—Effects of hysteresis on the stability boundaries for the Von Schlippe-Dietrich test model of references 3 to 5.

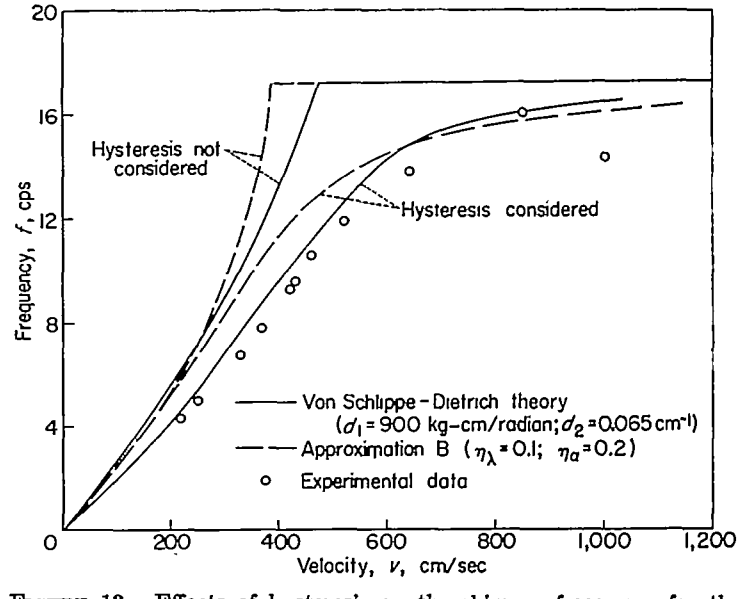

FIGURE 13.—Effects of hysteresis on the shimmy frequency for the Von Schlippe-Dietrich test model of references 3 to 5.

approximation B were calculated by using the equations for hysteresis effects derived in the present report (see appendix B). The values of η_λ and η_α indicated in these figures, which were used in these calculations, were estimated from static hysteresis-loop data, partly unpublished and partly published in reference 24. The values of d_1 and d_2 used were taken from reference 5. It is observed from these figures that there is a considerable difference between the calculations according to either theory, depending on whether hysteresis effects are included or omitted. Moreover, it is seen that either theory provides fairly good agreement with the experimental data when the hysteresis effects are taken into account. These facts suggest that hysteresis effects may be an important factor which must be taken into account in order to obtain good agreement between theory and experiment. On the other hand, neither the Von Schlippe-Dietrich nor the present report's consideration of the hysteresis effects seems to rest on a completely sound foundation. Thus it appears safe to conclude only that since two different approaches to the hysteresis problem indicate that hysteresis effects are important, a more rigorous analysis of the hysteresis problem would be worthwhile.

(c) Effect of l_1: The next test of the summary theory makes use of the experimental data of Melzer (ref. 10), who performed a series of tests with an untilted ($\kappa=0$) solid rubber tire 7 cm (3 in.) in diameter at sufficiently high speeds so that his data would be expected to fall considerably to the right of the curved-line low-speed stability-boundary curve in the first two sketches of figure 8. For this velocity range the predictions of the summary theory and approximations A to C2 are identical; they all predict that the undamped ($g=\tau=T_\lambda=T_\alpha=0$) motion is stable for all values of trail a greater than $l_1=N/K_\lambda$; that is, the critical value of trail a_c at which the motion changes from an unstable state to a stable one is given by the relation $a_c=l_1$. (Even if gyroscopic moments are taken into account, this equation is only slightly modified throughout a relatively large range of rolling velocity; however, for very large velocities this relation breaks down as a result of the gyroscopic moment and the motion becomes stable for all positive trails. This phenomenon will be discussed in a subsequent section.) The prediction $a_c=l_1$ is well confirmed by Melzer's tests, as is illustrated in the following table of data taken from reference 10, which lists the experimental values of l_1 together with the trail required for stability for several conditions of vertical loading:

F_z, kg	1	2	2.8	3.6
$l_1=N/K_\lambda$, cm	2.58	2.85	3.22	3.40
a_s, cm	2.5	3.0	3.1	3.4

These particular data were taken for the case where no spring restoring force acted on the model landing gear ($\rho=0$). Similar good agreement was obtained for the case where a strong linear spring restoring moment was present ($\rho>K_\alpha$). For this case, according to the summary theory and approximations A to C2, the stability boundary for the positive trail condition is the same as for the case of no spring restoring force. This prediction is well confirmed by Melzer's tests, as is illustrated in the following table of data also taken from reference 10.

F_z, kg	1	2	2.8	3.6
$l_1=N/K_\lambda$, cm	1.96	2.60	2.90	2.91
a_s, cm	2.0	2-2.25	≈2.7	≈2.8

(The difference between the values of l_1 in these two tables is merely a consequence of changes in tire characteristics between the corresponding tests.)

In order to assess the significance of the preceding comparisons of theory and experiment it should be noted that the theoretical relation $a_c=l_1$, calculated for $g=\tau=T_\lambda=T_\alpha=0$, is independent of spring restoring moment ρ and tire torsional stiffness K_α and, in the velocity range discussed, can be shown to be not strongly influenced by gyroscopic or hysteresis moments (τ, T_λ, and T_α) or by the higher l_n's (l_2, l_3, . . .). Consequently, this comparison tells practically nothing about the correctness of the manner in which these important quantities have been inserted into the summary theory. On the other hand, the theoretical relation $a_c=l_1$ depends almost entirely on the correctness of the kinematic equation of the summary theory which, for Melzer's test conditions, reduces to the kinematic equation of approximation C2 (eq. (85)):

$$\lambda_0=-l_1\alpha$$

Thus, the results of the preceding comparison indicate that there exists a range of rolling speeds in which the kinematic equation of the summary theory, as well as of approximations A to C2, is reasonably correct (except possibly for the terms involving ξ, which are as yet not evaluated and are not very important).

It can be said with safety that the range of velocity for which the theory gives good agreement with Melzer's model data corresponds to full-scale conditions somewhere inside the practical rolling speed range and possibly covering much of the practical range. However, the preceding comparison definitely does not prove anything about the adequacy of the summary theory for small velocities or for the highest velocities which may be encountered in practice.

Further confirmation of the preceding conclusions is provided by the experimental data of Schrode (ref. 17) who performed tests, similar to those of Melzer, for realistic pneumatic tires as large as 39 cm (15 in.) in diameter, as compared with the small 7 cm (3 in.) solid rubber tire tested by Melzer. Schrode obtained trail-velocity stability-boundary plots of the type illustrated in figure 7. These stability-boundary plots indicate the same result as Melzer's data, namely, that there exists a range of velocity in which the motion is stable above a certain critical trail a_c and unstable below it. (This velocity range for the data in figure 7 is approximately 60 to 160 km/hr.) It is not possible to check quantitatively the theoretical stability-boundary equation $a_c=l_1$ for Schrode's data because Schrode provides no information suitable for accurately evaluating l_1. However, some qualitative confirmation may be found, since the quantity l_1 always appears to be of the order of magnitude of the

tire radius r and for Schrode's data a_c is found to be of this same order of magnitude (e. g., see fig. 7). Thus Schrode's experimental data appear to confirm the previously drawn conclusion that there exists a velocity range in which the kinematic equations of the summary theory and approximations A to C2 are valid.

Dietz and Harling have presented some similar stability-boundary curves in reference 16 which also confirm the foregoing conclusions.

(d) Effect of ξ: Some insight into the effect of the tilt parameter ξ can be obtained by an examination of the effects of swivel-axis inclination κ on the stability boundaries according to the predictions of approximation C1 for the condition where damping, spring-restoring, and gyroscopic moments are neglected ($g=\rho=\tau=0$) in order to isolate the effects of inclination. (These assumptions appear to be justified for the experimental conditions discussed in this section.) Under these assumptions one theoretical stability boundary is given by the equation

$$a_c=l_1\cos\kappa+\frac{\xi Lh}{r}\sin\kappa \tag{142}$$

Experimental data suitable for testing this relation are available in reference 16 for an inclination range of $-20°<\kappa<20°$ for one constant-velocity condition. These experimental data, some of which had to be slightly extrapolated from the data in reference 16, are shown in figure 14 together with the predictions of equation (142) for values of ξ equal to 0 and 1. Although reference 16 does not supply the values of L, h, and l_1 needed for calculations, the assumed values indicated on the figure are probably accurate enough to justify the following more or less qualitative observations. (The value of l_1 was chosen so as to make the calculated and experimental values agree for the case $\kappa=0$.) It is noted that the experimental variations and the theoretical variations for $\xi=0$ are in fairly good agreement and also that these two variations are more or less symmetrical with respect to positive and negative values of κ. On the other hand, the theoretical curves for $\xi>0$, such as the indicated curve for $\xi=1$, will all be unsymmetrical. Thus, it appears that ξ is probably close to zero. In this connection it might be noted that Greidanus' theory, which is the only known theory that uses a term corresponding to ξ, implies a value of $\xi>1$ (compare eqs. (100) and (101)).

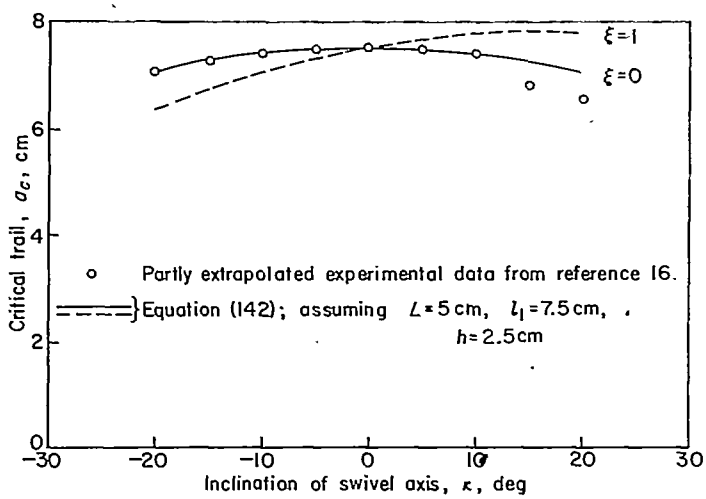

FIGURE 14.—Influence of swivel-axis inclination on the stability boundary. Tire approximately 12 cm in diameter; $F_z=6.25$ kg; $v=19$ km/hr.

(e) Effects of K_γ and c_λ: In order partly to assess the importance of the tire parameters K_γ and c_λ, the special case of approximation C2 where $\tau=\rho=0$ and $l_1\cos\kappa-a=0$ will be considered. While this particular case is of no practical importance in itself, its examination permits some insight into the effects of the tire parameters K_γ and c_λ. For this case the damping required to stabilize the motion is given by the inequality

$$[a(aN+K_\alpha\cos\kappa)+\rho_\kappa l_1]\,gvl_1+I_\psi gv^3+g^2v^2l_1>0$$

where ρ_κ is given by equation (115c). It is evident from this relation that ρ_κ is a stabilizing term if positive and destabilizing if negative. Also, according to reference 2, K_γ may be as large as F_z and, according to reference 24, $c_\lambda\approx0.75$. Thus, according to equation (115c), if the small $\sin^2\kappa$ term is neglected, ρ_κ may be positive for positive κ, whereas if the K_γ, c_λ, and c_γ terms are neglected (as has been done in all previous investigations except ref. 2) then ρ_κ is always negative for positive κ. Therefore, if situations should arise wherein ρ_κ is important, it is not necessarily safe to neglect the terms involving c_λ and K_γ that are used in the determination of ρ_κ. (See eq. (115c).)

(f) Effect of cornering power N: As a rough check on the variation of the tire cornering power N under dynamic conditions, there are available experimental frequency data obtained by Melzer in connection with his previously mentioned tests on an uninclined ($\kappa=0$) model landing gear equipped with a solid rubber tire of 7 cm (3 in.) diameter (ref. 10). For the higher velocity conditions of Melzer's tests, the predictions of the summary theory and approximations A to D1 lead to the frequency equation

$$f=\frac{1}{2\pi}\sqrt{\frac{aN+K_\alpha+\rho}{I_\psi}} \tag{143}$$

for an uninclined and undamped landing gear, that is, for $\kappa=\tau=g=0$. (Inclusion of the effect of finite τ in this equation would not significantly alter this equation for the test conditions to be discussed herein.) Some of Melzer's experimental data are compared with the predictions of this equation in the following table for the condition $\rho=0$. The

F_z, kg	2.8		3.6		
a/l_1	0.47	0.78	0.44	0.73	0.88
$f_{calculated}$, cps	3.8	4.5	4.0	4.8	5.1
$f_{experimental}$, cps	3.3	3.5	2.7	4.1	4.7

experimental data shown represent Melzer's data for the highest velocity conditions tested. The theoretical and experimental values are seen to be in fair agreement. However, the experimental values are somewhat smaller than the corresponding theoretical values. This discrepancy is believed to be largely due to the fact that these experimental tests were not conducted at sufficiently small values of shimmy amplitude for the assumptions of a linearized theory to be valid. Specifically, all of Melzer's frequency data

were obtained for maximum swivel angles of 5° or larger. (The data shown in the preceding table correspond to the condition $\theta_m=5°$.) Moreover, Melzer's data indicate that there is a fairly definite decrease in shimmy frequency with increasing maximum swivel angle. A sample plot of Melzer's data illustrating this effect is given in figure 15. Also shown is the theoretical calculation, which is valid only for $\theta_m=0°$. If allowance is made for a certain amount of experimental error, extrapolation of the experimental data to $\theta_m=0°$ could be considered as confirmation of the theory. It should be noted, however, that much of the rest of Melzer's data, while not necessarily disputing this conclusion, do not so clearly support it. Also, plots of the type of figure 15 are of limited significance since each test point shown corresponds to a different rolling velocity. In view of these considerations, the only reasonable conclusion that can be reached appears to be that Melzer's data roughly confirms the theoretical frequency and does not conclusively dispute its quantitative accuracy.

Melzer has also conducted frequency tests on the same model with an additional strong restoring spring (spring stiffness several times the tire torsional stiffness). A comparison of theoretical and experimental frequencies for this test is shown in the following table:

F_z, kg	2.0	2.8		3.6	
a/l_1	0.77	0.69	0.86	0.69	0.86
$f_{calculated}$, cps	5.2	5.4	5.7	5.5	5.8
$f_{experimental}$, cps	4.9	5.45	5.9	5.8	5.85

The much better agreement obtained for this case is explained by the predominant influence of the spring restoring moment, since for large values of ρ the model system approaches the condition of a simple torsional oscillator with moment of inertia I_ψ and spring constant ρ, for which condition the well-known frequency equation is $2\pi f=\sqrt{\rho/I_\psi}$.

In order to assess the significance of the preceding comparisons, the quantities involved in the theoretical equation (143)—a, N, K_α, ρ, and I_ψ—will be considered. The quantities a, ρ, and I_ψ are easily measured constants and, for most of Melzer's data, K_α is much smaller than aN; therefore, the preceding fair agreement between theory and experiment indicates that the quantity N (the tire cornering power), which was considered to be a constant in the preceding calculations, actually does not vary extremely with rolling velocity and shimmy frequency—at least not for Melzer's test conditions.

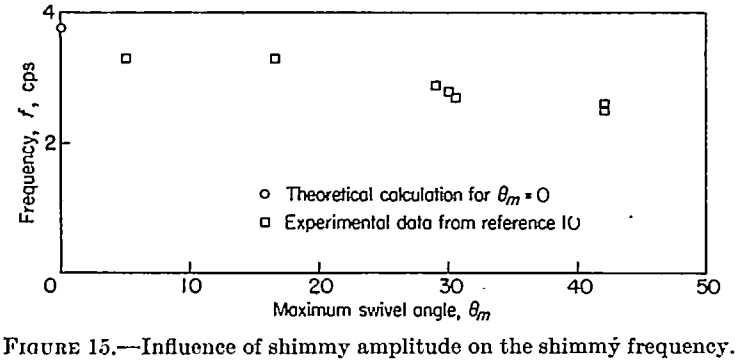

FIGURE 15.—Influence of shimmy amplitude on the shimmy frequency.

(g) Effect of gyroscopic torque: The next question to be considered is the influence of the gyroscopic torque resulting from lateral distortion of the tire. All pertinent experimental data obtained at very high speeds (e. g., ref. 10; see also fig. 7) demonstrate that at sufficiently high speeds the previously discussed conclusion that high-speed motion is unstable for trails less than l_1 is no longer valid. Instead, the experimental data show that at these very high speeds instability at any given positive trail ceases above a certain critical velocity. The existence of this critical velocity will now be shown to result, at least in part, from the gyroscopic action which was previously included only in Kantrowitz' theory (ref. 8) but was not specifically mentioned there. The simplest systematic approximation that adequately provides for this effect is approximation C2. In order to isolate the gyroscopic effect, the special condition of no tilt ($\kappa=0$) and no spring-restoring force ($\rho=0$) or damper ($g=0$) will be considered. For this condition the equation for the stability boundary of approximation C2 (or C1) reads

$$(I_\psi v_c^2+\underline{a\tau v_c^2 l_1})\,(a^2N+aK_\alpha+\underline{l_1\tau v_c^2})=I_\psi v_c^2 l_1\,(aN+K_\alpha) \quad (144)$$

where the underlined terms are the gyroscopic terms. For the computation of the critical velocity v_c this equation may be simplified still further if it is realized that the quantity $a\tau l_1$ is small in comparison with the moment of inertia I_ψ about the swivel axis; hence, for an approximate calculation the term $a\tau v^2 l_1$ can be omitted. Then solution of equation (144) for the critical velocity v_c above which the system is stable yields the expression

$$v_c=\sqrt{\frac{(l_1-a)(aN+K_\alpha)}{l_1\tau}} \quad (145)$$

which is observed to give an infinite critical velocity for zero gyroscopic action ($\tau=0$).

The only available experimental data containing enough information on the tire constants that are necessary for checking the validity of equation (145) are Melzer's data (ref. 10) and even these data do not provide the required gyroscopic moment; therefore, it can only be crudely estimated as follows: The mass of the tire will be of the order of magnitude $w_1[2\pi(r-r_4)]\pi r_4^2$, where r is the overall tire radius, r_4 the radius of the cross section of the tire torus, and w_1 the average tire density. The moment of inertia will be the mass times the radius of gyration r_g squared; thus, with $\tau_1=\frac{1}{2}$ according to Kantrowitz, τ (eq. (33)) becomes

$$\tau=\frac{\pi^2 w_1 r_4^2(r-r_4)r_g^2}{r(r+r_3)}$$

For the usual tire $r_4\approx 0.3r$, r_3 is slightly smaller than r (say $r_3\approx 0.9r$), and r_g is probably around $0.8r$. Then, to a crude approximation, $\tau\approx 0.21 w_1 r^3$. For Melzer's solid rubber tire $r=3.5$ cm and w_1 is probably about 10^{-6} kg-sec^2/cm^4 (specific gravity of 1); thus $\tau\approx 10^{-5}$ kg-sec^2/cm. Critical velocities calculated from equation (145) with this value of τ are compared in figure 16 with some of Melzer's experimental data for one test condition at various values of a/l_1. The calculated and experimental values of critical velocity are seen to be of the same order of magnitude.

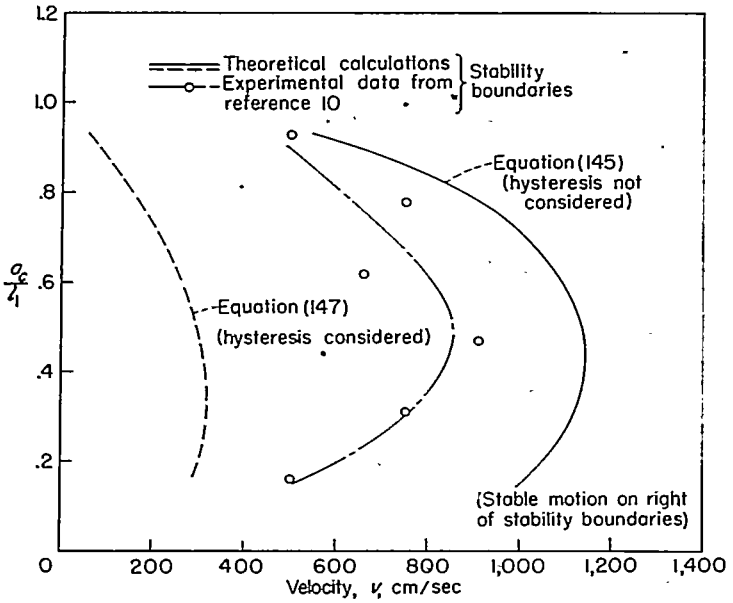

FIGURE 16.—Comparison of theoretical and experimental variations of critical trail with rolling velocity. $r=3.5$ cm; $l_1=3.22$ cm; $N=12.3$ kg; $K_\alpha=5.9$ kg-cm; $\eta_\lambda=.0;1$ $\eta_\alpha=0.2$.

Since neglect of the gyroscopic moment gives, theoretically, an infinite critical velocity, this agreement indicates that the gyroscopic moment is an important factor in producing stability at high velocities. Also, the theoretical calculation is conservative, that is, the unstable region is overestimated. The quantitative agreement between theory and experiment is fair but far from excellent. One probable reason for some of the disagreement is the relatively crude procedure used for estimating the parameter τ. Another possible explanation may lie in hysteresis effects, as follows:

If the differential equation for approximation C2 (see eq. (124a)) is modified to take into account hysteresis forces and moments in the manner suggested in this report, a modified differential equation results (see eq. (B2)), which has the stability boundary equation

$$(I_\psi v_c^2+\underline{a\tau v^2 l_1+a^2NT_\lambda v_c+aK_\alpha T_\alpha v_c})(a^2N+aK_\alpha+ l_1\tau v_c^2+aNT_\lambda v_c+K_\alpha T_\alpha v_c)=I_\psi v_c^2 l_1(aN+K_\alpha) \quad (146)$$

for the same conditions as the corresponding equation (144), namely, $\kappa=\rho=g=0$. After neglecting the underlined terms, which are relatively small at large velocities, this equation can be expressed in the simpler and more easily interpreted form

$$v_c^2+\frac{aNT_\lambda+K_\alpha T_\alpha}{l_1\tau}v_c=\frac{(l_1-a)(aN+K_\alpha)}{l_1\tau} \quad (147)$$

This equation indicates that the effect of finite hysteresis (that is, $T_\lambda\neq 0$; $T_\alpha\neq 0$) is to reduce the critical velocity below what it would be for no hysteresis effect ($T_\lambda=T_\alpha=0$). This result is also indicated in figure 16, where calculated and experimental curves are shown for the previously discussed high-speed conditions of Melzer's model tests. (The values of T_λ and T_α needed for these calculations were obtained from equations (60), (62), and (143), by using the previously mentioned estimated values of $\eta_\lambda=0.1$ and $\eta_\alpha=0.2$, based on static hysteresis loops.) In figure 16 the experimental data lie between the theoretical curves for "hysteresis considered" and "hysteresis not considered." The theoretical calculation that includes hysteresis is extremely unconservative. Two conclusions can be drawn from these observations. First, if the actual hysteresis effect at high speeds is only a fraction of the calculated effect, this fact might explain the difference between the experimental curve and the theoretical curve that does not include hysteresis. Second, as was previously noted, it is evident that the treatment of hysteresis effects in the present report is inadequate and unconservative at high velocities.

In concluding this discussion of gyroscopic torque, it should be noted that for the case of a rigid landing gear the critical design condition (velocity at which shimmy is most intense) occurs at low rolling speeds where the gyroscopic moment is insignificant. Thus, the inclusion of this gyroscopic moment in the theory is of somewhat academic interest (at least for case I) and it probably could be safely omitted in practical design calculations.

Unstable shimmy conditions.—As a further overall check of the summary theory and its systematic approximations, the experimental data of Kantrowitz (ref. 8) for unsteady shimmy conditions are available.

The significant features of unsteady shimmy motion are the divergence and frequency of the oscillation, which are simply the real and imaginary parts of the roots of the characteristic algebraic equation corresponding to the differential equation in question. Kantrowitz has made measurements of these quantities for a model tire of 4-inch diameter at inclination angles κ of 5° and 20° with corresponding trails of about $0.08r$ and $0.31r$, respectively (ref. 8). His experimental results for $\kappa=5°$ are presented in figure 17, together with corresponding theoretical calculations made according to approximation B, which is the simplest systematic approximation to the summary theory which describes, at least qualitatively, the shimmy phenomena throughout the complete range of rolling velocity. The theoretical and experimental frequencies are seen to be in fairly good agreement. The theoretical and experimental divergences are in fair qualitative agreement, but the experimental variation is sometimes considerably below the corresponding theoretical one. This quantitative disagreement may be due to several factors. First, hysteresis effects are neglected in the theoretical calculations. Although use of the hysteresis force and moment equations derived in this report would not completely explain the disagreement, it is believed that these hysteresis equations are not accurate enough, particularly at small trails ($a=0.08r$ for the data in fig. 17), to justify the conclusion that the disagreement cannot be explained by hysteresis effects. A second partial explanation of the disagreement arises from the fact that the theoretical calculations may be based on insufficiently accurate values of the necessary tire parameters, since Kantrowitz did not make direct measurements of all of the most fundamental tire parameters, such as h, a, N, and K_α. Specifically, he measured only the quantity L, a quantity approximately equal to $aN\cos\kappa+K_\alpha\cos^2\kappa$ for 2 values of κ, and the path frequency ν_1 and trail a for kinematic shimmy (shimmy with velocity approaching zero). The basic tire parameters used for calculating the theoretical curves in figure 17 were

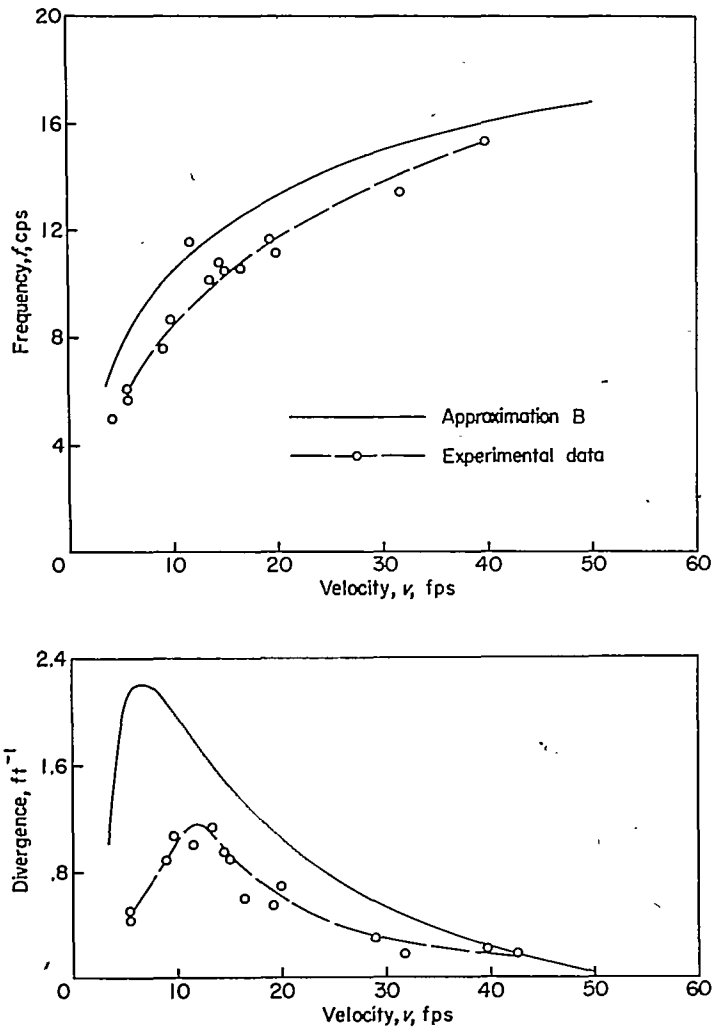

FIGURE 17.—Comparison of theoretical and experimental shimmy frequency and divergence for Kantrowitz' experimental data. $\kappa=5°$.

approximately deduced from these quantities as follows: The quantity h was obtained from equation (D1) after setting v equal to 0 and substituting Kantrowitz' experimental values of L, ν_1, and a for kinematic shimmy. This procedure for determining the quantity h is not necessarily accurate since equation (D1) neglects hysteresis effects. The tire deflection needed for calculating the trail was estimated from figure 8 of reference 2. The trail was computed from the tire radius, the tire deflection, and the inclination. With the aid of this estimated value of trail the tire parameters N and K_α can be obtained from Kantrowitz' approximate values for $aN\cos\kappa+K_\alpha\cos^2\kappa$. In addition, most tire tilt effects were neglected; specifically, ξ and ρ_κ were taken equal to zero. While the foregoing procedure will probably give roughly correct values for most of the fundamental tire constants, it is believed that the limitations of this procedure and the neglect of hysteresis effects are sufficient to prohibit the making of any strong point out of the discrepancies between theory and experiment in figure 17. Thus, to summarize, it appears that Kantrowitz' data furnishes only a rough overall confirmation of the summary theory. Although quantitative agreement is poorer than for most of the previously discussed experimental data, this poorer agreement is not necessarily significant.

This completes the discussion of case I with respect to the summary theory and its systematic approximations. Next, attention will be directed to a discussion of case I with respect to the predictions of some of the previously published theories.

PREDICTIONS OF SOME OF THE PREVIOUSLY PUBLISHED THEORIES

Some interesting features of the previously published theories in relation to case I are discussed in the following paragraphs. Comments on the influence of swivel-axis inclination will not be repeated here.

The theory of Von Schlippe and Dietrich gives predictions which are substantially the same as the predictions of the summary theory, as can be seen by a comparison of the predictions of these two theories in figures 9 and 10 for Von Schlippe and Dietrich's model test conditions. Hysteresis effects were neglected in computing both sets of theoretical curves. In comparing these two theories it should be noted that the only difference in the two sets of theoretical curves arises from a slight difference in the expressions used for the elastic forces and moments of the tire (see section entitled "Forces and Moments on the Wheel" and the comments after eq. (128)). The Von Schlippe-Dietrich theory also provides for some tire width effects, but these effects are believed to be relatively small for the present test conditions and were not taken into account in computing the theoretical curves in figures 9 and 10. From these figures it is seen that the differences between the stability boundaries and frequency curves for the Von Schlippe-Dietrich theory and the summary theory are usually small in comparison with the differences between the theoretical curves and the experimental data. Thus, it seems reasonable to conclude that there is no significant difference between the main features of the summary theory and the Von Schlippe-Dietrich theory.

Bourcier de Carbon's advanced theory provides essentially the same predictions as approximation B and will thus probably give a reasonable prediction of shimmy behavior for the complete velocity range. Similarly, Bourcier de Carbon's elementary theory, corresponding to approximation C2, will probably give reasonable predictions for the high velocity range.

Melzer's theory correctly predicts the existence of the large-trail stability boundary given by the equation $a_c=l_1$, but it also predicts the existence of stable motion in the small negative trail region between zero trail and a trail equal to $-\epsilon=-K_\alpha/N$. The latter prediction is in disagreement with the experimental data of Von Schlippe and Dietrich (ref. 5) who conducted some tests in this trail range and found the motion there to be unstable.

The stability boundary according to Moreland's advanced theory for the case of no damping or spring-restoring forces (see eq. (132a)) is given by the equation

$$v_c\sqrt{\frac{I_\psi}{Nl_1^3}}=\frac{1}{\sqrt{\tau_2}}\left(\frac{1}{1-\frac{\tau_2 a_c}{l_1}}-\frac{a_c}{l_1}\right) \tag{148}$$

where

$$\tau_2=\frac{Nl_1T^2}{I_\psi}$$

This equation is plotted in figure 18 for zero time constant

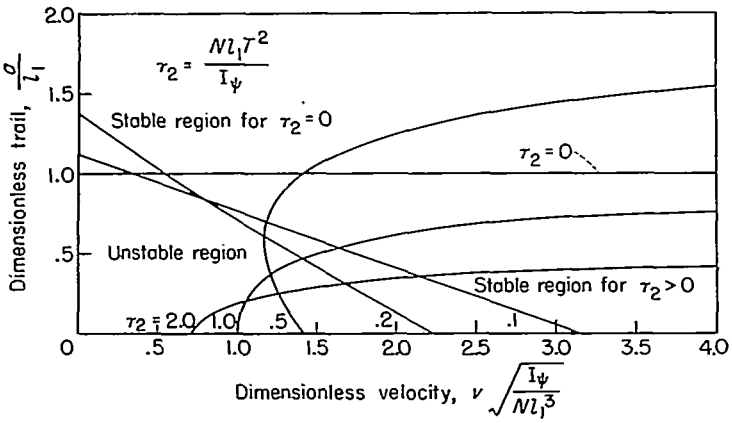

FIGURE 18.—Variation of critical trail with rolling velocity according to Moreland's advanced theory.

(for which case Moreland's theory reduces to the subcase of approximation C2 for which $\epsilon = K_\alpha = 0$) and for several finite values of the time-constant parameter τ_2. It is seen that if τ_2 is large, a large-trail stability boundary no longer exists at the trail $a_c = l_1$. Since the actual existence of this large-trail stability boundary has already been demonstrated, it appears likely that τ_2 cannot be very large. On the other hand, if τ_2 is small the introduction of the time-constant term produces an almost linear decrease of critical trail with increasing velocity until a certain limiting velocity (equal to l_1/T) is reached; above this velocity all motion is stable. Thus, the influence of the time-lag constant term is somewhat like that of the previously discussed gyroscopic moment due to tire distortion or the hysteresis force and moment, which may also produce stability at high velocities. However, in regard to the general shape of the critical trail-velocity curve, the variations predicted by consideration of the gyroscopic or hysteresis effects (see solid and dashed lines in fig. 16) appear more like those of the experimental data (figs. 7 or 16) than does the nearly linear variation predicted from Moreland's time-lag term for small τ_2.

Moreland's elementary theory, Temple's elementary theory, and Maier's and Taylor's theories are too crude to give any details for case I.

Kantrowitz' theory incorrectly predicts instability for all positive trails in the absence of damping or gyroscopic moments. (This prediction is a consequence of the fact that the third coefficient in Kantrowitz' differential eq. (137a) is zero.)

Wylie's theory (see eqs. (138)) correctly predicts the existence of stability at large trails; however, the predicted value of critical trail is given by the equation

$$a_c(a_c+\epsilon)Nl_2 = Iv^2L \qquad (149)$$

for $\kappa = 0$. This relation implies that the critical trail is a continuously increasing function of velocity, whereas the previously discussed experimental data clearly indicate that the critical trail rapidly reaches the maximum value l_1. Also it is noted that the last of Wylie's equations (138b) contains the factor $1+a/L$, which does not appear in any of the other theories. This term appears as a consequence of the earlier mentioned fact that Wylie's theory does not correctly predict the influence of trail for the yawed rolling condition. It might be noted that if Wylie's theory were modified to remove this difficulty, as suggested in equation (110), then this factor $1+a/L$ would be replaced by 1; thus the modified Wylie theory would be more consistent with the other equations. Also, for high velocities the modified Wylie theory would more correctly predict a definite critical trail according to the relation $a_c = L$.

PRACTICAL APPLICATION

Before concluding the discussion of case I, it is perhaps pertinent to comment on whether the preceding theoretical predictions for this idealized case can be applied to practical landing-gear problems. Moreland has demonstrated that neglect of the torsional and lateral elasticity of the landing-gear strut can sometimes lead to false predictions of stability in an actually unstable system (ref. 12). For example, for too large torsional damping the torsional damper unit effectively locks the swiveling structure against torsional movement with respect to its point of attachment to the landing gear strut, so that torsional movement of the swiveling structure is possible only as a consequence of the always finite torsional stiffness of the strut. In other words, for too large damping the damper unit and strut combination behaves like a pure torsion spring and is thus ineffective for damping purposes. In regard to lateral strut stiffness Moreland has pointed out that for a rigid tire, corresponding to approximation D3, if the strut is prohibited from lateral motion, as is assumed for case I, the motion is stable; on the other hand, if the strut is assumed to be of stiffness approaching infinity, the system may be unstable. While this particular criticism of the practical value of case I for infinite stiffness applies only to approximation D3, still for finite strut stiffness of the same order of magnitude as the tire lateral stiffness the theoretical equations of the other approximate theories may also be unconservative.

CASE II

This section is concerned with the idealized landing gear shown in figure 6. This landing gear consists of a wheel free to swivel about an uninclined always-vertical swivel axis that is attached by a horizontal linear spring, of spring constant k, to the supporting structure. This configuration, case II, is discussed here for two reasons: it illustrates the effect of structural elasticity on wheel shimmy, and it is better suited than case I for evaluating approximations D1, D2, and D3 as applied to landing-gear problems involving structural elasticity. (It may be recalled that these three approximations were of little value in dealing with a rigid landing-gear strut (case I); however, for a flexible strut these approximations may sometimes be of value.) In discussing case II, and also later cases, no further mention will be made of the previously published theories or of the question of agreement between theory and experiment; all discussion will be restricted to the summary theory and its systematic approximations.

The discussion of case II proceeds as follows: The equations of motion for case II are derived according to the summary theory and its systematic approximations. As for case I, it is more convenient to rederive these equations of motion in a slightly different manner rather than to apply the equations derived earlier for the completely general

case. After these derivations are made the equations for the stability boundaries are established. Finally, the damping required to prevent shimmy is presented in curves as a function of strut stiffness and rolling velocity for a specific sample landing-gear configuration according to the predictions of approximations C, D1, D2, and D3. (For the present case approximations C1 and C2 are identical and are henceforth referred to collectively as approximation C.) These curves are utilized to obtain some insight into the accuracies of the predictions of approximations D1, D2, and D3 with respect to the more advanced approximation C.

GENERAL DERIVATION

The derivation of the equation of motion for the summary theory proceeds as follows. The details of the landing gear considered are illustrated in figure 6. This gear has a rigid symmetrical swiveling part having a mass m and a moment of inertia about its center of gravity I_0. The nonswiveling part of the landing gear consists of a spring of stiffness k with an attached mass m_1. The lateral displacement of the swivel axis is designated as η_a.

Setting the sum of the lateral spring and inertia forces acting on the swiveling part equal to the inertia reaction of its center of gravity $m\,D_t^2(\eta_a-c_2\theta)$ yields the relation

$$K_\lambda\lambda_0-k\eta_a-m_1\,D_t^2\eta_a=m\,D_t^2\eta_a-mc_2\,D_t^2\theta \qquad (150)$$

Substitution for λ_0 from the relation

$$\lambda_0=y_0-\eta_0=y_0-\eta_a+a\theta \qquad (151)$$

(see fig. 6) yields, after rearrangement,

$$K_\lambda y_0-(m_1\,D_t^2+m\,D_t^2+K_\lambda+k)\eta_a+(mc_2\,D_t^2+aK_\lambda)\theta=0 \qquad (152)$$

Setting the sum of the moments about the center of gravity of the swiveling part equal to the inertia reaction yields the result

$$K_\alpha\alpha-K_\lambda\lambda_0c_1-k\eta_ac_2-m_1\,D_t^2\eta_ac_2-g\,D_t\theta-\rho\theta-\tau v\,D_t\lambda_0 = I_0\,D_t^2\theta \qquad (153)$$

(see fig. 6) where I_0 represents the moment of inertia of the swiveling structure at its center of gravity ($I_0=I_\psi-mc_2^2$). Substituting for α and λ_0 according to equations (23) and (151) then yields, after rearrangement,

$$(\tau v\,D_t-K_\alpha v^{-1}D_t+K_\lambda c_1)y_0+(m_1c_2\,D_t^2-\tau v\,D_t+kc_2-K_\lambda c_1)\eta_a+(I_0\,D_t^2+g\,D_t+\tau av\,D_t+\rho+K_\alpha+ac_1K_\lambda)\theta=0 \qquad (154)$$

The third equation for this system for the general case is given by the kinematic relation of equation (19a) or (19b). When γ is omitted, the space derivatives are replaced by time derivatives, and η_0 is set equal to $\eta_a-a\theta$, this relation becomes

$$-(1+l_1v^{-1}D_t+l_2v^{-2}D_t^2+\ \ldots\ )y_0+(l_1-a)\theta+\eta_a=0 \qquad (155a)$$

from equation (19a) or

$$-(1+Lv^{-1}D_t)e^{hv^{-1}D_t}\,y_0+(l_1-a)\theta+\eta_a=0 \qquad (155b)$$

from equation (19b).

The three equations (152), (154), and (155a) or (155b) completely describe the motion of the landing gear according to the summary theory in terms of the three variables y_0, η_a, and θ. The corresponding equations for the systematic approximations are obtained as follows.

SYSTEMATIC APPROXIMATIONS

Approximation A.—For case II, the three governing equations of motion for approximation A are the force and moment equations (152) and (154) and the kinematic equation:

$$-(1+l_1v^{-1}D_t+l_2v^{-2}D_t^2+l_3v^{-3}D_t^3)y_0+(l_1-a)\theta+\eta_a=0 \qquad (156)$$

Equation (156) is obtained by omitting all l_n's for $n>3$ in the general kinematic equation (155a).

Approximation B.—The three governing equations of motion for approximation B are the force and moment equations (152) and (154) and the kinematic relation

$$-(1+l_1v^{-1}D_t+l_2v^{-2}D_t^2)y_0+(l_1-a)\theta+\eta_a=0 \qquad (157)$$

which is obtained by omitting the l_3 term in equation (156).

Approximation C.—The kinematic equation for approximation C is obtained by omitting the l_2 term in equation (157). The resulting relation is

$$-(1+l_1v^{-1}D_t)y_0+(l_1-a)\theta+\eta_a=0 \qquad (158a)$$

or

$$\eta_a=\left(1+\frac{Nv^{-1}D_t}{K_\lambda}\right)y_0-\left(\frac{N}{K_\lambda}-a\right)\theta \qquad (158b)$$

The force and moment equations (152) and (154) also apply for this approximation. However, a slightly simpler form of these equations can be obtained by substituting for η_a, according to equation (158b), in the terms containing $K_\lambda\eta_a$ and $\tau\eta_a$ in these two equations. With this substitution, the force equation becomes

$$-Nv^{-1}D_ty_0-(m_1\,D_t^2+m\,D_t^2+k)\eta_a+(mc_2\,D_t^2+N)\theta=0 \qquad (159)$$

and (using the relation $K_\alpha=\epsilon N$) the moment equation becomes

$$\left[-\frac{N\tau D_t^2}{K_\lambda}-Nv^{-1}(c_1+\epsilon)D_t\right]y_0+(m_1c_2\,D_t^2+kc_2)\eta_a+\left[I_0\,D_t^2+g\,D_t+\frac{N\tau vD_t}{K_\lambda}+\rho+(c_1+\epsilon)N\right]\theta=0 \qquad (160)$$

Equations (158a), (159) (or (152)), and (160) (or (154)) describe the motion for approximation C.

Approximation D1.—The equations of motion for approximation D1 are obtained by setting λ_0 equal to 0, or

$$y_0=\eta_a-a\theta \qquad (161)$$

and

$$K_\lambda=\infty$$

in the force and moment equations (159) and (160). Thus

$$-(m_1\,D_t^2+m\,D_t^2+Nv^{-1}D_t+k)\eta_a+(mc_2\,D_t^2+aNv^{-1}D_t+N)\theta=0 \qquad (162)$$

$$[m_1c_2\,D_t^2-Nv^{-1}(c_1+\epsilon)D_t+kc_2]\,\eta_a+[I_0\,D_t^2+g\,D_t+aNv^{-1}(c_1+\epsilon)D_t+\rho+(c_1+\epsilon)N]\,\theta=0 \qquad (163)$$

Equations (162) and (163) completely describe the motion for approximation D1.

Approximation D2.—The equations for approximation D2 are obtained as follows. In the force equation (152) set α equal to 0, or

$$\theta=v^{-1}D_t y_0 \tag{164}$$

which gives the relation

$$(mc_2v^{-1}D_t^3+aK_\lambda v^{-1}D_t+K_\lambda)y_0- (m_1 D_t^2+m D_t^2+K_\lambda+k)\eta_a=0 \tag{165}$$

For the moment equation (153), set α equal to $-\lambda_0/l_1$ (eq. (85)) according to approximation C, and apply equations (151) and (164). The result is

$$[I_0v^{-1}D_t^3+gv^{-1}D_t^2+a\tau D_t^2+\tau v D_t+\rho v^{-1}D_t+a(c_1+\epsilon)K_\lambda v^{-1}D_t+ (c_1+\epsilon)K_\lambda]\, y_0+[m_1c_2 D_t^2-\tau v D_t-(c_1+\epsilon)K_\lambda+c_2k]\,\eta_a=0 \tag{166}$$

Equations (165) and (166) are the basic equations for approximation D2.

Approximation D3.—The basic equation for approximation D3 is obtained by first solving the equations (162) and (163) of approximation D1 simultaneously to eliminate either η_a or θ and then letting N approach ∞ so that all terms not multiplied by N vanish. The resulting equation, after dividing out the factor N and using the relation $c_1+c_2=a$, can be expressed in terms of θ as

$$\{[I_0+m_1a(a+\epsilon)+mc_1(c_1+\epsilon)]\, D_t^3+\{[m_1(a+\epsilon)+ m(c_1+\epsilon)]\, v+g\}D_t^2+[\rho+ak(a+\epsilon)]\, D_t+vk(a+\epsilon)\}\theta=0 \tag{167}$$

STABILITY BOUNDARIES

The stability boundaries for case II are obtained in the same manner as those for case I. For the summary theory they are obtained as follows.

Purely oscillatory boundaries.—The equations for the Purely oscillatory motion boundaries are obtained by substituting into the differential equations the expressions

$$\left.\begin{aligned}\theta&=\theta_{max}e^{i\nu t}\\ \eta_a&=\eta_{a_{max}}e^{i(\nu t+\sigma_1)}=\eta_{a_{max}}e^{i\nu t}(\cos\sigma_1+i\sin\sigma_1)\\ y_0&=y_{0_{max}}e^{i(\nu t+\sigma_2)}=y_{0_{max}}e^{i\nu t}(\cos\sigma_2+i\sin\sigma_2)\end{aligned}\right\} \tag{168}$$

Substitution of these relations into equations (152), (154), and (155b), differentiation and cancellation of $e^{i\nu t}$, and separation of real and imaginary parts into separate equations yields the expressions:

From equation (152),

$$K_\lambda(y_{0_{max}}\cos\sigma_2)+(m_1\nu^2+m\nu^2-K_\lambda-k)(\eta_{a_{max}}\cos\sigma_1)+ (aK_\lambda-mc_2\nu^2)\theta_{max}=0 \tag{169}$$

and

$$K_\lambda(y_{0_{max}}\sin\sigma_2)+(m_1\nu^2+m\nu^2-K_\lambda-k)(\eta_{a_{max}}\sin\sigma_1)=0 \tag{170}$$

From equation (154),

$$c_1K_\lambda(y_{0_{max}}\cos\sigma_2)-(\tau v\nu-K_\alpha v^{-1}\nu)(y_{0_{max}}\sin\sigma_2)+ (-m_1c_2\nu^2+c_2k-c_1K_\lambda)(\eta_{a_{max}}\cos\sigma_1)+\tau v\nu(\eta_{a_{max}}\sin\sigma_1)+ (-I_0\nu^2+\rho+K_\alpha+ac_1K_\lambda)\theta_{max}=0 \tag{171}$$

and

$$c_1K_\lambda(y_{0_{max}}\sin\sigma_2)+(\tau v\nu-K_\alpha v^{-1}\nu)(y_{0_{max}}\cos\sigma_2)+ (-mc_2\nu^2+kc_2-K_\lambda c_1)(\eta_{a_{max}}\sin\sigma_1)- \tau v\nu(\eta_{a_{max}}\cos\sigma_1)+(g\nu+\tau a v\nu)\theta_{max}=0 \tag{172}$$

From equation (155b),

$$-p_{1\infty}(y_{0_{max}}\cos\sigma_2)+p_{2\infty}(y_{0_{max}}\sin\sigma_2)+(l_1-a)\theta_{max}+(\eta_{a_{max}}\cos\sigma_1)=0 \tag{173}$$

and

$$-p_{2\infty}(y_{0_{max}}\cos\sigma_2)-p_{1\infty}(y_{0_{max}}\sin\sigma_2)+\eta_{a_{max}}\sin\sigma_1=0 \tag{174}$$

Equations (169) to (174) can be considered as six linear simultaneous algebraic equations with no constant terms in the five variables $y_{0_{max}}\cos\sigma_2$, $y_{0_{max}}\sin\sigma_2$, $\eta_{a_{max}}\cos\sigma_1$, $\eta_{a_{max}}\sin\sigma_1$, and θ_{max}. Then for this system of equations to have solutions other than zero it is necessary that the determinant of the coefficients of any group of five of these six equations should equal zero. The determinant for equations (169), (170), (171), (173), and (174) is

$$\begin{vmatrix} c_1K_\lambda & -\tau v\nu+K_\alpha v^{-1}\nu & -m_1c_2\nu^2+c_2k-c_1k_\lambda & \tau v\nu & -I_0\nu^2+\rho+K_\alpha+ac_1K_\lambda \\ K_\lambda & 0 & (m_1+m)\nu^2-K_\lambda-k & 0 & aK_\lambda-mc_2\nu^2 \\ 0 & K_\lambda & 0 & (m_1+m)\nu^2-K_\lambda-k & 0 \\ -p_1 & p_2 & 1 & 0 & l_1-a \\ -p_2 & -p_1 & 0 & 1 & 0 \end{vmatrix}=0 \tag{175}$$

and the determinant for equations (169), (170), (172), (173), and (174) is

$$\begin{vmatrix} \tau v\nu - K_a v^{-1}\nu & c_1 K_\lambda & -\tau v\nu & -mc_2\nu^2 + kc_2 - K_\lambda c_1 & g\nu + \tau a v\nu \\ K_\lambda & 0 & (m_1+m)\nu^2 - K_\lambda - k & 0 & aK_\lambda - mc_2\nu^2 \\ 0 & K_\lambda & 0 & (m_1+m)\nu^2 - K_\lambda - k & 0 \\ -p_1 & p_2 & 1 & 0 & l_1 - a \\ -p_2 & -p_1 & 0 & 1 & 0 \end{vmatrix} = 0 \qquad (176)$$

where $p_1=p_{1\infty}$ and $p_2=p_{2\infty}$ for the summary theory. The corresponding equations for approximation A are obtained by setting p_1 equal to $1-l_2\nu_1^2$ and p_2 equal to $l_1\nu_1-l_3\nu_1^3$, for approximation B by setting p_1 equal to $1-l_2\nu_1^2$ and p_2 equal to $l_1\nu_1$, and for approximation C by setting p_1 equal to 1 and p_2 equal to $l_1\nu_1$.

The two equations (175) and (176) completely describe the conditions governing purely oscillatory modes of motion according to the summary theory and approximations A to C (other groupings by fives of the equations merely lead to repetition of these two relations). The procedure for obtaining the stability boundaries for each of the other systematic approximations (D1, D2, and D3) is similar to that just outlined. The resulting stability-boundary equations for the other approximations are listed in appendix E.

Purely uniform motion.—For purely uniform motion all variables will have constant values which may be represented as

$$\theta=\theta_{max}$$

$$\eta_a=\eta_{a_{max}}$$

$$y_0=y_{0_{max}}$$

Substitution of these relations into equations (152), (154), and (155) yields the results

$$aK_\lambda\theta_{max}-(K_\lambda+k)\eta_{a_{max}}+K_\lambda y_{0_{max}}=0$$

$$(\rho+K_a+ac_1K_\lambda)\theta_{max}+(c_2k-c_1K_\lambda)\eta_{a_{max}}+c_1K_\lambda y_{0_{max}}=0$$

$$(l_1-a)\theta_{max}+\eta_{a_{max}}-y_{0_{max}}=0$$

For nonzero solutions of these three equations the determinant of the coefficients of θ_{max}, $\eta_{a_{max}}$, and $y_{0_{max}}$ must be zero. Evaluation of this determinant gives simply

$$a+\epsilon+\frac{\rho}{N}=0 \qquad (177)$$

CHARACTER OF THE MOTION BETWEEN STABILITY BOUNDARIES

In order to determine the character of the landing-gear motion (stable or unstable) between stability boundaries it is first convenient to solve the equations of motion for each approximation simultaneously to obtain a single linear differential equation in one variable for each approximation. From these differential equations the stability of the motion may be determined by examining the corresponding characteristic equations by any of the methods discussed in appendix C. These characteristic equations for case II, according to the various systematic approximations, are listed in appendix F.

EVALUATION OF APPROXIMATIONS D1, D2, AND D3

In the earlier discussion of case I it was not possible to present a fair relative evaluation of the three parallel approximate theories D1, D2, and D3 since for case I none of these theories provides any realistic information. However, for case II such a comparison can be made between the predictions of these three approximations and the more accurate approximation C, and a specific example will be discussed here for a sample landing-gear configuration having the relative dimensions and properties $L=0.8r$, $h=a=0.5r$, $c_1=c_2=0.25r$, $\epsilon=0.3r$, $m_1=0.35m$, $I_0=mr^2$, and $\tau=\rho=0$. The actual calculated behavior of this landing gear in terms of damping required for stability as a function of rolling velocity according to approximation C is shown in figure 19 for four values of the ratio of strut stiffness to tire stiffness k/K_λ. It is seen from this figure that as the stiffness of the

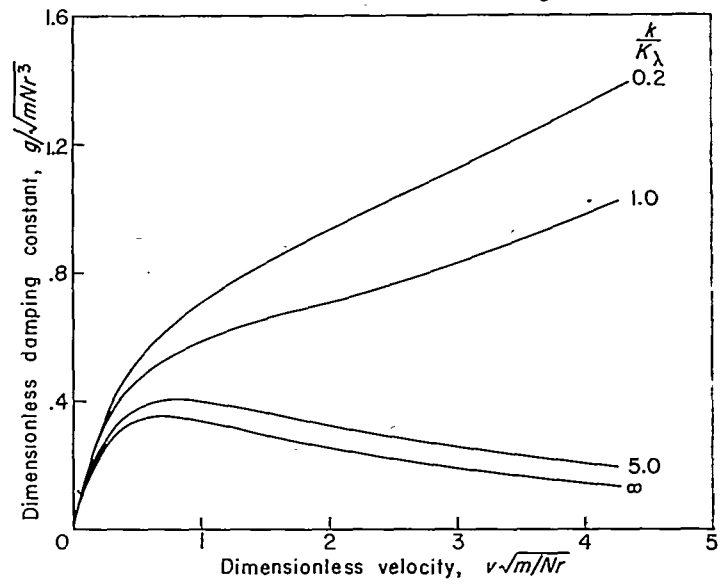

FIGURE 19.—Influence of strut stiffness on damping required for stability according to approximation C for a sample landing gear. $L=0.8r$; $h=a=0.5r$; $c_1=c_2=0.25r$; $\epsilon=0.3r$; $m_1=0.35m$; $I_0=mr^2$; $\tau=\rho=0$.

strut is decreased from infinity the damping requirement is increased. Also, for large values of strut stiffness the region of maximum damping required lies at low speeds, whereas for small values of strut stiffness it lies at higher speeds.

The theoretic predictions of the three theories D1, D2, and D3 for this sample landing gear are compared in figure 20 with the corresponding predictions of the more accurate approximation C (from fig. 19) for three values of strut stiffness, $k=0.2K_\lambda$, $1.0K_\lambda$, and $5.0K_\lambda$. It is seen that for each strut stiffness approximations D2 and D3 provide a considerable overestimate of the damping required for stability. On the other hand, approximation D1 gives results in good agreement with those of approximation C for the ratios $k/K_\lambda=0.2$ and 1.0, but this approximation greatly underestimates the damping for the large value of strut stiffness $k/K_\lambda=5.0$.

In view of the comparisons of figure 20, it appears that approximations D2 and D3 will not, in general, give reliable quantitative estimates of the damping required for stability. It appears that approximation D1 may give reasonable results for some cases in which the lateral stiffness of the strut does not greatly exceed the lateral stiffness of the tire. Since this latter conclusion is based on only one set of landing-gear parameters, the degree to which it is valid in general would require a more extensive investigation for a range of landing-gear properties.

PRACTICAL APPLICATION

One limitation on the practical application of the preceding equations for case II lies in the assumption that the damping is simply proportional to the angular swiveling velocity $D_t\theta$. As was previously mentioned, Moreland has demonstrated that this assumption is sometimes unreliable since it implies a neglect of the torsional flexibility of the landing-gear strut, which in turn can sometimes lead to a false prediction of stability for heavily damped systems (see ref. 11 or 12). Thus, for systems in which torsional flexibility of the strut is important, it will be necessary to replace the damper unit of case II by a damper and spring in series, as has been done by Moreland (refs. 11 and 12), where the spring represents the strut torsional stiffness. This particular case of a series damper-spring unit applied to the landing gear of case II is not considered separately in this report; it is, however, included in the more general case III to be considered next.

CASE III

The next type of landing-gear construction to be considered is chosen largely to illustrate the application of the summary and approximate theories to more complex problems than have previously been considered by now making use of transfer-function concepts. This landing gear is assumed to be of the same general type as that of case II except for the following generalizations. In case II the lateral deflection characteristics of the landing-gear strut were represented by a single spring and mass combination, or, more precisely, the force exerted on the swiveling part of the landing gear by the strut was set equal to

$$F_\eta=-(k+m_1 D_t^2)\eta_a \tag{178}$$

For case III it is assumed that the strut (or, more generally, the supporting structure) is a more complex linear system than is a spring-mass combination, so that the strut force-deflection relation of equation (178) can be generalized to the new form

$$F_\eta=-T_{10}(D_t)\eta_a \tag{179}$$

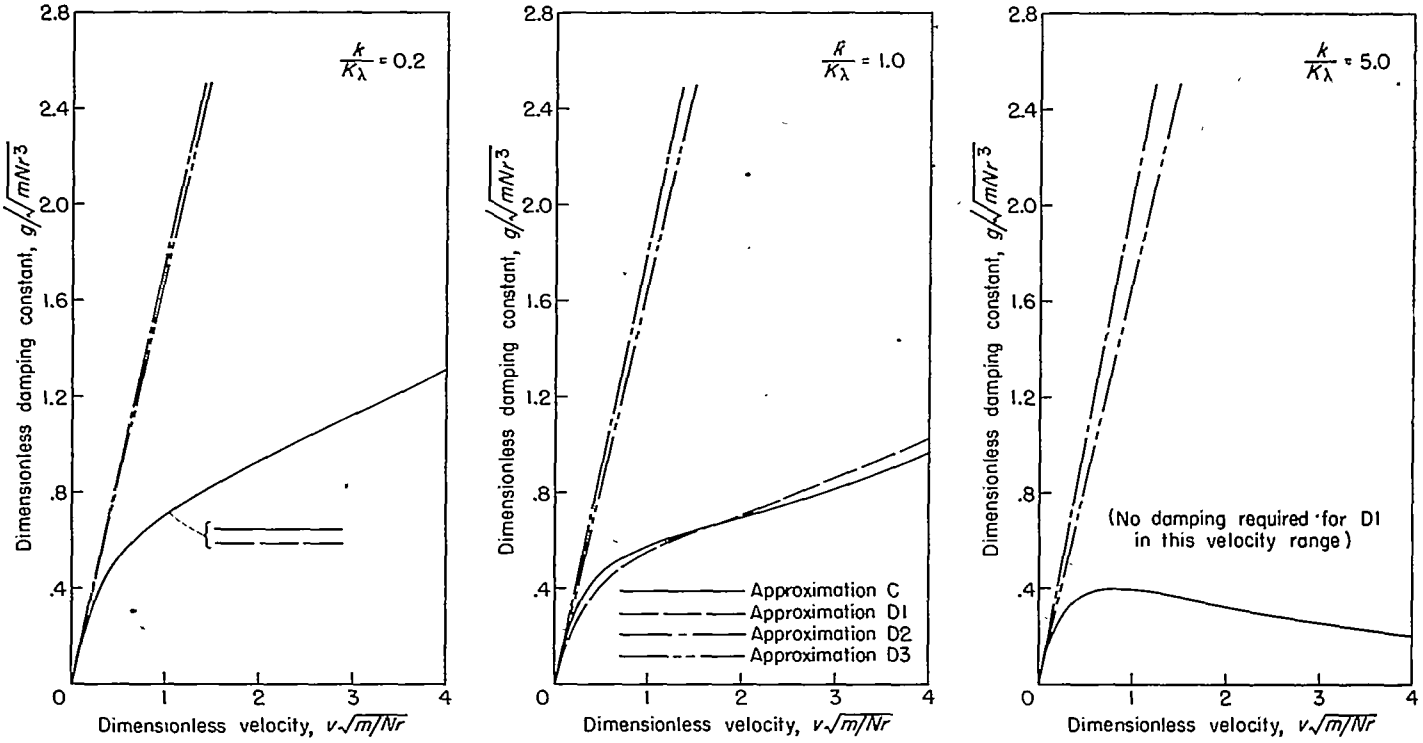

FIGURE 20.—Comparison of damping required for stability according to approximations C, D1, D2, and D3 for a sample landing gear. $L=0.8r$; $h=a=0.5r$; $c_1=c_2=0.25r$; $\epsilon=0.3r$; $m_1=0.35m$; $I_0=mr^2$; $\tau=\rho=0$.

where T_{10} is a function of the differential operator D_t which represents the transfer function correlating F_η and η_a.[3] Similarly, the moment on the swiveling part due to the strut, which was previously set equal to

$$M_\theta = -(\rho + gD_t)\theta \tag{180}$$

for case II, is now generalized to the form

$$M_\theta = -T_{11}(D_t)\theta \tag{181}$$

The differential equations for case III are easily obtained from the corresponding differential equations for case II by replacing $k+m_1D_t^2$ by T_{10} and $\rho+gD_t$ by T_{11}. For example, for approximation D1 equations (162) and (163) are replaced by the new relations

$$-[mD_t^2+Nv^{-1}D_t+T_{10}(D_t)]\eta_a+(mc_2D_t^2+aNv^{-1}D_t+N)\theta=0 \tag{182}$$

$$[-Nv^{-1}(c_1+\epsilon)D_t+c_2T_{10}(D_t)]\eta_a+[I_0D_t^2+aNv^{-1}(c_1+\epsilon)D_t+(c_1+\epsilon)N+T_{11}(D_t)]\theta=0 \tag{183}$$

which lead to a characteristic equation of an order depending on the order of the T's. If the T's are analytically defined functions, the calculation of the stability of the motion and the stability boundaries proceeds exactly as for case II. However, if the T's are not analytically defined functions (for example, if they are determined by experimental tests) a slightly different procedure of the following type is needed.

In order to determine partial information about T_{10}, the swiveling part of the landing gear can be removed and the remaining strut can be subjected to a periodical lateral force $F_\eta = F_{\eta_{max}}e^{i\nu t}$ (either by calculation or by actual vibration tests). The resulting lateral-deflection response of the structure will have a certain amplitude and phase shift which are given by the relation

$$\eta_a = -\frac{1}{T_{10}(i\nu)}F_\eta \tag{184}$$

which is obtained by substitution of the sinusoidal variation for F_η into equation (179). The function $1/T_{10}(i\nu)$ is a complex function of the circular frequency ν, the absolute value of which represents the amplitude response and the argument of which represents the phase shift; it is generally called the frequency-response function of the system.

Similarly, a frequency-response function is defined for the response of the landing-gear strut to torsional moment oscillations by the relation (see eq. (181))

$$\theta = -\frac{1}{T_{11}(i\nu)}M_\theta \tag{185}$$

With the aid of the experimental or calculated functions $T_{10}(i\nu)$ and $T_{11}(i\nu)$, the stability boundaries for any of the theories may be obtained by the usual procedure of substituting expressions of the form $e^{i\nu t}$ into the corresponding differential equation together with the T's. For example, for approximation D3 the basic differential equation is

$$\{[I_0+mc_1(c_1+\epsilon)]D_t^3+[m(c_1+\epsilon)v]D_t^2+[T_{11}(iv)+a(a+\epsilon)T_{10}(iv)]D_t+v(a+\epsilon)T_{10}(iv)\}\theta=0 \tag{186}$$

(obtained by converting eq. (167) to apply to case III), and the stability boundaries for purely oscillatory motion (obtained by setting θ equal to $e^{i\nu t}$ in eq. (186) and separating real and imaginary parts) are given by the simultaneous equations

$$-m(c_1+\epsilon)v\nu^2-\nu\mathrm{I}[T_{11}(i\nu)+a(a+\epsilon)T_{10}(i\nu)]+v(a+\epsilon)\mathrm{R}[T_{10}(i\nu)]=0 \tag{187}$$

$$-I_0\nu^3-mc_1(c_1+\epsilon)\nu^3+\nu\mathrm{R}[T_{11}(i\nu)+a(a+\epsilon)T_{10}(i\nu)]+v(a+\epsilon)\mathrm{I}[T_{10}(i\nu)]=0 \tag{188}$$

where R and I represent the real and imaginary parts of the bracketed functions. Analogous equations are obtained in a similar manner for the other approximations.

In regard to the question as to whether any particular motion between stability boundaries is stable or not, case III may present a more difficult problem if the forms of the T-functions are not known in terms of ratios of polynomials, that is, if only the frequency-response variations are known. In this event, for example, the usual form of the Routh-Hurwitz stability criteria (which is applicable to polynomial forms only) cannot be applied and criteria of the Nyquist type must be used. A brief discussion of these criteria is contained in appendix C.

The procedure for applying the summary and systematic approximation theories to cases of arbitrary complexity is essentially the same as the procedure discussed above for case III, the only important difference being that for the general case the equations of motion (eqs. (16) or (19), (63), (64), (65), (67), (69), and (71)) are more numerous and more complicated. No new concepts need to be discussed.

CONCLUDING REMARKS

This report has presented a correlation and evaluation of the previously published theories of linearized tire motion and wheel shimmy and has demonstrated that the major merits of all of these theories are contained in a summary theory which represents a minor modification of the basic theory of Von Schlippe and Dietrich. In cases where there are strong differences between the existing theories and the summary theory, the previously published theories have, in the main, been demonstrated to possess certain deficiencies except for Moreland's advanced theory, for which no adequate evaluation was possible.

A series of systematic approximations to the summary theory has been developed herein for the treatment of problems too simple to merit the use of the complete summary theory. These systematic approximations have been shown to resemble closely the previously published theories except that in some details they avoid some of the limitations encountered in these theories.

[3] Moreland, in reference 11, has advanced a similar generalization of the strut lateral-deflection characteristics by means of a concept of "virtual elasticity." However, Moreland's generalization is less general in that it does not provide for the existence of strut structural-damping forces.

Comparison of the existing experimental data with the predictions of the summary theory and its systematic approximations has indicated a fairly good degree of correlation between the higher approximations and the existing experimental data for the cases investigated. However, since the agreement is far from perfect in some respects and since most of the limited amount of existing experimental data was obtained with small models there still remains the question as to whether the theory is safely applicable to full-scale conditions. In particular, the importance of hysteresis damping remains undetermined.

In regard to the determination of the various tire constants required for theoretical shimmy calculations, it is noted that the existing pertinent experimental data, mostly contained in references 21, 24, and 32 to 37, are extremely limited and apply mostly to small, obsolete, or foreign tires. Furthermore, although various attempts have been made to correlate and to reconcile theoretically the experimental data (e. g., ref. 2 or 38), there still apparently does not exist any fully reliable theoretical means for predicting all of the needed elastic characteristics of tires. In view of these considerations, a need exists for additional experimental data on modern tire characteristics and also for a more adequate evaluation of the existing data to determine whether these data can be applied by scale laws to predict the characteristics of any tire with tolerable accuracy.

In regard to the adequacy of a linearized theory of tire motion, it can be stated only that there is as yet no strong indication that a nonlinear theory is required for prediction of the stability boundaries. If, however, a knowledge of the large-angle (nonlinear) behavior is required, a theoretical system for dealing with this problem could be developed on the basis of assumptions of the type advanced by Kelley, Rotta, and Temple (see refs. 18, 19, and 21 (p. 36), respectively).

LANGLEY AERONAUTICAL LABORATORY,
NATIONAL ADVISORY COMMITTEE FOR AERONAUTICS,
LANGLEY FIELD, VA., *January 13, 1956.*

APPENDIX A

CALCULATION OF EQUIVALENT VISCOUS DAMPERS

GENERAL CASE

In the derivations and equations in this report, only linear damping terms were introduced so that the resulting equations would remain linearized. However, the damping moments caused by friction, hysteresis losses, and the ordinary shimmy dampers are nonlinear and therefore it is necessary to replace these nonlinear moments with equivalent linear viscous moments. The equivalent viscous moment is usually determined by assuming that linear and nonlinear damping moments are equivalent if they dissipate the same amount of energy during each cycle of shimmy oscillation.

For a linear damper of moment $g D_t\psi$ the energy dissipated per cycle of sinusoidal oscillation is (for $\psi=\psi_{max}\sin \nu t$)

$$E=\int_0^{2\pi} g D_t \psi \, d\psi$$

and, since $D_t \psi=\psi_{max}\nu \cos \nu t$ and $d\psi=\psi_{max}\nu \cos \nu t \, dt$,

$$E=g\nu\psi_{max}^2\int_0^{2\pi} \cos^2 \nu t \, d(\nu t)$$

which gives

$$E=\pi g \nu \psi_{max}^2$$

Therefore the linear damping constant g is related to the energy loss per cycle by the relation

$$g=\frac{E}{\pi\nu\psi_{max}^2} \tag{A1}$$

By using this relation an effective value of linear damping constant can be calculated for any nonlinear damper if the energy dissipation per cycle is known.

VELOCITY-DEPENDENT DAMPING

By using equation (A1) Rotta (ref. 2) has calculated the effective damping constant for damping moments of the type

$$M_\psi=\left(M_0+q_n|D_t\psi|^{n_1}\right)\frac{D_t\psi}{|D_t\psi|} \tag{A2}$$

The first term represents friction damping and the second represents fluid damping. The exponent n_1 will probably always be between 1 and 2.

Rotta's calculations proceed essentially as follows: First, the total energy dissipated is calculated from the relation

$$E=4\int_0^{\psi_{max}} M_\psi \, d\psi \tag{A3}$$

where

$$\psi=\psi_{max}\sin \nu t \tag{A4}$$

After combining equations (A1) to (A4) and integrating, the following equation for g is obtained:

$$g=\frac{4M_0}{\pi\nu\psi_{max}}+q_n\psi_{max}^{n_1-1}\nu^{n_1-1}\frac{4}{\pi}\int_0^{\pi/2}\cos^{n_1+1}\nu t \, d(\nu t) \tag{A5}$$

It is seen that the damping constant depends on the amplitude ψ_{max}; for $n_1>1$ it is large at small angles due to the first term and is large at large angles due to the second term. The minimum value of the equivalent damping constant $\left(\text{obtained by setting } \frac{dg}{d\psi_{max}} \text{ equal to } 0\right)$ occurs at the angle

$$\psi_m=\left[\frac{M_0}{q_n\nu^{n_1}(n_1-1)\int_0^{\pi/2}\cos^{n_1+1}\nu t \, d(\nu t)}\right]^{1/n_1} \tag{A6}$$

and the corresponding minimum damping constant becomes

$$g=M_0^{\frac{n_1-1}{n_1}} q_n^{1/n_1} k_n \tag{A7}$$

where

$$k_n=\frac{4n_1}{\pi(n_1-1)^{\frac{n_1-1}{n_1}}}\left[\int_0^{\pi/2}\cos^{n_1+1}\nu t \, d(\nu t)\right]^{1/n_1} \tag{A8}$$

For the special case of velocity-squared damping ($n=2$) equation (A7) reduces to the relation

$$g=\frac{8}{3\pi}\sqrt{6M_0q_2} \tag{A9}$$

FRICTION DAMPING

The equivalent damping constant for friction damping (constant moment M_0), obtained by setting q_n equal to 0 in equation (A5), is

$$g=\frac{4M_0}{\pi\nu\psi_{max}} \tag{A10}$$

APPENDIX B

DIFFERENTIAL EQUATIONS FOR CASE I WITH INCLUSION OF HYSTERESIS EFFECTS

If the differential equations of approximations B and C2 for case I (see eqs. (122) and (124), respectively) are modified to take into account the hysteresis force and moment expressions derived in this report, the following differential equations are obtained:

For approximation B,

$$E_0 D^4 y_0+E_1 D^3 y_0+E_2 D^2 y_0+E_3 D y_0+E_4 y_0=0 \tag{B1a}$$

where

$$\left.\begin{aligned}
E_0&=I_\psi v^2 l_2\\
E_1&=I_\psi v^2 l_1+(a\tau v^2\cos\kappa+gv)l_2+(a^2K_\lambda T_\lambda+K_\alpha T_\alpha\cos^2\kappa)l_2 v\\
E_2&=Iv^2+(a\tau v^2\cos\kappa+gv)l_1+(a^2K_\lambda+K_\alpha\cos^2\kappa+\rho+\rho_\kappa)l_2+(a^2NT_\lambda+a'K_\alpha T_\alpha\cos\kappa)v\\
E_3&=a^2N+a'K_\alpha\cos\kappa+\rho l_1+\rho_\kappa l_1+gv+\sigma l_1\tau v^2\cos^2\kappa+(\sigma aNT_\lambda\cos\kappa+K_\alpha T_\alpha\cos^2\kappa)v\\
E_4&=\sigma aN\cos\kappa+K_\alpha\cos^2\kappa+\rho+\rho_\kappa+u_\kappa
\end{aligned}\right\} \tag{B1b}$$

For approximation C2,

$$E_0 D^3 y_0+E_1 D^2 y_0+E_2 D y_0+E_3 y_0=0 \tag{B2a}$$

where

$$\left.\begin{aligned}
E_0&=I_\psi v^2 l_1\\
E_1&=I_\psi v^2+(a\tau v^2\cos\kappa+gv)l_1+(a^2NT_\lambda+aK_\alpha T_\alpha\cos\kappa)v\\
E_2&=a^2N+aK_\alpha\cos\kappa+\rho l_1+\rho_\kappa l_1+gv+l_1\tau v^2\cos^2\kappa+(aNT_\lambda\cos\kappa+K_\alpha T_\alpha\cos^2\kappa)v\\
E_3&=aN\cos\kappa+K_\alpha\cos^2\kappa+\rho+\rho_\kappa+u_{\kappa 1}
\end{aligned}\right\} \tag{B2b}$$

APPENDIX C

STABILITY CRITERIA

In this appendix a brief review is presented of most of the existing methods for examining the stability of motion of systems whose motions are governed by linear differential equations of the type

$$f(D_t)\theta=0 \tag{C1}$$

The solution of this type of equation consists of terms of the form

$$\theta=e^{pt} \tag{C2}$$

whence

$$D_t^n\theta=p^ne^{pt}=p^n\theta \tag{C3}$$

Substitution of equation (C3) into equation (C1) yields the algebraic equation

$$f(p)=0 \tag{C4}$$

for the p's. Equation (C4) is called the characteristic equation of the differential equation (C1).

The type of motion for the linear system is determined by the character of the complex roots of the characteristic equation. Most important, the motion is entirely stable if and only if the characteristic equation possesses no roots having positive real parts. Several procedures are available for determining whether a particular characteristic equation has such roots with positive real parts.

One procedure which is useful in cases where the characteristic equation (C4) can be written in the polynomial form

$$a_0p^n+a_1p^{n-1}+\ldots+a_n=0 \tag{C5}$$

is the well-known Routh-Hurwitz criterion which makes use either of the Routh test functions (ref. 26) or of the equivalent Hurwitz determinants. In Hurwitz' form the requirement for stability (or no roots with positive real parts) is that a_0 and all of the n determinants

$$D_1=a_1$$

$$D_u=\begin{vmatrix} a_1 & a_3 & a_5 & \ldots & a_{2u-1} \\ a_0 & a_2 & a_4 & \ldots & a_{2u-2} \\ 0 & a_1 & a_3 & \ldots & a_{2u-3} \\ . & . & . & \ldots & . \\ . & . & . & \ldots & a_u \end{vmatrix}$$

for $u=1, 2, \ldots n$ must be greater than zero, or, in the alternate form of Cremer (ref. 39), all of the a_n's and either the even or the odd Hurwitz determinants must be positive.

This criterion is particularly suited for examining the stability of linear systems with polynomial-type differential equations of low order. However, for high-order polynomial-type differential equations this criterion may not be the easiest to use and for nonpolynomial-type equations the criterion is not directly applicable. For such cases use can be made of the graphical-type criterion originated by Nyquist (refs. 28 to 31). Some discussion of criteria of this type is contained in most books dealing with servomechanisms or feedback amplifiers (for example, refs. 29 and 31). These references provide the necessary theoretical information for applying these criteria and the theory will not be repeated here; however, it may be useful to set down here, together with an example, one mechanical procedure for applying this criterion and a few pertinent comments.

Consider a differential equation with the characteristic equation (B4) for a case where the function $f(p)$ cannot necessarily be easily expressed in a simple polynomial form which can be handled by the usual Routh-Hurwitz criterion. (This may be the case, for example, where part of the function $f(p)$ is evaluated from experimental frequency-response data.)

The function $f(p)$ is assumed to be a single-valued function of p which is real when p is real. It is also assumed that the function $f(p)$ has no poles in the region of the complex p-plane where the real part of p is greater than zero. When the equations of motion are set up in the manner followed in this report, the condition of no poles in this region is usually satisfied for actual landing gears since this condition implies only that the landing-gear strut, as represented by equations or experimental curves, possesses some damping or is at least not inherently an unstable structure. For example, for the equations of case III, only the poles of the functions $T_{10}(p)$ and $T_{11}(p)$ could lead to such poles. However, if, for example, $T_{10}(p)$ had such a pole, equation (161) would indicate the possibility of a steady or divergent oscillating force F_η corresponding to this pole, even if the lower end of the landing-gear strut were held fixed ($\eta_a=0$); this obviously cannot occur in actuality.

In order to decide whether the motion of the system described by equation (C4) is stable, the following procedure may be followed:

(1) Determine the variation of $f(p)$ in equation (C4) for the case of pure sinusoidal oscillations, that is, for $p=i\nu$ in the range $0<\nu<\infty$.

(2) Plot the real part of $f(i\nu)$ against the imaginary part for the complete range $0<\nu<\infty$. This will give a curve such as is illustrated in figure 21 for a sample case. As ν varies from 0 to ∞ this curve will move about the origin through a net angle of $J\pi$ radians, this angle being considered positive in a counterclockwise sense. ($J=1$ for the case illustrated in fig. 21.)

(3) Determine the asymptotic behavior of the characteristic function $f(p)$ of $f(i\nu)$ for $p\to\infty$ or $\nu\to\infty$; at this limit the function will behave as $f(p)\propto p^j$ or $f(i\nu)\propto\nu^j$, whence j can be determined.

(4) Under the preceding restrictions $f(p)$ being a single-valued function of p, real when p is real, and having no poles in the half-plane $R(p)>0$, it can be shown that the motion corresponding to the differential equation is stable if and only if $2J=j$. (In the sample case of fig. 21, where $J=1$ and $j=2$, the motion is therefore stable.)

In conclusion it might be noted that, although either the preceding Nyquist type stability criterion or the Routh-Hurwitz criterion can usually be applied to most of the approximate equations discussed in this report, they cannot be directly applied to some equations of transcendental form such as those of the summary theory, since such equations may correspond to infinite-order linear differential equations (for example, see eq. (120)); hence, an infinite number of Hurwitz determinants would have to be evaluated or the Nyquist type plot would circle the origin an infinite number of times.

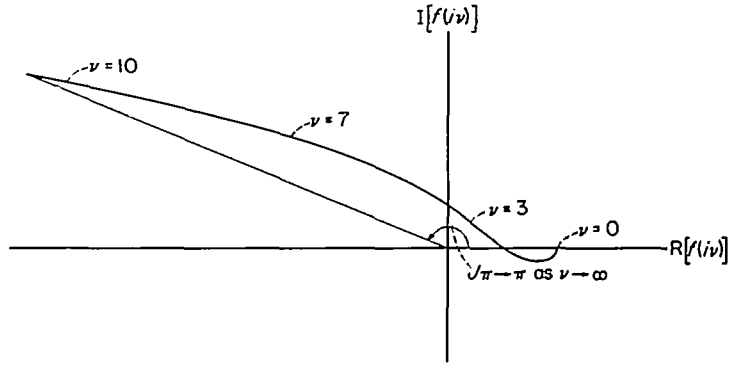

FIGURE 21.—Variation of the function $f(i\nu)$ for the linear differential equation having the characteristic equation

$$f(p)=\frac{p^4+6p^3+23p^2+50p+50}{p^2+2p+2}=0$$

APPENDIX D

STABILITY BOUNDARIES FOR CASE I

The following equations describe the conditions under which purely oscillatory motion is possible for case I for the summary theory and the systematic approximations.

For the summary theory and approximations A to C2,

$$v^2=\frac{(a^2K_\lambda+K_\alpha\cos^2\kappa+\rho+\rho_\kappa)(p_1^2+p_2^2)+[(aK_\lambda+c_\lambda F_z\sin\kappa)p_1-\nu_1p_2K_\alpha\cos\kappa](\sigma l_1\cos\kappa-a)}{I_\psi\nu_1^2(p_1^2+p_2^2)-\tau\nu_1p_2(\sigma l_1\cos\kappa-a)\cos\kappa} \tag{D1}$$

and

$$g=\frac{(\sigma l_1\cos\kappa-a)[p_2(aK_\lambda+c_\lambda F_z\sin\kappa)+\nu_1p_1(K_\alpha-\tau v^2)\cos\kappa]}{\nu_1v(p_1^2+p_2^2)}-a\tau v\cos\kappa \tag{D2}$$

where, for the summary theory,

$$p_1=p_{1\infty}=\cos\nu_1h-L\nu_1\sin\nu_1h$$

$$p_2=p_{2\infty}=\sin\nu_1h+L\nu_1\cos\nu_1h$$

for approximation A,

$$p_1=1-l_2\nu_1^2$$

$$p_2=l_1\nu_1-l_3\nu_1^3$$

for approximation B,

$$p_1=1-l_2\nu_1^2$$

$$p_2=l_1\nu_1$$

and for approximations C1 and C2,

$$p_1=1$$

$$p_2=l_1\nu_1$$

For approximations D1 and D3 purely oscillatory motion does not exist.

For approximation D2,

$$v^2=\frac{a^2K_\lambda+a\epsilon K_\lambda\cos\kappa+\rho+\rho_\kappa+\tau v^2\cos^2\kappa}{I_\psi} \tag{D3}$$

$$g=v\left[\frac{I_\psi(aK_\lambda\cos\kappa+\epsilon K_\lambda\cos^2\kappa+c_\lambda F_z\sin\kappa\cos\kappa)}{a^2K_\lambda+a\epsilon K_\lambda\cos\kappa+\rho+\rho_\kappa+\tau v^2\cos^2\kappa}-a\tau\cos\kappa\right] \tag{D4}$$

The stability boundaries for uniform motion are obtained by setting the coefficient of the y_0 terms in the various differential equations equal to zero. For example, for the summary theory and approximations A and B the equation

$$\sigma aN\cos\kappa+K_\lambda\cos^2\kappa+\rho+\rho_\kappa+u_\kappa=0$$

describes this stability boundary.

APPENDIX E

STABILITY BOUNDARIES FOR CASE II

The equations governing purely oscillatory modes of oscillation for case II are as follows for approximations D1, D2, and D3:
For approximation D1,

$$v^2=\nu^2N^2\frac{[I_0+mc_1(c_1+\epsilon)+m_1a(a+\epsilon)]\nu^2-[\rho+ak(a+\epsilon)]}{[(m_1+m)\nu^2-k]\{-[I_0(m_0+m)+mm_1c_2^2]\nu^4+[I_0k+mkc_2^2+m_1N(a+\epsilon)+mN(c_1+\epsilon)+\rho(m_1+m)]\nu^2-k[\rho+N(a+\epsilon)]\}} \tag{E1}$$

$$g=-Nv^{-1}\frac{\{[m(c_1+\epsilon)+m_1(a+\epsilon)]\nu^2-k(a+\epsilon)\}[(m_1a+mc_1)\nu^2+N-ak]}{[(m_1+m)\nu^2-k]^2+N^2v^{-2}\nu^2} \tag{E2}$$

For approximation D2,

$$v^2=\frac{[I_0(m_1+m)+mm_1c_2^2]\nu^4-[I_0(K_\lambda+k)+\rho(m_1+m)+mc_2^2k+m_1K_\lambda a(a+\epsilon)+mK_\lambda c_1(c_1+\epsilon)]\nu^2+[\rho(K_\lambda+k)+kK_\lambda a(a+\epsilon)]}{\tau\nu^2(m_1+m)-\tau k} \tag{E3a}$$

$$g=\frac{-v\{(\tau am_1+\tau c_1m)\nu^4-[a\tau k+m_1K_\lambda(a+\epsilon)+mK_\lambda(c_1+\epsilon)]\nu^2+kK_\lambda(a+\epsilon)\}}{\nu^2[(m_1+m)\nu^2-(K_\lambda+k)]} \tag{E3b}$$

For approximation D3,

$$\nu^2=\frac{\rho+ak(a+\epsilon)}{I_0+m_1a(a+\epsilon)+mc_1(c_1+\epsilon)} \tag{E4a}$$

$$g=v[k(a+\epsilon)\nu^{-2}-m(c_1+\epsilon)-m_1(a+\epsilon)] \tag{E4b}$$

APPENDIX F

CHARACTERISTIC EQUATIONS FOR CASE II

The characteristic equations for case II are as follows for the summary and systematic approximation theories:
For the summary theory and approximations A to C2,

$$\begin{vmatrix} K_\lambda & -(m_1+m)p^2-K_\lambda-k & mc_2p^2+aK_\lambda \\ (\tau v-K_av^{-1})p+c_1K_\lambda & m_1c_2p^2-\tau vp+kc_2-K_\lambda c_1 & I_0p^2+(g+\tau av)p+\rho+K_a+ac_1K_\lambda \\ -f(p) & 1 & l_1-a \end{vmatrix}=0$$

where, for the general theory,

$$f(p)=(1+Lv^{-1}p)e^{h\theta^{-1}p}$$

for approximation A,

$$f(p)=1+l_1v^{-1}p+l_2v^{-2}p^2+l_3v^{-3}p^3$$

for approximation B,

$$f(p)=1+l_1v^{-1}p+l_2v^{-2}p^2$$

and for approximation C1 or C2,

$$f(p)=1+l_1v^{-1}p$$

For approximation D1 the characteristic equation is

$$[I_0(m_1+m)+mm_1c_2^2]p^4+\{g(m_1+m)+Nv^{-1}[I_0+m_1a(a+\epsilon)+mc_1(c_1+\epsilon)]\}p^3+[(I_0+mc_2^2)k+\rho(m_1+m)+mN(c_1+\epsilon)+m_1N(a+\epsilon)+gNv^{-1}]p^2+\{[a(a+\epsilon)Nv^{-1}+g]k+\rho Nv^{-1}\}p+[\rho+(a+\epsilon)N]k=0$$

For approximation D2,

$$[I_0(m_1+m)+mm_1c_2^2]v^{-1}p^5+[\tau m_1a+\tau mc_1+g(m_1+m)v^{-1}]p^4+[I_0(K_\lambda+k)v^{-1}+\rho(m_1+m)v^{-1}+\tau v(m_1+m)+kmc_2^2v^{-1}+m_1a(a+\epsilon)K_\lambda v^{-1}+mc_1(c+\epsilon)K_\lambda v^{-1}]p^3+[\tau ak+g(K_\lambda+k)v^{-1}+m(c_1+\epsilon)K_\lambda+m_1(a+\epsilon)K_\lambda]p^2+[\tau vk+\rho(K_\lambda+k)v^{-1}+akK_\lambda(a+\epsilon)v^{-1}]p+kK_\lambda(a+\epsilon)=0$$

For approximation D3 see equation (167).

REFERENCES

1. Dengler, Max, Goland, Martin, and Herrman, Georg: A Bibliographic Survey of Automobile and Aircraft Wheel Shimmy. WADC Tech. Rep. 52–141 (Contract no. AF33(038)–21994), Wright Air Dev. Center, U. S. Air Force, Dec. 1951.
2. Rotta, J.: Properties of the Aeroplane During Take-Off and Alighting. Reps. and Translations No. 969, Dec. 15, 1947, and No. 970, Feb. 1, 1948, British M.A.P. Völkenrode.
3. Von Schlippe, B., and Dietrich, R.: Zur Mechanik des Luftreifens. (The Mechanics of Pneumatic Tires.) Junkers Flugzeug- und Motorenwerke, A.-G. (Dessau). (Translation available from ASTIA as ATI 105296.)
4. Von Schlippe, B., and Dietrich, R.: Das Flattern eines bepneuten Rades. (Shimmying of a Pneumatic Wheel.) Bericht 140, L.G.L., 1941, pp. 35–45, 63–66. (Available in English translation as NACA TM 1365, 1954, pp. 125–160, 217–228.)
5. Von Schlippe, B., and Dietrich, R.: Das Flattern eines mit Luftreifen versehenen Rades. (Flutter of a Wheel With Pneumatic Tire.) Tech. Berichte, Bd. 11, Heft 2, ZWB, 1944. (Available in English translation from ASTIA as ATI 51760.)
6. Bourcier de Carbon, Christian: Étude Théorique du Shimmy des Roues d'Avion. (Analytical Study of Shimmy of Airplane Wheels.) Office National d'Études et de Recherches Aéronautiques, Publication No. 7, 1948. (Available in English translation as NACA TM 1337, 1952.)
7. Greidanus, J. H.: Besturing en stabiliteit van het neuswiel-onderstel. (Control and Stability of the Nose-Wheel Landing Gear.) Rep. V 1038, Nationaal Luchtvaartlaboratorium, Amsterdam, 1942.
8. Kantrowitz, Arthur: Stability of Castering Wheels for Aircraft Landing Gears. NACA Rep. 686, 1940.
9. Wylie, Jean: Dynamic Problems of the Tricycle Alighting Gear. Jour. Aero. Sci., vol. 7, no. 2, Dec. 1939, pp. 56–67.
10. Melzer, M.: Beitrag zur Theorie des Spornradflatterns. (Contribution to the Theory of Tail-Wheel Shimmy.) Tech. Berichte, Bd. 7, Heft 2, ZWB, 1940, pp. 59–70. (Available in English translation as NACA TM 1380, 1954.)
11. Moreland, William J.: Landing-Gear Vibration. AF Tech. Rep. No. 6590, Wright Air Dev. Center, U. S. Air Force, Oct. 1951.
12. Moreland, William J.: The Story of Shimmy. Jour. Aero. Sci., vol. 21, no. 12, Dec. 1954, pp. 793–808.
13. Temple, G.: Preliminary Report on the Theory of Shimmy in Aeroplane Nose Wheels and Tail Wheels. Rep. No. A.D. 3148, British R.A.E., July 1940.
14. Maier, E.: Theoretische Untersuchungen über die Stabilität von Flugzeugfahrwerken. FB Nr. 1166, ZWB, 1940.
15. Taylor, J. Lockwood: Oscillation of Castoring Wheels. Aircraft Engineering, vol. XIII, no. 143, Jan. 1941, p. 13.
16. Dietz, O., and Harling, R.: Experimentelle Untersuchungen über das Spornradflattern. (Experiments on Tail-Wheel Shimmy.) FB Nr. 1320, ZWB (Berlin-Adlershof), Nov. 1940. (Available in English translation as NACA TM 1376, 1954.)
17. Schrode, H.: Verminderung der Flatterneigung von Sporn- und Bugwerken durch Einbau besonders geformter Reifen. (Reduction of the Shimmy Tendency of Tail and Nose-Wheel Landing Gears by Installation of Specially Designed Tires.) Tech. Berichte, Bd. 10, Heft 4, ZWB, Apr. 15, 1943, pp. 113–116. (Available in English translation as NACA TM 1391, 1955.)
18. Kelley, Henry J.: Prediction of Yawing Stability Characteristics of Airplanes During Catapulting. Jour. Aero. Sci., vol. 19, no. 8, Aug. 1952, pp. 529–539.
19. Rotta, J.: Rechnerische Behandlung des Flatterns schwenkbarer Laufräder mit Gummibereifung. Focke-Wulf Flugzeugbau G.m.b.H. (Bad Eilsen), Sept. 1944. (Available from ASTIA.)
20. Marstrand, O. J. (with Appendix I by J. B. Shearlaw): Prevention of Castor Shimmy by the Twin-Contact Tyre. R. & M. No. 2508, British A.R.C., Mar. 1942.
21. Hadekel, R.: The Mechanical Characteristics of Pneumatic Tyres. S & T Memo. No. 5/50, British Ministry of Supply, TPA 3/TIB, Mar. 1950.
22. Fromm, H.: Kurzer Berichte über die Geschichte der Theorie des Radflatterns. (Brief Report on the History of the Theory of Wheel Shimmy.) Bericht 140, L.G.L., 1941, pp. 53–56. Available in English translation in NACA TM 1365, 1954, pp. 181–190.)
23. Broulhiet, M. G.: La Suspension de la direction de la voiture automobile—Shimmy et dandinement. Bull. Soc. Ing. Civ. (France), vol. 78, July 1925, pp. 540–554.
24. Horne, Walter B.: Static Force-Deflection Characteristics of Six Aircraft Tires Under Combined Loading. NACA TN 2926, 1953.
25. Temple, G.: Note on American Work on Kinematic and Dynamic Shimmy. Rep. No. A.D. 3158, British R.A.E., Nov. 1940.
26. Routh, Edward John: Dynamics of a System of Rigid Bodies. Part II. Sixth ed., rev. and enl., Macmillan and Co., Ltd., 1905.
27. Guillemin, E. A.: The Mathematics of Circuit Analysis. John Wiley & Sons, Inc., c. 1949.
28. Nyquist, H.: Regeneration Theory. Bell Syst. Tech. Jour., vol. XI, no. 1, Jan. 1932, pp. 126–147.
29. James, Hubert M., Nichols, Nathaniel B., and Phillips, Ralph S.: Theory of Servomechanisms. McGraw-Hill Book Co., Inc., 1947.
30. Frey, W.: A Generalization of the Nyquist and Leonhard Stability Criteria. The Brown Boveri Rev., Brown, Boveri & Co., Ltd. (Switzerland), vol. XXXIII, no. 3, Mar. 1946, pp. 59–65.
31. Bode, Hendrik W.: Network Analysis and Feedback Amplifier Design. D. Van Nostrand Co., Inc., 1945.
32. Horne, Walter B., Stephenson, Bertrand H., and Smiley, Robert F.: Low-Speed Yawed-Rolling and Some Other Elastic Characteristics of Two 56-Inch-Diameter, 24-Ply-Rating Aircraft Tires. NACA TN 3235, 1954.
33. Evans, R. D.: Properties of Tires Affecting Riding, Steering and Handling. SAE Jour., vol. 36, no. 2, Feb. 1935, pp. 41–49.
34. Bull, A. W.: Tire Behavior in Steering. SAE Jour., vol. 45, no. 2, Aug. 1939, pp. 344–350.
35. Evans, R. D.: Cornering Power of Airplane Tires. The Goodyear Tire & Rubber Co., Oct. 17, 1946.
36. Maier, E.: Zur Frage der Seitenbeanspruchungen von Flugzeugfahrwerken. (Lateral Stresses on Aircraft Undercarriages.) Bericht 169, L.G.L., 1943, pp. 19–27.
37. Boeckh: Ermittlung der elastischen Konstanten von Flugzeugreifen. (Determination of the Elastic Constants of Airplane Tires.) Focke-Wulf Flugzeugbau G.m.b.H. (Bremen), Dec. 1944. (Available in English translation as NACA TM 1378, 1954.)
38. Thorson, K. R.: A Rational Method for Predicting Tire Cornering Forces and Lateral Stiffness. Boeing Doc. No. D-11719, Boeing Airplane Co., Mar. 28, 1951.
39. Cremer, L.: Die Verringerung der Zahl der Stabilitätskriterien bei Voraussetzung positiver Koeffizienten der charakteristischen Gleichung. Z.a.M.M., Bd. 33, Heft 7, July 1953, pp. 221–227.